Article:
Reithmeier, RAF, Casey, JR, Kalli, AC orcid.org/0000-0001-7156-9403 et al. (3 more authors) (2016) Band 3, the human red cell chloride/bicarbonate anion exchanger (AE1, SLC4A1), in a structural context. Biochimica et Biophysica Acta (BBA) - Biomembranes, 1858 (7, Part A). pp. 1507-1532. ISSN 0005-2736

https://doi.org/10.1016/j.bbamem.2016.03.030

Band 3, the Human Red Cell Chloride/Bicarbonate Anion Exchanger (AE1, SLC4A1), in a Structural Context*

Reinhart A.F. Reithmeier[1], Joseph R. Casey[2], Antreas Kalli[3], Mark S. P. Sansom[3], Yilmaz Alguel[4] and So Iwata[4]

[1]Department of Biochemistry, 1 King's College Circle, University of Toronto, Toronto, Canada, M5S 1A8

[2]Department of Biochemistry, Membrane Protein Disease Research Group, University of Alberta, Edmonton, Alberta, Canada, T6G 2H7

[3]Department of Biochemistry, University of Oxford, South Parks Road, Oxford, UK, OX1 3QU

[4]Division of Molecular Biosciences, Imperial College London SW7 2AZ

[1]Corresponding author. Tel.: +1 416 978 7739

E-mail address: r.reithmeier@utoronto.ca (R.A.F. Reithmeier).

*This article is dedicated to the (great) grandfathers in the Band 3 field: mentor Guido Guidotti, Bob Gunn, Harvey Lodish, Hermann Passow, Aser Rothstein, Ted Steck and Michael Tanner who all inspired future generations of scientists including colleagues Seth Alper, Lesley Bruce, Naotaka Hamasaki, Mike Jennings, Phil Knauf, Ron Kopito, Phil Low, Jim Salhany, Ashley Toye and others to devote their continued interest to this membrane transport glycoprotein with such a poor name.

Running Title: Band 3 in a Structural Context

ABSTRACT

The crystal structure of the dimeric membrane domain of human Band 3[1], the red cell chloride/bicarbonate anion exchanger 1 (AE1, SLC4A1), provides a structural context for over four decades of studies into this historic membrane glycoprotein. In this review we highlight the key structural features responsible for anion binding and translocation and have integrated the following topological markers within the Band 3 structure: blood group antigens, N-glycosylation site, protease cleavage sites, inhibitor and chemical labeling sites, and the results of scanning cysteine and N-glycosylation mutagenesis. Locations of mutations linked to human disease, including those responsible for Southeast Asian ovalocytosis, hereditary stomatocytosis, hereditary spherocytosis and distal renal tubular acidosis, provide molecular insights into their effect on Band 3 folding. Finally, molecular dynamics simulations of phosphatidylcholine self-assembled around Band 3 provide a view of this membrane protein within a lipid bilayer.

Keywords: Anion exchanger, Band 3, bicarbonate transport, chloride/bicarbonate exchange, distal renal tubular acidosis (dRTA), glycoprotein, hereditary spherocytosis (HS), hereditary stomatocytosis (HSt), membrane proteins, molecular dynamics, N-glycosylation, protein folding, protein quality control, solute carrier 4 (SLC4), Southeast Asian ovalocytosis (SAO), trafficking, transporters

[1]For the purpose of this review, Band 3 refers to the native protein as found in red blood cells, AE1 to the protein expressed from its cDNA, *SLC4A1* as the gene and SLC4A1 as the gene product.

1.0 A brief history of Band 3

Band 3 or anion exchanger 1 (AE1), the founding member of the Solute Carrier 4 family of bicarbonate transporters (SLC4A1), is the predominant glycoprotein of red blood cell membrane where it carries out chloride/bicarbonate anion exchange across the plasma membrane – a process necessary for efficient respiration (Fig. 1). In the tissues, carbon dioxide that diffuses into the red cell by diffusion is hydrated by intracellular carbonic anhydrase II (CAII) to produce bicarbonate, which is in turn transported out of the cell in electroneutral exchange for chloride [1, 2]. Driven by the shift to a lower pCO_2 environment, in the lungs the system is reversed. Bicarbonate that enters the red cell via Band 3 in exchange for chloride is converted by CAII to carbon dioxide, which then diffuses out across the plasma membrane to be expired by the lungs. This central part of the respiratory system increases the blood's capacity to transport carbon dioxide as soluble plasma bicarbonate.

Over the last 45 years, major advances have been made in our understanding of the structure and function of Band 3, culminating with the publication of the crystal structure of the membrane domain responsible for its transport function in 2015 [3]. Band 3 earned its unique moniker in 1971 as the third major band from the top of Coomassie blue-stained gels of red cell ghost membrane proteins resolved in early SDS polyacrylamide gel electrophoresis experiments [4]. Next, proteolytic digestion and chemical labeling studies showed that Band 3 spanned the membrane [5], while crosslinking [6] and hydrodynamic studies [7] showed that Band 3 was a dimer. The fourth major advance was the labeling of Band 3 with the radiolabelled stilbene disulfonate inhibitor, [^{3}H]H_2DIDS [8] and other reagents [9] that characterized Band 3 as a red cell anion exchanger [10]. In 1977 Band 3 Memphis was the first variant identified, due to the altered mobility of a proteolytic fragment in SDS gels [11, 12]. The next major advance was the cloning of the cDNA and deduction of the amino acid sequence of murine AE1 in 1985 [13], followed by the human sequence in 1988 [14] and in 1989 [15]. A truncated form of Band 3 missing the N-terminal 64 residues, expressed in the kidney (kAE1), was also identified in 1989 [16]. Many mutations in the *SLC4A1* gene have been subsequently identified as responsible for blood group antigens classified as Diego [17] and others [18-20], and various diseases and conditions, including Southeast Asian ovalocytosis (SAO) [21, 22], hereditary stomatocytosis (Hst) [23], hereditary spherocytosis (HS) [24] and distal renal tubular acidosis (dRTA) in the truncated kidney form [25, 26]. Glu681 was identified as an essential active-site residue using elegant chemical labelling methods [27, 28]. In 2000 the crystal structure of the cytosolic domain of Band 3 under acidic conditions was published [29], with a higher resolution structure at neutral pH published in 2013 [30]. Electron crystallography of two-dimensional crystals of the Band 3 membrane domain provided a low resolution structure and the dimensions of the dimer [31]. The crystal structure of Band 3 membrane domain labelled with H_2DIDS and in complex with a Fab antibody fragment was published in 2015 [3]. In this review, we place the findings of over four decades of work on Band 3 into the structural context, provided by the high-resolution crystal structure, with an emphasis on key functional residues and mutations linked to human disease.

2.0 Band 3 structure

Human Band 3 consists of 911 residues arranged into two major domains: an N-terminal cytosolic domain (cdAE1) and a C-terminal membrane domain (mdAE1) [5, 14, 15]. The two

domains can be separated by mild protease treatment of red cell "ghost" membranes. Cleavage at Lys360 by trypsin defined an early internal topological marker [5, 7, 32]. The protease sensitive sites are located in a poorly-conserved linker region joining the cytosolic domain (residues 1-360) to the membrane domain (residues 361-911). The conserved portion of the amino acid sequence of the membrane domain of SLC4A1 proteins across species begins at Phe379 [33]. The membrane domain, responsible for the transport function of Band 3, is fully functional in the absence of the cytosolic domain when produced by proteolysis [34] or by expression of mdAE1 in transfected cells [30]. The crystal structure of the isolated cytosolic domain revealed a dimeric structure consisting of an interacting domain and a dimerization domain [29]. The membrane domain of Band 3 has also been the subject of intense structural analysis, but until now only low resolution structures of two-dimensional crystals typically examined by electron microscopy were available [31, 35-37]. These studies confirmed the dimeric nature of the membrane domain and revealed some features of its dimensions, but provided no clear insights into its mechanism of action. Crystals of Band 3 membrane domain have been produced, but they diffracted to low resolution [38]. Breakthrough to a high resolution structure came with the use of monoclonal antibodies [39] that allowed the formation of well-ordered crystals of the dimeric membrane domain of human Band 3-Fab complex, which diffracted to 3.5 Å [3]. This review will focus on the membrane domain of Band 3 and the structural insights provided by the crystal structure (PDB entry: 4YZF). Excellent reviews on the cytosolic domain of Band 3 are available [40, 41].

3.0 Band 3 topology

Band 3 consisting of 14 transmembrane (TM) segments, with the N- and C-termini facing the cytosol, is portrayed spectrally blue to red in Fig. 2. The membrane domain begins with a helical segment (H1) that lies parallel to the inner membrane surface and ends with a disordered C-terminal cytosolic region not visible in the crystal structure. The single site of N-glycosylation at Asn642, located in an unresolved region between TM7 and 8, marks the extracellular side of the membrane. All the blood group antigens [42], located in loops connecting TM segments, also face the cell exterior providing strong validation of the crystal structure (Fig. 2). As expected for an intrinsic membrane protein, most of the TM segments in Band 3 have a predominant α-helical conformation. The crystal structure defines the beginning and end of the helical portions of the TM segments quite accurately, but defining the corresponding boundaries of the lipid bilayer for a membrane protein in a detergent micelle is less reliable. The limits of the TM segments may be determined by other methods such as scanning N-glycosylation mutagenesis or by molecular dynamics (MD) simulations of the protein in a lipid bilayer (see below). Of particular note in the structure are two half-helices that make up TM3 and TM10 (Fig. 2). Proteolytic digestion [43, 44] and biosynthetic studies [45-48] showed that the regions encompassing TM3 and TM10 do not form stable TM helical segments but rather form so-called "re-entrant loops" that are initially in the ER lumen but fold back into the protein during biosynthesis to form the final transmembrane disposition. Thus, not all TM segments in Band 3 span the ~30 Å thickness of the hydrophobic phase of a lipid bilayer as classical 20-residue α-helices. Additionally, short helical segments (H2-6) link many TM segments, mostly on the cytosolic side of the membrane.

A ribbon diagram of the structure of the membrane domain of Band 3 monomer is shown in Fig. 3A again coloured spectrally from blue (N-terminus) to red (C-terminus). A corresponding model illustrates the arrangement of the 14 TM segments in Band 3 highlighting the complex

folding topology of this membrane protein (Fig. 3B). The residues visible in the crystal structure begin at Gly381 and end at Asp887 with gaps in disordered regions of loops connecting TM segments, particularly the long N-glycosylated segment (green) that runs across the structure joining the extracellular ends of TM7 and 8. The 14 TM segments are highly α-helical in conformation in agreement with early circular dichroism measurements [49]. Two of the segments (TM3 and 10), however, have an unusual feature also observed in the bacterial UraA uracil transporter that has a similar fold [50], an extended structure followed by a half-helix [51]. In UraA, the two extended structures interact to form a short anti-parallel β-sheet not resolved in the Band 3 structure. The N-termini of the two helices provide positive helical dipoles facing each other ~12 Å apart that likely play a direct role in anion binding (Fig. 3B). This distance provides space for chloride (1.8 Å diameter), bicarbonate (2.3 Å diameter) or even larger anions transported by Band 3 like pyridoxal-5-phophate (8.8 Å diameter) probably in a hydrated state.

Each Band 3 monomer is arranged into two inverted repeats (TM1-7 and TM 8-14) that have a similar fold, yet the two halves share little sequence identity between them. Furthermore, each monomer consists of a core domain (TM1-4 and TM 8-11) and a gate domain (TM5-7 and TM12-14) with the anion passage located between the domains. The core domain contains the anion-binding site and the gate domain contains the lysine residues in TM5 and 13 that can be crosslinked by H_2DIDS (Fig. 3B). A recent crystal structure of a bacterial member of the SLC26 family of anion transporters revealed the same 14 TM 7+7 inverted topology as Band 3 and UraA [3]. The relative rocking movement of the gate and core domains in these proteins changes the accessibility of the single substrate-binding site from one side of the membrane to the other to accomplish anion translocation [52].

4.0 Band 3 dimer

Band 3 exists as a mixture of dimers and tetramers in the membrane and in detergent solutions [53, 54]. Tetramers are formed by dimerization of AE1 dimers, mediated by the cytoplasmic domain and stabilized by interaction with ankyrin [55]. The isolated membrane domain is dimeric [7] as is the cytosolic domain [29, 41]. Dissociation of Band 3 into its constituent subunits required the use of denaturing detergents like SDS [56, 57]. Transport studies have shown that blocking one subunit of Band 3 with an inhibitor does not prevent transport by the other subunit [58, 59]. Thus, although Band 3 exists as a dimer, the two subunits operate independently from one another. Band 3 dimers form in the ER during biosynthesis and proper folding and oligomer formation are essential for its trafficking to the cell surface [60]. This is particularly important in some dominant disease states where a defective subunit is associated with a wild-type subunit often retaining the heterodimer in the ER. Heterodimer formation of normal and mutant forms of Band 3 occurs in heterozygotes as well as between two mutant forms in homozygotes and in compound heterozygotes in disease states such as dRTA [61].

The crystal structure of the Band 3 membrane domain confirmed its dimeric nature (Fig. 4A). The dimer interface (1092 $Å^2$) consists primarily of a four-helix bundle contributed by TM5 and 6 with the predominant interactions occurring on the extracellular ends of these two helices at Leu572 at the N-terminal extracellular end of TM6 (Fig. 4B). There is also some contribution from TM7 and on the cytosolic side of the membrane from H4 and the loop connecting it to TM13. Viewed from the cytosolic surface (Fig. 4B) there is a funnel-shaped entry between the two subunits, with few interactions between the two subunits on the cytosolic side of the dimer

in the H_2DIDS-labelled form. The dimer interface, which is entirely contributed by the gate domain, may change during the transport cycle as the constituent subunits move from an outward to an inward-facing conformation. Alternatively, the dimer interface may remain fixed and the core domain may move during the translocation cycle.

Band 3 in red cells can be crosslinked quantitatively to a covalent dimer by the membrane impermeant reagent bis(sulfosuccinimdyl)suburate (BS^3) [62]. This reagent forms an intramolecular crosslink between the two H_2DIDS-reactive lysines residue and an intermolecular crosslink between Band 3 subunits. One end of the intermolecular crosslink has been localized to a lysine residue close to the extracellular chymotrypsin cleavage site at Tyr553 – likely Lys551 or Lys562 [63]. These two residues are located in the extracellular loop connecting TM5 and TM6 at the dimer interface. BS^3 crosslinking of Band 3 in the presence of the inhibitor 4,4'-dinitro-2,2'-stilbene disulfonate promotes the formation of SDS-resistant tetramers made up of non-covalent dimers of crosslinked dimers [64].

In Dent's disease, mutations in the ClC-5 chloride transporter cluster at the dimer interface [65]. Phosphorylation of a critical threonine at the dimer interface of the plant nitrate transporter NRT1.1 results in dissociation to a monomer [66]. Mutations located at the dimer interface of Band 3 may affect dimerization and the ability of the protein to exit the ER. No such mutants have yet been identified in the human *SLC4A1* gene. It would be interesting to generate a stable monomeric version of Band 3 and assay its transport function as was done with the ClC transporter [67].

5.0 The DIDS inhibitor-binding site

Anion transport in red blood cells can be inhibited by some organic anions [68], most notably 4,4'-diisothiocyano-2,2'-stilbene disulfonate (DIDS) or its reduced dihydro derivative (H_2DIDS). NMR studies of $^{35}Cl^-$ binding to Band 3 [69-71] revealed three classes of inhibitors: channel blockers like DIDS, transport site inhibitors, and translocation inhibitors. H_2DIDS, which binds to an outward-facing inhibitor site [63, 72-74], reacts irreversibly with Lys539 in TM5 at neutral pH and crosslinks to Lys851 in TM13 under alkaline conditions, thereby bridging the ~13.2 Å distance between the ends of the two lysine residues within each Band 3 monomer (18.6 Å from the Cα backbones) [63, 75, 76]. This is clearly seen in a top view of the crystal structure (Fig. 5A) where the inhibitor is sandwiched between the core and gate domains of the protein. Lys539, located two helical turns in from the extracellular end of TM5, is in a hydrophobic environment, which lowers its pKa and makes it a reactive nucleophile.

Energy transfer occurs between tryptophan residues in Band 3 and bound fluorescent stilbene disulfonates [72]. Fluorescence of the inhibitors is increased upon binding consistent with a hydrophobic environment [74]. Trp848 is located one turn proximal to Lys851 on the extracellular end of TM13 and is likely the predominant tryptophan residue responsible for energy transfer. Trp831 is located near the end of TM13 on the cytosolic side of the membrane. Both tryptophan residues are at the interface region of the membrane, typical of tryptophan residues in membrane proteins [77]. Mutation of Trp492 or Trp496 within TM4 to Phe or Ala causes Band 3 to misfold. These two residues face outward from the same side of TM4 and are in close contact with the N-terminal region of TM8. Replacement of the bulky tryptophans could disrupt this interaction. Mutation of Trp648, Trp662 or Trp723 to Ala but not Phe had the same effect, while mutation of Trp831 or Trp848 had no effect on the folding or functional expression

of AE1 in HEK-293 cells [78]. Trp648 is located in the long strand connecting TM7 and 8 just residues distal for the N-glycosylation site at Asn642 and is not visible in the crystal structure. Trp662 is located near the beginning of TM8 at the membrane interface region, facing towards the end of TM3. Trp723 is located in the extended region of TM10 and is buried within the Band 3 structure. Trp 831 is located at the beginning of the TM13 helix in the membrane interface region, while Trp848 is located one turn in from the extracellular end of this helix facing towards TM5.

DIDS once bound to Band 3 is not accessible to anti-DIDS antibodies [73], consistent with its lack of exposure in the crystal structure (Fig. 5B). In the crystal structure, H_2DIDS is located in a deep cleft on the external aspect of Band 3 between the core and gate domain. The binding of DIDS within a cleft is in agreement with fluorescent energy transfer experiments. These experiments indicated that the inhibitor is located 34-43 Å away from probes located on the cytosolic domain. Although the spatial arrangement between the membrane and cytosolic domain is not known, this distance is less than the thickness of the bilayer indicating the DIDS binding site is buried within Band 3 not on its outer surface [72, 79]. More recent FRET experiments by the Knauf lab showed that that stilbene disulfonate site is located over 60 Å away from the cysteines in the cytosolic domain [79]. This would place the inhibitor binding site near the middle or outer leaflet of the bilayer further towards the external surface than Glu681, as shown by the crystal structure (Fig. 5). One end of H_2DIDS is attached to Lys851, which is located at the extracellular end of TM13. The other end of H_2DIDS is attached to the very reactive Lys539, located two helical turns in from the extracellular end of TM5. Both lysine residues are indeed closer to the external side of Band 3 than Glu681, which is located closer to the cytosolic end of TM8.

H_2DIDS sits between the core and gate domains in a passage that leads to the anion-binding site in Band 3, located some distance below. As such it may impede the relative movement of the two domains, blocking translocation. One H_2DIDS sulfonate group is exposed to solvent, facing the outside of the inhibitor cavity, whereas the second is held in place by interactions with positive dipole between TM3 and TM10 in the gate domain reaching across to Arg730 within TM10 in the core domain (Fig. 5C).

Mutation of Lys539 does not affect the AE1 anion transport activity [80] and this residue is therefore not directly involved in anion transport. Similarly, mutation of the DIDS-reactive lysine residues in murine AE1 (Lys558, Lys869) [81] does not affect anion transport, but does affect inhibitor binding [82]. Inhibitor binding induces a conformational change in Band 3 that locks the protein into an outward-facing state, consistent with an alternating sites model for transport [83, 84]. The centers of the two DIDS molecules are 50 Å apart in the dimer, consistent with energy transfer and other spectroscopic experiments that suggested the sites are greater than 20 Å apart [59, 72, 85]. The crystal structure thus represents an outward-facing conformation of Band 3 with DIDS blocking external access to the central anion-binding site. The binding of DIDS at the interface between the gate and core domain may also inhibit the relative rocking movement between the two domains necessary for anion translocation.

6.0 The substrate anion-binding site

The Band 3 crystal structure did not directly reveal the location of the substrate anion-binding site, although the location of the buried sulfonate of the DIDS molecule interacts directly with

Arg730 that faces back towards the space between the helical ends of TM3 and 10. In bacterial UraA, a protein with similar structure to Band 3, the uracil substrate bound to a central cavity comprised of the extended portions of TM segments 3 and 10 [50]. As suggested in 1989 [86], the partial positive helical dipole charge at the N-terminal end of helices, within disjointed Band 3 TM segments can provide binding sites for anions. Thus, the N-terminal ends of the helical portions of TM3 and TM10 facing in the opposite orientation may provide the binding site for substrate anions in Band 3. The involvement of helix dipoles in anion binding is similar to the chloride-binding site in the bacterial ClC proton/chloride exchanger [87]. Band 3 was initially proposed to show some structural resemblance to a portion of the bacterial ClC based on low-resolution (8.5 Å) electron microscopy analyses of Band 3 crystals [36, 37, 88]. A model of Band 3 based on UraA [89] rather than ClC turned out to be a better fit with the actual Band 3 structure.

The anion-binding site could be located at the N-terminal, positive end of helix dipoles created by the short apposing helices with TM3 and 10 (Fig. 6). The side chain of Glu681 in TM8 may occupy this site in the absence of anions, acting as an active site blocker or gate (Fig. 7). Glu681 was identified as the proton-binding site in Band 3 involved in H^+-sulfate co-transport [27, 28]. Mutation of the homologous residue in murine Band 3 (E699Q) resulted in loss of chloride-mediated anion exchange [90, 91]. The E681Q mutation in human Band 3 also severely impaired Cl^-/HCO_3^- exchange, but accelerates sulfate transport, rendering it largely pH independent [30]. The presence of the negative charge on Glu681 may preclude binding of divalent anions like sulfate due to ionic repulsion, while eliminating the charge on Glu681 would permit sulfate binding. Glu681 is in the position corresponding to active site Glu241 in UraA (Fig. 8). Interestingly, the side chain of Glu681 is only 5.3 Å away from the side chain of the H_2DIDS reactive Lys851 in TM13, suggesting a possible ion interaction between these two residues. Perhaps Lys851 is the ionic partner for Glu681 when it is displaced from the anion-binding site. The relative position of these two residues may be different in Band 3 without the H_2DIDS crosslink and their positions may change during the transport cycle.

The side chain of Arg730 in the helical portion of TM10 faces back towards the active site in Band 3 located 7.5 Å from Glu681 (Fig. 7). Arg730 thus provides the positively-charged environment to accommodate anions. Recall that one sulfonate of H_2DIDS interacts directly with the guanidinium group of Arg730. Arg730 is found at the same position as the active site Glu290 in UraA (Fig. 8). The ends of the side chains of Glu241 and Glu290 involved in binding uracil in UraA are spaced ~8.5 Å apart. In Band 3 Arg730 may interact directly with the negative charge on bicarbonate (and chloride), with the –OH group of bicarbonate forming a hydrogen bond either directly or via water with the side chain of Glu681. In murine Band 3, mutation of Arg748 (equivalent to Arg730 in human AE1) inactivates the protein while mutation of Arg509 (equivalent to Arg490 in human AE1) leads to a mis-folded protein [92]. Arg490 is located one turn from the TM4 end and points inward towards Glu472 in TM3 helix, the side-chains being 2.3 Å apart. Disruption of this salt bridge could be the cause of the mis-folding seen in the mutant.

His834, located near the end of the TM10 helix one turn distal on the same side of the helix as Arg730, was identified as an essential residue in the conformational change that occurs during anion transport [93]. This residue is conserved in all 10 human members of the SLC4 bicarbonate transport family. Mutation of the equivalent His752 in murine Band 3 reduced

transport [91], however this effect was reversed by mutation at the DIDS-reactive Lys558 [94]. These two residues are far apart in the crystal structure, so allosteric changes in long-range interactions may be involved.

There are also a number of hydroxyl-containing residues in the extended regions of TM 3 (Ser465) and TM10 (Ser725, Thr727, Thr528) that could participate in binding anions by replacing bound water molecules as proposed for the dehydration of chloride when bound within ClC channels [95].

7.0 Band 3 Transport Mechanism

Band 3 operates by an alternating access model [96] with the empty carrier tending to face the cell interior [97]. DIDS locks Band 3 into the outward-facing state [98] as seen in the crystal structure [3]. Simple, yet elegant, NMR chloride-binding studies by Falke and Chan [84, 99, 100] showed that Band 3 contains a single buried anion binding site and that the mechanism of transport follows a simple ping-pong mechanism where the transition from outward to inward facing is the rate-limiting step. The ion-binding site was proposed to remain stationary, with access through a gate that rapidly alternates between inward and outward when an ion was bound. These studies further showed that the stilbene disulfonate DNDS and phenylglyoxal modification blocked the chloride binding site [69], while 1,2-cyclohexanedione (CHD) and dipyridamole (DP) block a channel leading to the site [70], and compounds like niflumic acid are translocation inhibitors [71].

The Band 3 crystal structure represents an outward-facing conformation of the protein, locked in place by the inhibitor H_2DIDS. The 14 TM segments in Band 3 consist of two inverted 7 TM repeat regions (TM1-7 and TM8-16) that have a similar fold (Fig. 9). Thus, TM1 and 8, 2 and 9, 3 and 10, 4 and 11, *etc*. have a similar but inverted topology as the segments run in opposite directions. This inverted topology is most important in positioning TM3 and TM10, where their N-termini face each other in the center of the protein to form the anion-binding site.

The membrane domain of Band 3 is composed of two domains: a core domain and a gate domain. The anion passage across the membrane is formed at the interface between these two domains and their relative rocking movement is responsible for anion transport. The core domain consists of TM1-4 and the inverted repeat TM 8-11 bundled together, while the gate domain consists of TM5-7 tightly associated with the inverted repeat TM12-14. It is possible to overlay the corresponding repeats of the core domain, however the gate domain repeats do not overlay (Fig. 10). Conversely, it is possible to overlay the gate domain repeats but then the core domains repeats do not overlay. Thus, in the DIDS-labelled outward-facing structure, the relative positions of the repeats in the core and gate domains are different.

The Band 3 structure represents an outward-facing conformation, while the related UraA structure represents an inward-facing state. We used UraA as a template to thread the Band 3 sequence and produce a model of Band 3 in the inward-facing conformation using Phyre2 Protein Fold Recognition Server (http://www.sbg.bio.ic.ac.uk/phyre2/html/page.cgi?id=help) developed by Lawrence Kelley [101]. Observing the superimposed structures of Band 3 aligned with the UraA structure on their core domains reveals a highly similar domain structure with an RMSD of 1.9 Å (Fig. 11). In contrast to the core domain, the gate domain appears with high differences revealing conformational changes between the Band 3 outward-facing state and the

inward-facing state of UraA. Note the major shift in the positions of the gate domain relative to the core domain, indicated by changes in the positions of the helices. While the TM helices 6, 7 and 13, 14 appear peripheral in both structures, TM helices 5 and 12 are centered and cover the substrate-binding site. In the inward open conformation TM5 and 12 of Band 3 modelled on UraA are translated by ~8 Å and rotated by ~30° relative to the equivalent TM5 and 12 positions in the outward open Band 3. A similar shift in position can be seen for equivalent pairs of helices due to the relative movement of the entire gate and core domains. This alternating access is also seen by fixing the gate domains in the dimerization interface and allowing the core domain to move during the cycle (not shown). In the outward open conformation TM3 would open to the outside of the cell membrane and allow substrate access to the binding site whereby TM10 would close the substrate access from the inside of the membrane. In the inward open state the conformations would change by TM3 closing the substrate access from the outside and TM10 opening it up into the cytosol.

As mentioned earlier, the side chain of Lys851 in TM13 is only 5.3 Å away from the side-chain of Glu681 in TM8 in the H_2DIDS labeled Band 3 structure. In the inward facing model of Band 3 based on UraA, Lys851 is now over 30 Å away from Glu681. Recall that TM8 is in the anion-binding core domain while TM5 and 13 are in the gate domain (Fig. 3B). The change in the distance reflects the dramatic movement of the two domains. The distance between the side chain of Lys852 in TM13 and Lys539 in TM5 is ~20 Å in the inward-facing state compared to 15 Å in the H_2DIDS-crosslinked structure. Thus, there is some relaxation of the Band 3 gate domain structure in the absence of the crosslink.

Band 3 is the world's fastest transporter with a turnover number of some 10^5 chloride ions per second per molecule [102]. The large conformational change in Band 3 that occurs during the transport cycle must involve an equally rapid movement of the core and gate domains. The binding of an anion lowers the activation energy of the protein to allow this rapid conformational change. Band 3 continually oscillates back and forth rapidly when the substrate-binding site is occupied. The energy barrier for the empty carrier is high and does not permit Band 3 to undergo the conformational change. In the empty state, the active site may be occupied by the side-chain of Glu681, locking Band 3 into an inactive conformation. This results in tight coupling of anion binding and translocation resulting in 1:1 exchange, with very limited anion leakage or unidirectional channel activity. One reason for the high turnover number is the high (~30 mM) Km values for chloride. This low affinity for anions allows for rapid de-binding of anions to occur. The key structural feature here is likely that the anion is bound, not by multiple basic side-chains, other than perhaps Arg730, but rather weakly between two helix dipoles, with a neighbouring negative charge provided by Glu681 acting as a gate to displace bound anions. In contrast, the bound uracil in UraA is held in place by multiple interactions that must be made and broken in every transport cycle, resulting in a much slower transport rate.

Band 3 is the founding member of the solute carrier SLC4 family of bicarbonate transporters that includes bicarbonate/chloride exchangers and sodium-coupled bicarbonate transporters [103-107]. Thus, these exchangers and co-transporters share a common ancestor and are related in sequence and structure. They likely operate by a similar transport mechanism with a central substrate-binding site alternately facing the cytosolic or extra-cytosolic side of the membrane [96]. In the exchange mode, the conformational change between inward and outward facing only occurs when anions are bound; the empty carrier cannot undergo the conformational change. In

the co-transporter mode both sodium and bicarbonate must be bound to the active site for the conformational change from outward-facing to inward facing state to occur. In this co-transport mode, the empty carrier must be able to change its conformation from inward-facing to outward facing to complete the transport cycle.

8.0 Band 3 N-glycosylation

The single N-glycosylation site at Asn642 in human Band 3 defined an early extracellular topological marker [108]. This site is located in a largely unresolved region in the middle of a long polypeptide segment (Gln625 – Pro660) that stretches across the entire outer surface of Band 3 linking the extra-cellular ends of TM 7 and 8 in the gate and core domains, respectively (Fig. 3). Asn642 is located about half-way between Gln625 and Pro660, which are about 60 Å apart. This positions the N-glycosylation site near the centre of the outer surface of the Band 3 monomer, although this location would depend upon the conformation of the various regions between Gln625 – Pro660. Also, the oligosaccharide may lie across Band 3 covering much of its external surface.

The complex oligosaccharide on Band 3 is not essential for the functional expression of this membrane glycoprotein. When expressed in transfected HEK-293 cells, Band 3 retains a high mannose oligosaccharide and its anion transport activity [109]. Mutation of the oligosaccharide acceptor site (N642D) does not impair the trafficking of Band 3 to the cell surface or its transport function [110]. Likewise, enzymatic removal of the oligosaccharide chain from mature Band 3, using N-glycanase F, does not affect its transport activity in red cells [111]. During its biosynthesis, Band 3 can interact transiently with the ER chaperone, calnexin, in a N-glycosylation-dependent manner [112]. This transient interaction is neither required for the proper folding of Band 3 nor its trafficking to the cell surface [113]. The N-linked oligosaccharide does play a role in the retention of some Band 3 mutants in the ER via an interaction with calnexin, particularly important in the kidney but not in the developing red cell [113]. Indeed, calnexin is lost during erythroblast development prior to the maximal production of the major red cell glycoproteins, Band 3 and Glycophorin A [114]. Glycophorin A has a role in facilitating the cell surface expression of Band 3, particularly mutants of Band 3 (e.g. SAO and the dRTA mutant G701D) that would otherwise be retained intracellularly [115-119].

9.0 Band 3 Fatty Acylation

Cys843 has been identified as a fatty acylation site in Band 3 [120]. Chemical analysis showed that palmitate at a mole ratio of ~0.7, with stearate making up the remainder, was bound to Band 3 or an 8.5 kDa C-terminal peptide fragment. Thus, in red blood cells every Band 3 molecule is fatty acylated at Cys843. This modification is not required for trafficking of AE1 to the plasma membrane [121] or its functional expression [122]. Unexpectedly, Cys843 is located in the middle of TM13 (Fig. 2). This indicates that palmitoylation may arise from conformational dynamics in this region of Band 3 or protein unfolding that positions Cys843 at the interior membrane interface where it can be palmitoylated by a non-enzymatic acylation reaction. Unfolding of Band 3 may play a role in red cell senescence due to exposure of novel epitopes to the cell surface or increased sensitivity to proteolytic degradation [123]. As such, palmitoylated Band 3 may serve as a marker for red cell aging. It would be interesting to look at changes in the level of palmitoylation of Band 3 as red cells age.

10.0 Band 3-Associated Blood Group Antigens

Single amino acid changes in Band 3 give rise to several blood group antigens on the surface of red cells (Table 1). As such, these epitopes define regions of Band 3 that face the cell exterior, thereby providing valuable topological information (Fig. 2). The first antigen-associated mutation found in Band 3 (P854L) was known as Diego and thus, a new Diego blood group system was formed. This mutation is in the last extracellular loop of Band 3 [124], and is genetically associated with the Memphis K56E mutation present in the cytosolic domain. As expected all antigens are located on the extracellular side of the protein, where the epitope (~6 residues) must be accessible to reactive antibodies. Diego antigens are located on EC1, 2, 3 and 4, as well as the last loop EC7. The correct topological positioning of the blood group antigens to the external surface provides strong validation to the Band 3 crystal structure.

11.0 Topology Studies of Band 3

Extensive studies of Band 3 topology using sequence analysis [13, 125], proteolysis [5, 43], chemical labeling [126], scanning N-glycosylation [45, 46, 127, 128] and scanning cysteine mutagenesis [129, 130] revealed that the membrane domain consists of 12-14 transmembrane (TM) segments. Some regions in Band 3 were proposed to form "re-entrant" loops that do not span the membrane as completely helical segments and are likely involved in the transport mechanism. The crystal structure now confirms that Band 3 contains 14 TM segments with TM3 and 10 containing half extended and half α-helical structures that span the membrane. This fold is also found in the bacterial UraA uracil transporter [50] and SLC26 fumarate transporter [131].

11.1 Proteolytic Cleavage Sites

Early studies found that Band 3 protein was sensitive to proteolytic cleavage by chymotrypsin but not trypsin treatment of intact red blood cells [5]. Chymotrypsin cleaves at two closely-spaced extracellular sites, Tyr555 and Tyr558, in an unresolved region of the protein structure, releasing a small peptide from Band 3 without affecting its ability to transport anions [32] or bind inhibitors [74]. This shows that the integrity of EC loop 3, connecting TM5 and 6, is not essential for anion transport as the two complementary parts of Band 3 remain tightly associated [7, 76]. Pronase or papain treatment of red blood cells has more drastic effects on Band 3, resulting in a loss of transport function [132-134]. In reconstitution experiments using cloned fragments of AE1, TM 6/7 was not required for functional expression of anion transport activity mediated by TM1-5 and TM 8-14 [135, 136]. TM6 and 7 are located on the periphery of the structure at the dimer interface (Fig. 4B).

Band 3 can be cleaved at Lys360 on the intracellular side of the membrane by mild trypsin treatment of ghost membranes, showing that Band 3 spans the membrane [5, 32]. A second site sensitive to trypsin from the cytosolic side of the membrane was localized to Lys743 [137]. This site can however be N-glycosylated in cell-free translation systems when mutated to Asn, showing that this loop is exposed to the luminal side of the ER during biosynthesis in a rabbit reticulocyte lysate supplemented with canine pancreatic microsomes [45]. An acceptor site at Lys743 was however not N-glycosylated when the mutant Band 3 protein was expressed in HEK-293 cells [127]. In the final folded state of Band 3, Lys743 is located in a short intracellular loop connecting TM segments 10 and 11 (Fig. 2). It is proposed that the helical

hairpin encompassing TM10 and 11 folds into the Band 3 structure as a "reentrant" loop during the biosynthesis of the protein (see below).

Denaturation of Band 3 by alkali-treatment of ghost membranes exposes a number of TM segments that were characterized to form "re-entrant" loops (TM2/3 and TM9/10) [138]. TM3 and TM10 are not typical TM helices and they do not interact strongly with the lipid bilayer. TM2 does not act as a strong stop-transfer sequence, which allows the translocation of the TM2/3 region across the membrane during biosynthesis [46]. TM10 is also a weak stop-transfer sequence, allowing the TM9/10 region to translocate across the membrane [139]. TM3 and TM10 turn out to be half extended, half helical TM segments, rather than fully helical TM segments. This unusual TM conformation accounts for the exposure of these TM segments to aqueous solution under strong alkaline conditions and their subsequent sensitivity to trypsin digestion [44]. DIDS labeling stabilizes Band 3 [140, 141] and makes it resistant to alkaline denaturation. Thus, proteolysis reveals three classes of sites: 1) loops sensitive in the native protein, 2) TM segments involved in protein-protein interactions that become sensitive upon denaturation, and 3) stable TM segments that have a strong interaction with other portions of the protein or the lipid bilayer [142].

11.2 Chemical labeling sites

Eosin maleimide, normally a sulfhydryl-directed reagent, reacts with Lys430 located in the first extracellular loop of Band 3 [143], but which is accessible to quenching reagents from the cytosolic side of the membrane [83]. It inhibits anion transport with the eosin located in the anion transport channel [144], but it does not block chloride binding to Band 3, suggesting an indirect or allosteric mechanism [145, 146]. Lys430 is located near the extracellular end of TM1 helix and its side-chain points backwards in between the core and gate domains. It is in a hydrophobic environment, which accounts for its reactivity. The hydrophobic eosin moiety would be sandwiched between the two domains, thereby inhibiting the conformational changes necessary for transport.

Pyridoxal phosphate, a transport substrate of Band 3 can label the protein at Lys851 (the second H_2DIDS-reactive lysine) equivalent to Lys869 in the mouse sequence [126, 147, 148]. This lysine defines part of the translocation pathway between the core and gate domains. Lys851 is located at the extracellular end of TM13 with its side chain facing into the DIDS binding site.

Diethylpyrocarbonate (DEPC) reacts with histidine residues and locks Band 3 into the inward-facing conformation [149, 150]. DEPC reacts from the cytosolic side of the membrane with His834 identified as the primary reaction site [93]. His834 is located one helical turn in from the cytosolic end of TM13. Stilbene disulfonates, which lock Band 3 in the outward-facing conformation, prevent the reaction with DEPC, while DEPC modification in turn, reduces stilbene disulfonate binding [151]. Thus, His834 should be accessible from the cytosolic side of the membrane when Band 3 is in the inward-facing conformation, but should be inaccessible when Band 3 is locked in the outward-facing conformation. In the H_2DIDS-labelled Band 3 structure the side chain of His834 is bound by a pocket formed by the cytosolic loop connecting TM12 and 13 that contains four proline residues (–$P^{815}P^{816}$KWHP^{820}DVP^{823}–). TM12 is unusual (Fig. 3A). It is composed of a N-terminal helical TM segment (Leu785–Ser801 running parallel to the membrane that is connected to a C-terminal helical segment (Leu805–Lys814) by a ~90° bend formed by the sequence –S^{801}GIQ^{804}. The end of TM12 is then connected to the beginning

of TM 13 by the proline-rich loop. The helix-loop-helix structure of this region and the mobile nature of the proline-rich loop were determined by early NMR studies of a synthetic peptide encompassing residues 796-841 [152].

Region 812–830 and more particularly the limit Phe813–Trp818 in the proline-rich cytosolic loop has been defined as a red cell senescence antigen [153]. If this region is displayed to the cell surface in aged red cells, Band 3 must unfold dramatically to display this normally cytosolic region to the extracellular surface. The identification of this sequence is based on a competitive screen using short synthetic peptides. The conformation of the peptides may not reflect the conformation of the same sequence in the context of the intact protein.

Phenylglyoxal compounds react with 1-3 arginine residues in Band 3 and inhibit transport [154, 155]. The reaction is blocked by stilbene disulfonates and reduced by chloride [154, 156]. There are multiple sites of modification on Band 3, with 2/3 of [^{14}C] phenylglyoxal label located in the N-terminal 60 kDa chymotryptic fragment [157]. The modification affects anion binding suggesting that an arginine is directly involved in anion binding [154]. Under selective labeling condition one site in the 35 kDa fragment of Band 3 can be labeled with phenylglyoxal [158]. Arg730 has been identified as a residue required for anion transport [159]. Interestingly, the last arginine residue in the protein, Arg901 [149], which is located on the cytosolic tail of the protein well beyond the end of the helix (Leu874) forming TM14 is modified by hydroxyphenylglyoxal resulting in inhibition of transport [149].

12.0 Cysteine Scanning Mutagenesis

Human Band 3 contains five cysteine residues, two in the cytosolic domain (Cys201and 317) that can be cross-linked to each other [160], and three others in the membrane domain (Cys479, 843 and 885) [161]. Cys479 is located near the extracellular end of TM3; Cys843 in the middle of TM13; and Cys885 in the cytosolic tail of the protein. None of these cysteine residues can be labeled from the cell exterior. Band 3 does not contain any disulfide bonds, which would be located on the extracellular aspect of the protein. As mentioned above, Cys843 has been identified as a site of palmitoylation [120].

A cysteine-less Band 3 is functional [109], allowing the introduction of cysteine residues into defined sites in Band 3 by cysteine-scanning mutagenesis and a subsequent measurement of their accessibility to chemical modification [162]. There is a possibility that the Cys-less version of Band 3 is less stable than the wild-type protein and could sample rare conformational states. Introduced cysteine residues located within TM segments and exposed to the hydrophobic phase of the lipid bilayer, retain their proton and are unreactive. Cysteine residues on loops exposed to solvent, or more interestingly to an aqueous passage through which hydrated anions flow can be labeled by cysteine-directed reagents. If no labeling of sites within TM is observed, this defines the extent of the sequence that is in a hydrophobic and un-reactive environment. Using this method the limits of TM8 were defined as extending from Met664 to Gln683 [163], with the active site residue Glu681 located just within the cytosolic end of TM8. Further studies of TM8 found that small hydrophilic sulfhydryl probes inhibited transport after reaction with cysteine residues placed along one face of a helix in a region from Ala666-Ser690 [164], which extended the C-terminal end of the helix to one identical with the crystal structure.

Protein chemical studies provide additional insight into the structure of the long extended segment between TM7 and TM8. Introduced Cys mutants in the Trp648-Leu655 region immediately following glycosylation site, Asn642, were poorly accessible to biotinylation, whereas Arg656-Met663 could be labeled, with a progressive decline in reactivity moving toward Met663. Towards the C-terminal end, labeling is consistent with an aqueous region extending below the surface of the bilayer. Since the extracellular loop region was poorly resolved in the crystal structure, we can only speculate that core portion of the oligosaccharide at Asn642 sterically blocked labeling in the Trp648-Leu655 region.

Cysteine labeling may provide some insight into the conformational changes of Band 3. The crystal structure defines the outward facing state of the transporter, while labeling studies capture the full conformational spectrum of the protein. The crystal structure reveals TM13 as starting at Thr830, but residues as deep as Leu835 could be labeled from the cell exterior when mutated to cysteine [165]. This suggests that in the inward conformation, the aqueous pore may open more at the N-terminus of TM13. The limits of TM13 and 14 were localized by these studies to Phe836-Lys851 and Ser856-Arg871, respectively, in good agreement with the crystal structure (Fig. 2).

The Band 3 crystal structure was obtained for protein fixed in the outward conformation with H_2DIDS. What effect does this have on the protein? One protein chemical study examined the structure changes occurring upon stilbene disulfonate binding by treating Band 3 with 4, 4'-dinitro stilbene-2,2'-disulfonate (DNDS). Changes in the ability to label introduced cysteine residues with biotin maleimide were assessed [166]. The Ile661-Met663 region at the extracellular end of TM8 became much less able to be biotinylated, either because of steric hindrance by DNDS, or because the end of TM8 becomes less open to solvent.

Overall the ability to biotinylate introduced cysteine residues was accurate in identifying aqueous accessible regions, and thus defining topology of the Band 3 [129, 163, 165]. To differentiate intracellular from extracellular regions, membrane impermeant compounds were used, leading to one result inconsistent with the crystal structure [165]. The monoclonal antibody BRIC132 binds to the sequence Phe813-Tyr824 from the intracellular side of the erythrocyte membrane [167], consistent with the disposition of the region in the Band 3 structure. The Lys814-Val828 region, spanning the cytosolic region between H4-H5, all of H5 and up to the end of TM13 could be labeled by the small, charged, hydrophilic compound, monobromotrimethylammoniobimane (qBBr). Labeling cannot easily be explained by a systematic artifact of qBBr leakage into cells, as cytosolic Cys201 and the Leu873-Cys885 regions were not labeled by qBBr. Given the Band 3 crystal structure, the biochemical data can be explained by two possibilities: 1, qBBR can transit through Band 3 and label the cytosolic region it reaches immediately upon entering the cytosol, or 2, in some extreme conformation, the cytosolic region H4-H5 can pull out of the Band 3 structure and access the extracellular milieu. Consistent with the latter idea, Phe813–Tyr818 has been identified as a red cell senescence antigen [168]. Together this suggests that the H4-H5 region under normal circumstances transiently becomes accessible to the outside of the cell and that in senescence the region becomes "fixed" in this position. Labeling with qBBr occurred for 10 min, which is a long time in the conformational life of Band 3, with its transport rate of 10^5 ions per second. Thus qBBr may trap a rare conformational form of Band 3. Note that in the structure TM13 and 14 are quite short and are connected to the rest of the structure by an exotic cytosolic loop containing two helical segments (H4 and 5).

Cysteine scanning mutagenesis was also used to define the regions of AE1 involved in dimer formation [169]. Single cysteine residues were substituted into 16 different positions in AE1 in putative extracellular and intracellular loops and the protein was expressed in HEK-293 cells. Zero-distance crosslinked disulfide dimers were generated with mutants T431C, Y486C, Y555C, G565C and A751C. None of the crosslinks had any significant effect on anion transport activity. Based on the structure of the Band 3 dimer, Tyr555 and Gly565 in EC loop 3 between TM5 and TM6 are at the dimer interface (Fig. 4B). The crosslinking results with T431C are inconsistent with the crystal structure. Thr431 is at the extracellular end of TM1 and the two equivalent residues are over 70 Å apart in the Band 3 dimer. Furthermore, Thr431 is centrally located at the interface between the core and gate domains, which suggests that crosslinks between pairs of dimers in a membrane is unlikely. Similarly, Tyr486 is at the extracellular beginning of TM2 and the equivalent residues are over 90 Å apart in the Band 3 dimer. An inter-molecular crosslink between Band 3 dimers is possible in this case as TM2 is on the periphery of the dimer. Ala751 is located in an unresolved intracellular loop region between TM10 and 11 about 30Å apart in the dimer. This loop may have a dynamic aspect facilitating crosslinking within the dimers or between dimers.

Fluorescence resonance energy transfer (FRET) was used to measure distance within the Band 3 dimer. The distance between cysteine residues introduced in place of Gln434 in the short loop between TM1 and 2 was measured as 49±5 Å [170]. The crystal structure reveals the distance from the two Cα atoms to be 75 Å. The difference in the distances might be due to the large size of the fluorescent probe, the relative orientation of the probes or the conformational dynamics of Band 3. That is, the crystal structure illustrates an H_2DIDS-locked outward conformation. Whereas, without inhibitor, the FRET data represent the inward and outward conformations with the inward conformation dominating as demonstrated by the use of inhibitor probes and flux measurements [97, 171].

Additional studies examined the sulfhydryl-reagent sensitivity of Cl^-/HCO_3^- exchange by AE1 introduced Cys mutants. In the Val806-Cys885 region (H4- C-terminal end of TM14) function was inhibitable for only 10 mutants in the region Val849 to Leu863 [130]. These all cluster toward the external ends of TM13-14 and the short loop extracellular connecting them. The crystal structure reveals that the region lies close to the Band 3 active site. Inhibitable mutant Leu863Cys extends most deeply into the plane of the bilayer, well aligned with Glu681, indicating that the inhibitors used (pCMBS and MTSEA) could not move past the constriction point at the active site. The ability of chloride to block inhibition by the negatively charged mercurial, pCMBS, varied amongst the residues. The Band 3 structure shows that residues deepest in the plane of the bilayer and thus closest to active site Glu681, were most sensitive to chloride, indicating that substrate selection was present near the active site.

A study focused on the TM8 region [164] accurately identified a sequence of sulfhydryl-reagent-sensitive introduced Cys mutants that the crystal structure reveals as facing toward the anion translocation pore. That study also found that pCMBS would not inhibit mutants beyond Glu681, but that membrane-permeant MTSEA would. Again, this reveals that the region around Glu681 marks a restriction point in Band 3 past which substrate movement is restricted.

Finally, a homology model developed for AE1 on the basis of the ClC structure [87], was used to identify possible functionally important residues in AE1 [88]. Although UraA is a better model

for Band 3 than ClC, ClC also has an inverted repeat structure of two sets of seven TMs and features discontinuous helices in the transmembrane region. The ClC homology model was combined with Ala scanning mutagenesis to identify critical residues. In this way, Gly463 and Ser465, were identified as functionally sensitive. Both residues are at the C-terminal end of the extended TM region, just before the start of TM3, where they may play a role in forming the substrate anion binding site. Phe792 in TM12 faces directly into the cleft between the gate and core domains, directly across form Glu681. As a hydrophobic residue facing into the active site, Phe792 may assist in positioning of the substrate anion. More difficult to explain is the loss of activity associated with Phe878Ala, which the Band 3 structure reveals as in the short linker between TM14 and H6. This position was tolerant of mutation to Tyr, or Leu, but not Ala or Thr, suggesting that a bulky residue is required. Sensitivity of this position may be explained by effects on positioning of neighbouring residues at the N-terminus of TM13.

13.0 N-glycosylation scanning mutagenesis

N-glycosylation of membrane proteins is a co-translational event that occurs on the luminal side of the ER membrane. As mentioned above, Band 3 contains a single site of N-glycosylation at Asn642, consistent with the extracellular location of this long strand. Removal of this site through mutagenesis does not impair the functional expression of Band 3. The utilization of introduced acceptor site (-Asn-X-Ser/Thr-) into defined sites in Band 3 is consistent with exposure of this loop to the oligosaccharyl transferase enzyme on the luminal side of the membrane *during biosynthesis*. Furthermore the acceptor site must be located 12 or more residues from the end of the preceding TM segment and 14 or more residues from the beginning the following TM segment [45]. Thus, it is possible to map the ends of TM segments in Band 3 during the biosynthesis and folding of this membrane protein. Using this method, the luminal end of TM1 during biosynthesis was localized to Phe423. In the crystal structure, TM1 helix terminates at Thr431 (Fig. 2). TM2 was not stably integrated into the membrane and forms part of a reentrant loop. The luminal end of TM4 was localized to Ile487. In good agreement, the TM4 helix begins at Tyr486, with this aromatic residue located at the membrane interface. The luminal ends of TM5 and TM6 were localized to Phe544 and Pro568 respectively. In the structure TM4 helix terminates at Asp546 while the TM 5 helix begins at Thr570, in excellent agreement with the scanning N-glycosylation results. The luminal ends of TM7 and 8, which border the N-glycosylated loop were localized to residues Ile624 and Met663 respectively. The TM7 helix begins at Phe623 and the TM8 helix at Ile661, again in excellent agreement with the biosynthetic studies. TM9 and 10 form a reentrant loop, since residues located on the cytosolic side of the membrane in the folded protein (e.g. Lys743) could be N-glycosylated on the luminal side of the ER membrane in cell-free translation systems. The luminal ends of TM9 and 12 (the region encompassing TM10 and part of TM11 were luminal) were defined as residues Pro722 and Leu764 respectively with the intervening sequence exposed to the ER lumen during biosynthesis. In the Band 3 structure the extracellular end of the helix forming TM9 is located at Phe719 followed by Gly720 as a helix terminator in good agreement with the topology assay. Leu764 is however located within TM11 suggesting that the region between TM9 and TM12 undergoes dramatic conformational changes during biosynthesis and upon Band 3 attaining its final folded state. This would involve insertion of the reentrant loop consisting of TM10 and 11 into the protein with Leu764 moving from the membrane surface to the middle of TM11 and placing TM12 into its final position. Clearly the C-terminal region of Band 3 (TM10-14) exhibits dramatic conformational flexibility during biosynthesis.

14.0 A Proposed Model for the Folding of Band 3 During Its Biosynthesis

Results of cell-free translation seen in the light of the topology of the final folded structure (Fig. 3B) provide insight into the Band 3 folding pathway. TM1 is known to act as a signal sequence to target the nascent chain to the ER via an initial interaction with the signal recognition particle (SRP) [48, 172]. H1 preceding TM1 may interact with the head-groups of lipids to help position the first TM segment. We hypothesize that TM2 and 3 are translocated entirely across the ER membrane into the lumen during biosynthesis. Indeed, in cell-free translation studies using reticulocyte lysates and dog pancreatic microsomes, TM2 has been shown to be an inefficient stop transfer sequence and that TM3 is a poor signal sequence [47, 48]. TM4 acts as an efficient stop transfer sequence, suggesting a folding intermediate with two TM segments (TM1 and 4) spanning the ER membrane (perhaps still held within the translocon), with TM2 and 3 being located entirely within the ER lumen perhaps bound to chaperones. Indeed, Band 3 truncated after TM4 can be stably integrated into the ER membrane [173] and the proper integration of TM2 and 3 required TM4 [174]. We suggest that this folding intermediate then can move from the translocon laterally into the lipid bilayer. We further suggest that TM5 and 6 then insert into the translocon and form a hairpin loop, which then moves into the bilayer. TM7 follows and acts as a signal sequence to translocate EC loop 4 across the membrane [173], which is know to be co-translationally N-glycosylated at Asn642 allowing interaction with the ER chaperone calnexin [112]. TM2 and 3 are proposed to remain in the ER lumen and not insert into the protein to form the native transmembrane loop until TM8-11 are synthesized to form the remainder of core domain (Fig. 3B). TM8 follows joined to TM7 by a long intervening N-glycosylated segment and acts as a stop-transfer sequence within the translocon. TM9 then acts as an internal signal sequence and is know to translocate the sequence containing TM10 and 11 into the ER lumen followed by part of TM11 and TM12 acting as the stop-transfer sequence [45, 127]. TM10 and 11 are proposed to then fold into the protein and assume a transmembrane disposition to form the core sub-domain with TM12 assuming a transmembrane disposition [139]. TM13 and 14 insert into the translocon as the final hairpin loop. The stop codon is reached following residue 911, allowing release of TM13 and 14 from the translocon and the final part of the nascent polypeptide inserts into the lipid bilayer. TM12-14 now can interact with TM5-7 to form the gate domain. Thus, it is clear that Band 3 does not fold in a linear fashion with TM segments forming sequential hairpin loops. Rather, pairs of non-interacting hydrophobic TM segments are positioned in the bilayer (e.g. 1, 4 and 5, 6) and can only collapse to form the two domains when distal TM segments move into the bilayer. Once the monomer has folded in the bilayer upon completion of translation, we propose that Band 3 becomes ready to form a dimer, through interactions of extracellular portions of TM5 and 6, as revealed in the crystal structure.

Certain complementary fragments of Band 3 can assemble to form a functional transporter, including TM1-8 + TM9-14 and TM1-12 +TM13-14 [135]. This indicates that these regions of Band 3 can insert into the ER membrane, interact directly and assemble into a functional transport unit [175]. The integrity of EC loop 2, which connects TM3 and 4, is required to reconstitute transport. EC3, which contains the chymotrypsin cleavage site and EC4, which contains the site of N-glycosylation, are not, however, required for transport function [176]. Surprisingly, complementary fragments encompassing TM1-5 and TM8-14, but leaving out the fragment encompassing TM6 and 7 in the gate domain are able to reconstitute transport activity when expressed in *Xenopus* oocytes [136]. TM6 and 7, which are part of the gate domain, are located at the interface of the Band 3 dimer, suggesting that the complementary fragments could

form a functional unit, perhaps as a monomer. These experiments show that complementary fragments of Band 3 can move into the lipid bilayer, find each other and assemble a functional transporter [177].

15. Band 3-Glycophorin A Protein Interactions

Glycophorin A is a type I single-span membrane protein that interacts with Band 3 in the mature red cell membrane forming the Wright (Wr) blood group antigen [116, 178]. The Band 3/Glycophorin A complex is not resistant to detergent extraction, as Band 3 can be readily purified without any contaminating Glycophorin A [179, 180]. Patients with the Wr (a+b-) blood group have an E658K mutation in Band 3 [178]. Glu658 of Band 3 is proposed to interact with Arg61 in the extracellular domain of Glycophorin A to form the Wr antigen. Glu658 is exposed on the extracellular side of the membrane near the beginning of TM8, which is located on the opposite far end sides of the Band 3 dimer, distanced ~120 Å apart (Fig. 4A). Glu658 is located at juxta-membrane position at the beginning of TM8, exposed to solvent in a position to form a salt-bridge with Glycophorin A. The dimeric TM segments (residues 82-101) of Glycophorin A may interact with this hydrophobic surface in Band 3 encompassing parts of TM8.

Glycophorin A promotes the cell surface expression of Band 3 [116-119, 181]. Glycophorin A interacts with Band 3 in the ER, suggesting that these two protein assemble and traffic together to the cell surface [115]. Perhaps Glycophorin A stabilizes an intermediate in the folding process. Indeed red cells of Band 3 knock-out mice are devoid of Glycophorin A [182, 183]. In contrast, Band 3 can be found in human red cells devoid of Glycophorin A, but with a decrease in transport activity suggesting that Band 3 does not fold perfectly in the absence of Glycophorin A [183, 184]. The Glycophorin dimer may promote a linear polymerization of multiple Band 3 dimers causing clustering of the proteins at ER exit sites. It is interesting to speculate that perhaps the C-terminal tail of Glycophorin A interacts with Sec23/24 of the COP II complex facilitating vesicle formation. Furthermore, perhaps Glycophorin A blocks the relative movement of the core and gate domain rendering Band 3 inactive until the two protein dissociate when they reach the plasma membrane. This would prevent rapid bicarbonate movement across the membranes of the ER and Golgi, which might interfere with the regulation of the internal pH of these organelles

Glycophorin A is essential for the movement of the G701D dRTA mutant to the plasma membrane [119]. Gly701 is located in the cytosolic loop connecting TM8 and 9, while Glu658 is on the opposite side of the membrane at the beginning of TM8. The interaction of Glycophorin A with Glu658 may induce a transmembrane change in the Band 3 mutant transmitted by TM8, facilitating its folding. Glycophorin A contains a cluster of basic residues in its cytosolic juxta-membrane region, which may interact directly with Asp701 in the dRTA mutant, stabilizing or masking this region of Band 3 to allow the protein to fold and traffic beyond the Golgi to the plasma membrane. The G701D mutation causes the dRTA disease due to the absence of Glycophorin A in the kidney, resulting in intracellular retention of the mutant.

16. Band 3 Mutations in a Structural Context

Mutations in the Band 3 gene are linked to several human diseases and conditions (Tables 1-3) [104, 185-188]. Many of these mutations affect the folding of Band 3 and its subsequent

trafficking from its site of synthesis in the ER, through the Golgi and to its final destination in the plasma membrane. Some also directly affect its transport function. In the following sections the mutations are positioned within the structure of Band 3 and an assessment is made of the impact of the mutations on the folding and stability of the protein.

16.1 Band 3 Memphis and High Transport Mutant

The Memphis Band 3 variant, described by Mueller and Morrison in 1977 [11], was the first polymorphism found in Band 3. It arises from a K56E point mutation located at the beginning of the first β strand in cdAE1 [12]. Treatment of intact red blood cells with Pronase or chymotrypsin produces a 60 kDa N-terminal fragment and a complementary ~35 kDa C-terminal N-glycosylated fragment [189]. In heterozygotes with the Memphis mutation, proteolytic treatment of Band 3 produces a doublet of 63 kDa and 60 kDa polypeptide bands of equal intensity on SDS gels, with the upper band carrying the Memphis point mutation. This gel shift assay provides a convenient biochemical assay for the presence of Band 3 Memphis, which is often linked to other mutations. Genetic analysis in non-human primates revealed that Band 3 Memphis is the ancestral *SLC4A1* gene [190].

A high transport (HT) variant (P868L) also carries the Memphis mutation. Band 3 HT exhibits increased anion transport activity in red cells and results in an abnormal red cell shape (acanthocytosis) [191]. It was originally discovered by Marguerite Kay as a Band 3 protein with a slower than normal migration rate on SDS gels [168]. The mutation is located within TM14 of Band 3, suggesting an important role of this region in the transport mechanism. The proline to leucine mutation is expected to remove a slight kink found in the last TM14 helical segment. The removal of proline would also be expected to create a stable α-helical segment due to the creation of a complete hydrogen-bonding network of back-bone carbonyls and amide groups. The straightening of TM14 may enhance anion transport by creating a conformational state that is an intermediate in the transport cycle, lowering the activation energy of the process.

16.2 Southeast Asian Ovalocytosis Deletion

The SAO deletion of nine amino acids (Ala400-Ala408) is located on the cytosolic boundary region of TM1 [22, 192]. The resulting mutant protein is found at near-normal levels in the red cell membrane of heterozygotes where it has some negative impact of the transport activity of the normal subunit [193]. The structure (Fig. 12) shows that this sequence creates a sharp turn at Pro403, linking an amphipathic helix H1 that lies parallel to the membrane to TM1. The SAO deletion removes the first six helical residues of TM1, which would disrupt its interaction with neighbouring TM segments, such as TM3, 8, 10 and 11. This deletion results in a severely mis-folded protein, unable to bind inhibitors or transport anions [194, 195]. The deletion also removes a bend induced by Pro403 as shown by NMR studies of synthetic peptides corresponding to TM1 [196]. This may change the orientation of TM1 and the preceding amphipathic H1 helix that normally lies across the cytosolic surface of the protein. This could change the disposition of the cytosolic domain relative to the membrane domain.

The crystal structure shows that N-terminal amphipathic helix H1 has extensive interactions with the cytosolic ends of TM4, 9, 11 and the loop connecting TM2 and 3 (Fig. 3A & 4B). Gly455 terminates the TM2 helix and is in a short sequence (-GAQP-) that forms a tight turn leading to the beginning of TM3 at Pro458 that folds into a bend in the amphipathic H1 helix at Pro391.

The beginning of the amphipathic helix is close to the cytosolic end of TM4. TM9 starts with Asp705. The preceding cytosolic loop (Lys691-Leu704) is close to a trio of arginines, particularly Arg388, located the beginning of the amphipathic helix H1. Asp396 is close enough to form an ionic interaction with Arg760 at the beginning of TM11. R760Q/W are HS mutations and disruption of this ionic interaction may result in protein misfolding affecting not only the membrane domain but its interaction with the cytosolic domain (Table 1).

Pro403 at the N-terminus of TM1 may play a role in initiating formation of this helix during biosynthesis. As mentioned above, TM1 of Band 3 acts as a signal sequence directing the protein to the ER membrane and its insertion into the lipid bilayer, translocating the following TM2 and 3 into the ER lumen with TM4 acting as a stop-transfer sequence [46]. The SAO deletion impairs the ability of TM1 to act as a signal sequence, resulting in poor translocation of the TM2/3 loop into the lumen. A fraction of SAO TM1 can assume a transmembrane topology with the luminal end of the helix located in a similar position to the normal TM1 [197]. Part of the hydrophilic sequence proximal to TM1 is likely drawn into the membrane in the SAO mutant. AE1 SAO is retained in the ER in transfected cells but can traffic to the cell surface with the aid of Glycophorin A or by forming a hetero-dimer with WT Band 3 [114, 198]. Glycophorin A may interact with Band 3 on the cytosolic side of the membrane, helping to correct the defect induced by the SAO deletion. There is solid biochemical evidence for the presence of Band 3 heterodimers in ovalocytes and that the deletion mutant affects the structure and function of the normal subunit [193, 199].

16.3 Hereditary Stomatocytosis Mutants

Mutations in Band 3 are associated with hereditary stomatocytosis (HSt) [23]. Typically in HSt the mutant Band 3 is expressed although it has no anion exchange activity but induces a conductive cation leak in affected red cells [23, 200]. The leak is blocked by classic inhibitors of anion transport suggesting that the mutated Band 3 provides a trans-membrane passage for cations. This channel-like feature was confirmed by expression of the mutants in *Xenopus* oocytes [201]. Band 3 mutations causing HS (see below) can occur throughout the sequence and generally cause protein misfolding and trafficking defects, resulting in loss of expression at the cell surface and membrane instability. In contrast, the HSt mutations result in a protein that is expressed properly, is defective in chloride/bicarbonate exchange, but forms a cation channel inducing a red cell Na^+ and K^+ leak. There can be an ~100 fold increase in the leak of cations, however this leak is extremely small compared with the normal rate of anion transport in red blood cells. Thus, the HSt mutations convert Band 3 from an excellent anion transporter into a poor cation channel.

Many HSt mutations cluster in or around TM10 on the cytoplasmic half of the core domain in TM8, 9, 10, 11 and 12 and may directly affect anion binding (Fig. 13, Table 2). In particular, Arg730 in the TM10 half-helix likely forms part of the bicarbonate-binding site, and a R730C mutation likely leads directly to loss of anion binding and transport activity. Mutation to lysine preserved activity while changing the arginine to histidine, isoleucine, or glutamate resulted in loss of activity [202]. Two other mutations in the TM10 half-helix are S731P and H734R, both mutations resulting in a 100-fold increase in cation leak in patients' red cells measured at 0°C. L687P is located near the C-terminus of TM8 and places a strong helix-breaking residue in a helical region. The E758K mutant required GPA co-expression in order to traffic to the cell

surface of oocytes with near normal anion transport activity but appeared to induce a cation leak through an endogenous pathway not directly through the mutant Band 3 protein [203]. The S762R mutation is located near the N-terminus of TM11 in close contact with the essential His734 in TM10. The G796R mutation [204] is located in the middle of TM12 where it introduces a large residue with a strong positive charge that would certainly interfere with packing of this helix against TM5. Many of these naturally-occurring mutations that eliminate anion transport activity are located in the half-helix TM10 highlight the central importance of this region in anion binding and translocation. Furthermore, the structural alterations in this region induced by the mutations provide a passageway for cations, allowing K^+ and Na^+ to move across the red cell membrane down their electrochemical gradients.

16.4 Hereditary spherocytosis mutations

Single amino acid changes in Band 3 can cause hereditary spherocytosis (HS), a hemolytic anemia resulting from smaller misshapen red cells. Most of these dominant mutations cause Band 3 to mis-fold and be retained in the ER in transfected cells [205]. Loss of Band 3 results in membrane instability and blebbing of membrane vesicles producing smaller spheroidal red cells. Importantly, dominant HS mutants can form heterodimers with the wild-type protein and retain the wild-type protein in the ER, exaggerating the loss of Band 3 at the cell surface [205].

HS mutations are found in both the membrane domain [205] and the cytosolic domain of Band 3 [40]. Cytosolic mutations affect the interaction of Band 3 with the protein components of the underlying cytoskeleton, which leads to membrane instability. Band 3 Tuscaloosa (P327R) is associated with a 30% deficiency of protein 4.2 in the heterozygous state [206]. This mutation is associated with the asymptomatic Memphis mutation (K56E). Three HS mutations (E40K, G130R and P327R) in cdAE1 do not affect the stability of the domain or the expression of Band 3, but diminish binding to protein 4.2 [207, 208]. Cytosolic domain mutations do not dramatically affect the domain's structure [209]. Furthermore, the three mutations do not cluster, but are located on the same surface of the protein. The three mutations all involve the introduction of positive charges into a largely acidic protein surface. This suggests that the interaction of protein 4.2 with the cytosolic domain is electrostatic and may involve a large surface area [207].

HS mutations are common in the Band 3 membrane domain. A selection of these mutations is summarized in Table 3. The crystal structure provides valuable insights into the effect of the mutations on the folding of Band 3 (Fig. 15, Table 3). A common theme that emerges for the HS mutations is that most are located close to the ends of TM helical segments. As such, the substitution could de-stabilize the helix, its position in the bilayer during biosynthesis or compromise helix-helix interactions required to achieve the final folded state.

Arg760 at the N-terminal region of TM11 points towards the cytosolic end of TM2, perhaps stabilizing the negative helix dipole. Arg760 may also interact with the phosphate group of lipids as it is on the surface of the protein positioned at the lipid interface, particularly during biosynthesis in the ER. Similarly, Arg870 is located one turn from the cytosolic end of the TM14 helix and may also be involved in interactions with lipid head groups, helping to position this final helix in the membrane (see MD simulation below). There is some overlap between HS and HSt. The R760Q and D705Y mutants have features of both conditions, namely low expression levels and a cation leak. Details of other mutants are found in Table 3.

16.5 Distal Renal Tubular Acidosis Mutations

SLC4A1 mutations also cause a kidney disease, distal renal tubular acidosis (dRTA) [26, 61, 210] as summarized in Table 4. Kidney Band 3 (kAE1), a truncated form of Band 3 missing the first 64 residues, is expressed at the basolateral membrane of acid-secreting α-intercalated cells of the kidney, where it mediates bicarbonate re-absorption into the blood in exchange for chloride [211, 212]. Protons are transported into the urine by an apical V-type H^+ ATPase to acidify the urine. Mutations that cause dRTA have been introduced into kAE1 and the effect of the mutations on functional expression have been studied in different cell systems, include HEK-293 cells, human K562 erythroleukemic cells that express endogenous Glycophorin A, non-polarized and polarized Madin-Darby canine kidney (MDCK) cells and in *Xenopus* oocytes that are amenable to transport measurements [26, 213, 214]. Some dRTA mutants show different trafficking patterns depending on the cell expression system and the degree of polarization achieved [213, 215].

One of the first dRTA mutations to be identified and studied is a C-terminal truncation missing the last 11 amino acids in the protein (Band 3 Walton, 901STOP) [216]. This mutation causes impaired exit of the protein from the ER and mis-sorting to the apical membrane in highly polarized epithelial cells [217-219]. The portion of the Band 3 sequence distal to Asp887 was not visible in the crystal structure, which is located by the cytosolic loop connecting TM 12 and 13 and begins with the L^{886}DADD region that forms the CAII binding site on Band 3 [220, 221]. The interaction of CAII with Band 3 promotes bicarbonate/chloride transport activity [2] by forming a membrane transport metabolon, a functional complex of a transporter with its cognate enzyme that metabolizes the imported substrate [222]. The truncation could impair the ability of TM14 to interact with TM13 since it would be buried within the ribosome upon termination of translation. Finally, it has been demonstrated [223] that the eleven terminal residues in Band 3 contains a phosphorylation-dependent sorting signal at Tyr904 that works in cooperation with Tyr359 in the cytosolic domain to target kAE1 to the basolateral membrane [224].

The kidney disease, dRTA presents in dominant and recessive forms [210, 225]. In the dominant disease, kAE1 typically retains function but is retained in the ER. In recessive dRTA, kidney Band 3 has impaired trafficking to the BLM in polarized MDCK epithelial cells often resulting in a decrease in functional expression. Dominant mutants of kAE1 like R589Q can form heterodimers with wild-type AE1, and retain the wild-type protein in the ER [226]. Recessive mutants can also form heterodimers with wild-type kAE1, but in this case, the wild-type protein can promote trafficking of the heterodimer to the cell surface [226]. Glycophorin A can facilitate the trafficking of certain dRTA mutants, including S667P and G701D (G719 in mouse), to the cell surface [119, 227, 228].

Compound heterozygous recessive mutants such as G701D and A858D can form hetero-dimers that are predominantly retained in the ER [229, 230], while hetero-dimers with the wild-type protein can traffic to the plasma membrane when expressed in transfected HEK-293 cells. Compound heterozygotes can also carry one dominant and one recessive mutation. In the case of the A858D/V850del compound heterozygote, the recessive and inactive V850del, which, by itself is retained in the ER, reached the basolateral membrane when co-expressed with the dominant, mildly misfolded A858D [231]. There are also compound heterozygotes of dRTA mutations with SAO. Recall that the SAO mutant is completely non-functional and retained in

the ER in the absence of Glycophorin A. SAO Band 3 can form a heterodimer with wild-type, or with dRTA mutants and retain the partner subunit in the ER [198, 232]. In these examples, Band 3 SAO exhibits a dominant-negative effect on its partner subunit, preventing its exit from the ER and trafficking to the cell surface. Thus, SAO Band 3 in compound heterozygote combination with a dRTA mutation can cause not only SAO in red cells, but severe dRTA in the kidney. Note that SAO heterozygotes with wild-type kAE1 do not exhibit dRTA, showing that a reduction in the expression of kAE1 alone is not sufficient to cause dRTA.

The crystal structure reveals how the dRTA mutations may affect the proper folding of kidney Band 3 (Table 4 and Fig. 15). Arg589 is located near the cytosolic end of TM6, one turn in from the end of the helix (Fig. 15). The side-chain points directly towards to a cluster of hydroxyl groups donated by Thr798, Ser799 and Ser800 one turn away from the cytosolic end of TM12 helix. This suggests a polar interaction between the guanidinium group and the oxygen atoms, particularly Thr798. The R589H/S/C dRTA mutations would be predicted to disrupt this interaction and change the interaction of TM7 and 12. The dominant R589H dRTA mutant is retained in the ER, but can be rescued to traffic to the cell surface by blocking its interaction with the ER chaperone calnexin [113].

A homozygous G701D mutation causes dRTA [233] as well as in a compound heterozygous state with an A858D mutation [230]. The G701D mutant can exit the ER but is retained predominantly in the Golgi [225]. Gly701 is located in a hydrophilic loop connecting TM8 and 9 on the cytosolic side of the membrane. The cytosolic end of TM9 is close to H1. The G701D mutation would place the Asp residue close to a cluster of Arg residues in H1, promoting a non-native ionic interaction. Mutating Gly701 to Asp or even Lys, however, results in retention of the mutant protein in the Golgi while an Ala substitution, but not Leu, results in normal trafficking [225]. Thus, it is likely that the replacement of the small glycine residue with bulkier residues alters the native structure of the loop, affecting the packing of TM8 and 9.

The trafficking of G701D mutant (G719D in mouse) can be rescued by the co-expression of Glycophorin A [228]. Since Glycophorin A interacts with Band 3 in the ER during biosynthesis it may correct the folding defect induced by the G701D mutation. Glycophorin A interacts directly with Glu658 at the beginning of TM8 on the extracellular side of the membrane but may also interact with the TM portion of Band 3 and on its cytosolic side. This interaction may "correct" the altered positioning of TM8 induced by the G701D mutation. Details of other dRTA mutations are given in Table 4.

17. The SLC4 family of anion transporters

Band 3 is the founding and best-characterized member of the SLC4 family of anion transport proteins [234]. There are 10 human SLC4 members: SLC4A1-5 and SLC4A7-11, as well as SLC4A6, a pseudogene [235-237]. SLC4A2 and SLC4A3 are closely related to SLC4A1 and are typically designated as AE2 and AE3 respectively; they all mediate anion (Cl^-/HCO_3^-) exchange [103, 238, 239]. The second group of SLC4 transporters is the electrogenic (e) sodium bicarbonate co-transporters, of which there are two members: NBCe1 and NBCe2 that share about 50% sequence identity [105, 240-242]. The third group is the electroneutral (n) sodium-coupled bicarbonate transporters that includes NBCn1, NBCn2 and the sodium-dependent chloride/bicarbonate exchanger (NDCBE) that are highly related with over 70% sequence identity [105]. Two other members of the human SLC4 family have been identified based on

sequence homology, and these have been designated AE4 and BTR1. AE4 clusters phylogenetically with Na^+-coupled transporters, and has been suggested to facilitate either Na^+/bicarbonate co-transport [243, 244] or Cl^-/HCO_3^- exchange. BTR1 (SLC4A11) shows less than 20% sequence identity to other members of the SLC4 family and many transport functions have been proposed. SLC4A11 plant orthologs mediate borate transport [245, 246]. The human protein is unlikely to share this function, and most recently is reported to mediate NH_3 [247] and water transport [248-250].

Like Band 3 (AE1), AE2 and AE3 have a similar two-domain structure with an N-terminal cytosolic domain and a C-terminal membrane domain made up of 14 TM segments [103, 107, 238]. Fig. 16 shows homology models of the membrane domains of the exchangers, SLC4A2 (AE2) and SLC4A3 (AE3) and the sodium-bicarbonate co-transporter, SLC4A4 (NBCe1) based on their sequence alignment with Band 3 (SLC4A1, AE1). The proteins display the same 7 + 7 topology as Band 3, not surprising given their high level of sequence identity. The key features involved in the transport mechanism are conserved across the AE1-3. Namely, Glu681 in Band 3 is retained as Glu1011 in AE2 and Glu1003 in AE3. Similarly, Arg730 is conserved in the three AE proteins, as Arg1060 in AE2 and Arg1052 in AE3. AE1-3 differ from all other SLC4 proteins by the presence of a three amino acid insertion (AE1 L655-R656-S657) just before the N-terminus of TM8. The region is in an extended structure, far from the dimeric interface, near the lipid head groups. Among the three anion exchangers the sequences are not conserved, but all contain a Lys or Arg. These residues are positioned where they could potentially interact with negatively-charged lipids, as further suggested by data in the next section. Some important role of this sequence is indicated by the reduction of transport function to 5-60% of WT level upon mutation to cysteine [163].

Na^+-coupled SLC4 proteins have some key differences from AE1-AE3. While Glu681 is conserved in all exchangers, it is replaced by aspartate in all sodium-bicarbonate co-transporters, except SLC4A11, which is likely a NH_3/water transporter. Glu681 provides the proton-binding site in Band 3 required for sulfate transport and likely provides the sodium-binding site in the NBCs. Arg730 is also not conserved in the Na^+-coupled SLC4 proteins, rather being a leucine or isoleucine. Fig. 16 shows a homology model of human SLC4A4 (NBCe1), including a zoom-in of the active site. We hypothesize that Asp799 in NBCe1 binds the sodium ion. Loss of the positive charge at Band 3 Arg730 by conversion to Ile803 in NBCe1 may be necessary to accommodate and translocate the sodium ion.

AE2 and AE3 differ from Band 3 (AE1) in having a larger extracellular loop (so-called Z-loop) between TM5 and TM6, 19 or 27 residues longer than AE1, respectively. This disordered loop contains the sites of N-glycosylation in AE2 and AE3 consistent with their exposure to the extracytosolic side of the membrane. The poorly-conserved loop region is not likely related to transport function as the region is remote from the transport site and AE2 and AE3 transport faster and slower than AE1, respectively. That said, this loop region contains the AE3 A867D mutation, which predisposes carriers to idiopathic epilepsy [251]. The A867D mutation does not affect the protein's ability to process to the cell surface, but reduces Cl^-/HCO_3^- exchange activity by about two-fold [252]. While this site is clearly not involved in ion transport, it may guide substrate to the transport site, such that anion movement is slowed past the acidic Asp. Like AE1, AE2 and AE3 have a long extended strand that runs across the external face of the protein

connecting TM 7 and 8 that, in contrast to AE1, is devoid of N-glycosylation acceptor sites (Fig. 16 top).

Homology modeling suggests that AE2 contains a novel cytosolic β-hairpin loop (coloured magenta in Fig. 16) with a turn centered on Pro1077. In AE3 this region contains a short helix (coloured green in Fig. 16). While the secondary structure is not established, these exposed loops may provide sites of cytosolic protein interaction. Band 3 is, in fact, unusual in the short length of loop between TM6 and TM7, as this region is also about 59 residues larger in Na^+-coupled SLC4 proteins than in AE1. Electrogenic NBCe2 stands out from all other SLC4 proteins in having a 16 amino acid insertion between the C-terminal end of TM12 and the H4 sequence. The unique role of this region will require additional attention.

A role of TM5 in substrate selection by SLC4 proteins is suggested by the observation that NBCe1a D555E mutant manifests a Na^+-independent Cl^- conductance [253]. The position of this mutation is homologous to E535 in human AE1 and is thus close to the key DIDS-binding residue, K539. Interestingly, this residue is conserved as glutamate in all AE proteins and in electroneutral Na^+/HCO_3^- co-transporters. Amongst electrogenic SLC4 proteins the residue is aspartate. Together this suggests an involvement of the residue in charge selection of substrates, the aspartate perhaps providing room for the sodium ion.

Disease-causing mutations of NBCe1, associated with pRTA and ocular deficits [254-258] arise in positions suggesting that the protein shares a fold with Band 3. Strikingly, the mutations G486R and A799V are homologous to positions one residue before the N-terminal end of TM3 and TM10, respectively. This provides additional support for the role of these short helical regions in function of SLC4 proteins. Interestingly, the N-terminus of TM3 is particularly sensitive to functional disruption as T485S also causes disease. Other NBCe1 mutations localize to positions homologous to TM1, TM4 and H4 in Band 3.

SLC4A11 stands apart from the other SLC4 family members as not demonstrating bicarbonate transport and for its phylogenetic distance. Unlike Na^+-coupled SLC4 proteins, SLC4A11 conserves the Glu681 residue found in AE1-AE3. Unique amongst the SLC4 proteins at the position homologous to Arg730, SLC4A11 has a His residue. Functionally this would be consistent with Na^+-independent transport, but also raises the possibility of pH-dependent transport or H^+ co-transport.

The preponderance of data indicates that SLC4 proteins share a common fold as illustrated by homology modeling shown in Fig. 16. The AE1 membrane domain has 30-45% amino acid identity and 37-54% similarity with other members of the SLC4 family [237], and folding is likely to follow sequence. The positions of disease mutations (above) lend further support to a common fold for SLC4 proteins. Substituted cysteine mutagenesis studies of NBCs [259-262] provide protein chemical data fundamentally consistent with the Band 3 crystal structure. In particular, the functional importance of TM1, which is in the core domain, but interfacial with the gating domain, was better appreciated in NBCe1 than in AE1 [260]. Biotinylating sulfhydryl reagents did not sharply define the ends of TMs, rather labeling residues residing somewhat beneath the surface of the bilayer, in some cases. For example, NBCe1 TM1 was defined as extending nine residues C-terminally longer than shown by the Band 3 crystal structure [260]. At the N-terminal end of TM1, the C-terminal end of H1 and start of TM1 were not accessible to biotinylation [263]. The protein chemical data are, however, beautifully consistent with the open

structure at the C-terminal end of TM1, which forms part of an aqueous-accessible cleft going beneath the plane of the bilayer outer leaflet phosphate head groups. The Band 3 crystal structure also reveals a tight protein packing of the pre-TM1 region that could not be biotinylated in NBCe1 introduced Cys mutants [263]. Moreover, the functional sensitivity of NBCe1 introduced cysteine mutants to small, hydrophilic probes along one helical face, is entirely consistent with the crystal structure and the proposed mechanism of Band 3 conformational change.

18. Band 3 in a Lipid Bilayer

To investigate the position of Band 3 in a membrane, coarse-grained molecular dynamics simulations of the membrane domain of Band 3 in a 1-palmitoyl-2-oleoyl phosphatidylcholine (POPC) bilayer were performed (Kalli, Sansom and Reithmeier, in progress). This is an established protocol to predict the position and interaction of integral membrane protein in a more realistic membrane environment [264]. In the simulations, the crystal structure of Band 3 dimer, after it was converted to a coarse-grained representation, was placed in the center of a simulation box. Lipids were randomly placed in the simulation box along with water and counter ions (Na^+ and Cl^-). Simulations of 200 ns with the protein restricted were performed, allowing POPC bilayer to self-assemble around Band 3. At the end of the simulation protein restraints were removed and further five additional 1 μs simulations were performed with the protein free to diffuse in the bilayer, thus optimizing its position and interaction with the bilayer lipids. Note that for these simulations the missing flexible regions of Band 3 in the crystal structure (residues: 554-566, 641-648, 743-752) were modeled in resulting in an intact structure from residue 381 to residue 887.

At the end of the simulations the Band 3 dimer is almost completely buried in the POPC bilayer with the ends of most of the helical regions positioned in the lipid head-group region rather than extending beyond into the aqueous phase (Fig. 18A). Besides TM3 and 10, some helices (e.g. TM2, 9, 11, 13 and 14) are shorter than others and do not fully span the bilayer. At end of the simulations the flexible region, Y553-L567 in the extracellular part of the protein, which was missing from the crystal structure and modeled in our simulations, lays at the protein/water interface interacting mainly with the external surface of Band 3. At the beginning of the simulations, this region was disordered and extended as a loop away from the rest of the protein. The cytosolic H1 segment (before TM1) lies parallel to the membrane surface and is located close to the lipid phosphate groups in these simulations. Cytosolic helices H4 (between TM12 and 13), H6 (after TM14) and H3 (extracellular, between TM11/12) were also located close to the lipid phosphate groups, similar to H1. H5 (cytosolic, following TM12 and H4), however, was located in the lipid head-group/water interface. Calculation of the interactions between the lipids and lipid phosphate groups (Fig. 18B) suggest that the amino acids that form the highest number of interactions with the lipids are predominantly positively charged arginine and lysine residues, as well as tryptophan residues. However, it should be noted that this is a simple bilayer containing only one phospholipid, POPC. In more complex bilayers, as found in the erythrocyte, Band 3 interaction with the lipids, such as cholesterol [265-267], may be selective. We found a similar outcome in our simulations of the UraA, a bacterial uracil transporter with a similar 14 TM fold to Band 3, which showed specific interactions with the lipid cardiolipin [268]. Interaction of specific positively-charged residues with lipid head groups may play a key role in

the insertion of Band 3 into the ER membrane, the lipids acting as chaperones to assist in the folding process.

Further studies are underway to produce a full atomistic model of Band 3 in a lipid bilayer. At the beginning of the simulation Band 3 is in the outward-facing conformation with bound H_2DIDS. Simulations are performed in the absence of H_2DIDS with the goal of visualizing the outward open state of Band 3. Simulations are performed in the presence of NaCl. It may therefore be possible to visualize the position and dynamics of chloride ions during the simulations. Of particular interest would be the detection of immobilized chloride ion located at the anion-binding site. Our simulations with UraA revealed a novel closed state of the protein in the absence of substrate. Removing H_2DIDS creates a temporary vacuum in the protein that can be filled with water or by a conformational change in the protein, perhaps forming an intermediate closed state in the transport cycle.

16. Future Perspectives

Determination of the crystal structure of the Band 3 membrane domain is another major milestone on the long and winding road to understanding the mechanism of action of this transport protein and how mutations linked to human disease affect the ability of it to fold properly and be functionally expressed at the cell surface. However, we are not yet at our final destination. Indeed, the Band 3 structure is but another major way station that leads to many different roads. One road leads to homology modeling and structural studies of other members of the SLC4 bicarbonate transport family. A second road leads to the study of site-directed mutants of Band 3 guided by the crystal structure, sharply focused on the mechanism of transport. Band 3 operates in a membrane and is influenced by surrounding lipids like cholesterol [265, 269]. MD simulations of Band 3 in a lipid bilayer (Fig. 18) can be used to study this membrane protein in a more native environment than detergent micelles. We still need a structural model of full length Band 3, to explore interactions that occur between the two domains, especially important in regulating the activity of other members of the SLC4 family like AE2 and AE3. The available crystal structure of Band 3 is of an outward-facing conformation, covalently modified by H_2DIDS. An inward-facing form would reveal the second key state of the transport protein and would provide clues as to the nature of conformational transitions that must occur to move from one state to the other, driven by anion binding to lower the energy barrier between the two states. Ideally, a combination of structural and computational biology will allow the production of a 10 μs movie to show the catalytic cycle of Band 3 in molecular action.

Abbreviations: AE1, anion exchanger 1; BLM, basolateral membrane; CAII, carbonic anhydrase II; cdAE1, cytosolic domain of AE1; dRTA, distal renal tubular acidosis; EC, extracellular loop; ER, endoplasmic reticulum; GPA, Glycophorin A; HS, hereditary spherocytosis; HSt, hereditary stomatocytosis; HT, high transport; kAE1, kidney anion exchanger 1; MD, molecular dynamics; mdAE1, membrane domain of AE1; SLC, solute carrier; SAO, Southeast Asian Ovalocytosis; SLC, solute carrier; TM, transmembrane.

Figure Legends

Fig. 1. Role of the Band 3 Cl^-/HCO_3^- anion exchanger 1 (AE1) in red blood cells. In the tissues, carbon dioxide (CO_2) that diffuses through the red blood cell membrane (represented as red oval) or enters via aquaporin channels is rapidly converted with water to bicarbonate and a proton by the action of carbonic anhydrase II. The bicarbonate is transported out of the cell in exchange for chloride and the proton is buffered by hemoglobin, which lowers its affinity for oxygen delivering it to the tissues. In the lungs, the system reverses (not shown); bicarbonate enters the cell in exchange for chloride via the anion exchanger, bicarbonate and a proton are converted to carbon dioxide and water by carbonic anhydrase II, the carbon dioxide then diffuses out of the red blood cell and is expired by the lungs.

Fig. 2. Linear topology of human Band 3 with 14 TM helices coloured from N-terminus (blue) to C-terminus (red). The cytosolic surface is at the bottom. The residues located at the beginning and end of each helix are given. Note that most of the helices, except TM3 and 10, are longer than the 20 residues minimally required to span the 30 Å thick hydrophobic interior of a lipid bilayer. Indicated are the single site of N-glycosylation at N642 and the positions of blood group antigens (italics) within loops on the extracellular side of the membrane. Also indicated are the positions of the two H_2DIDS reactive lysines in TM5 (K539) and TM13 (K851) as well as an intracellular trypsin-sensitive site (K743). The active site residue (E681) in TM8 is indicated. Note again that TM3 and 10 consist of half helices preceded by extended chains. Helices labeled H1-H6 are within hydrophilic sequences that connecting TM segments.

Fig. 3. (A) Ribbon representation of the human Band 3 monomer as viewed in the plane of the membrane, coloured from blue at the N-terminus to red at the C-terminus. The cytosolic surface is at the bottom. The protein begins with an amphipathic helix (H1) followed by 14 transmembrane segments (1-14). Note that TM3 and TM10 each consist of half-helices with their N-termini facing each other in the center of the protein forming the anion-binding site. (B) Topology diagram of human Band 3 with TM helices coloured blue from N-terminal to red to the C-terminal. α helices are represented by cylinders, shown in proportion to their length. The star indicates the substrate-binding site between the amino-termini of TM3 and 10. AE1 is inhibited by the H_2DIDS molecule that crosslinks TM helices 5 and 13. Amphipathic helices (H1-6) on the protein surface are coloured in grey. The protein is arranged in two domains: a core domain (left) consisting of TM1, 2, 3, 4, 8, 9, 10 and 11 that contains the anion binding site and a gate domain (right) consisting of TM 5, 6, 7, 12, 13 and 14. The single site of N-glycosylation is located at Asn642, in a long disordered region linking TM7 and 8.

Fig. 4. (A) Dimeric structure of the membrane domain of human Band 3. Transmembrane segments are labeled 1-14 in one subunit and 1'-14' in the second subunit and coloured from N-terminus (dark blue) to C-terminus (red). The cytosolic surface is at the bottom. Helices running parallel to the membrane are labeled H1-H6 and H1'-H6' respectively. The cytosolic side of the membrane is on the bottom and the extracellular side on the top. Note the positions of TM6 (6') and TM7 (7') at the dimer interface. (B) Band 3 dimer as viewed from the intracellular side. The dimerization interface creates a funnel shape, narrowing to the extracellular side with closest contact between the ends of TM6. Also, the two sub-domains are visible in this view and consist of TM1-4 and 8-11 forming the core domain and TM5-7 and 12-14 forming the gate domain located at the dimer interface. Note also the amphipathic H1 (and H1') on the intracellular side

of the protein makes contact with the membrane surface and the ends of TM2, 4, 9 and 11 of the core domain.

Fig. 5. H_2DIDS inhibitor binding site in Band 3. (A) Ribbon representation of Band 3 coloured as above with the H_2DIDS inhibitor located in the cleft between the core domain and gate domain. (B) H_2DIDS is covalently bound to the residues K851 and K539, placing it external to the substrate recognition site and the residue E681 in TM8. (C) Transparent surface representation shows the position of H_2DIDS in Band 3, with R730 stabilizing one sulfonate facing down into the protein, while the other sulfonate faces up into solvent. Red shading indicates acidic regions and blue shading basic regions.

Fig. 6. Structure of the Band 3 anion binding site. (A) N-termini of the TM helices 3 (cyan) and 10 (brown) face each other with their positive dipoles creating an anion binding site. (B) The anion, indicated by the red gradient circle is located close to crossing point of the two extended sequences.

Fig. 7. The Band 3 active site. (A) View of active site in Band 3 from outside with H_2DIDS removed. Numbers indicate TMs. (B) Zoom-in of Band 3 active site located between the N-termini of TM3 and 10. E681 from TM8 faces towards the anion-binding site as does R730 in TM10. H_2DIDS-reactive K539 and K851 are located exterior to the anion-binding site, with the side chain of K851 located close to the side-chain of E681.

Fig. 8. Comparison of substrate binding in Band 3 and UraA. (A) Anion binding site in Band 3 (A) (yellow) and (B) the uracil binding site (cyan) are illustrated with E681 in Band 3 positioned at the same location as E241 in UraA and R730 in Band 3 at the same location as E290 in UraA. Arg730 may play a direct role in anion binding, while Glu681 may occupy the anion-binding site, acting as a molecular gate.

Fig. 9. Ribbon diagram representation of two inverted repeat modules of Band 3. (A) TM 1-7 and (B) TM 8-14 exhibit a similar fold with TM1 equivalent to TM8, TM2 to TM9, TM3 to TM10, etc. but running in opposite directions.

Fig. 10. Superposition of the inverted repeat occurring in each of the inverted repeats. (A) TM 1/8, 2/9, 4/11, 3/10 superimpose in one component and (B) TM 5/12, 6/13, 7/14 in the second component. Note that only one of the sub-domains can be overlaid: A, core domains overlaid; B, gate domains overlaid) and that the other is in a different conformational state.

Fig. 11. Superposition of Band 3 (outward conformation) and Band 3 modelled on UraA (inward conformation). Ribbon diagram of the superimposition of the outward open conformation of Band 3 (yellow) and the inward open conformation of Band 3 modelled on the Uracil transporter (UraA) (cyan) from the cytoplasmic view. The core domain (marked by red dashed line) of both structures, including the TM helices 1, 2, 3, 4, 8, 9, 10 and 11, superimpose whereas the gate domain (marked by blue dashed line), including the TM 5, 6, 7, 12, 13 and 14, adopt different conformations defining the outward (yellow) and inward (cyan) conformations of Band 3.

Fig. 12. Location of the SAO deletion in Band 3 structure. Ribbon representation of the human Band 3 monomer as viewed in the plane of the membrane, coloured from blue at the N-terminus

to red at the C-terminus. The deletion region (coloured black) removes a turn that connects H1 to TM1, removing a critical bend between the two helical segments and a portion of TM1.

Fig. 13. Location of hereditary stomatocytosis mutations in Band 3. A, view from side; B, view from cytosolic surface. Note that most mutations are located near the active site of the protein, including within TM10.

Fig. 14. Location of hereditary spherocytosis mutations in Band 3. A, view from side; B, view from cytosolic surface. Note that most mutations are located near the ends of TM segments.

Fig. 15. Location of distal renal tubular acidosis mutations in Band 3. A, view from side; B, view from cytosolic surface. Note that most mutations are located near the ends of TM segments.

Fig. 16. Models of human SLC4A2 (AE2), SLC4A3 (AE3) and SLC4A4 (NBCe1) based on Phyre2 threading using the crystal structure of Band 3 as a template. The amino acid sequences of the membrane domains of SLC4A2, 3, 4 are 75%, 69% and 45% identical to Band 3 (SLC4A1) and have the same predicted 14 TM fold. Top, zoom-in of outside surface of protein; middle, side-view of SLC4A2, 3 and 4; Bottom, zoom-in of cytosolic loops showing putative β-hairpin in AE2 (magenta) and short helix in AE3 (green) connecting TM10 and 11.

Fig. 17. The human NBCe1 active site. (A) View of active site in NBCe1 from outside. TMs are numbered and coloured from blue at the N-terminus to red at the C-terminus (B) Zoom-in of NBCe1 active site located between the N-termini of TM3 and 10. D799 from TM8 is located in the same position as E681 in Band 3 and faces towards the anion-binding site as does I847 in TM10, which is in the same position as R730 in Band 3. We hypothesize that Asp799 provides the sodium ion-binding site as it is conserved in all NBCs.

Fig. 18. Simulation of Band 3 in a POPC lipid bilayer, generated by molecular dynamics. (A) Snapshot from the end of one of the five simulations performed with Band 3 dimer in a POPC bilayer. Each subunit is colored using the rainbow color scheme from blue to red and the positions of the lipid phosphate groups shown as grey spheres. (B) Normalized average (over all repeat simulations) number of contacts between Band 3 and the lipid phosphate groups. Note that for this histogram the number of contacts of the two Band 3 subunits were added together. In the histogram, 0 means no/low number of contacts whereas 1 means maximal number of contacts observed. Note that the N-terminal amphipathic helix (H1, V383-F401) has numerous contacts with lipids as do a number (but not all) of the loops connecting TM segments including the long N-glycosylated segment F623-I661) and residues within helices H2-5. The residues forming the highest number of contacts with the lipid phosphate groups are arginine, lysine and tryptophan.

Table 1. Band 3 Mutations and Blood Group Antigens			
Mutation	**Name**	**Structural Context**	**References**
Band 3 Memphis			
K56E	Memphis	N-terminal mutation. Altered mobility on SDS gels.	[11, 12]
Diego (Di) Blood Group Antigens			
P854L	Memphis II Di1	EC7. Altered DIDS reactivity	[124]
R432W	ELO Di18	EC1	[20]
E480K	Froese FR+ Di20	EC2	[270]
P548L	Rba Di6	EC3	[19]
K551N	Tra Di19	EC3	[19]
T552I	Warrior Di7	EC3	[18]
Y555H	VanVugt, Vga	EC3	[20]
V557M	Wda Di5	EC3	[19, 271]
P561S	BOW	EC3	[20]
G565A	Wulfsberg (Wu)	EC3	[20, 272]
P566S	In Di17	EC3	
P566A	Di18	EC3	

N569K	Bishop (Bpa) Di10	EC3	[20]
R646Q	Swan SW+ Di14	EC4	[273]
R646W	Swan SW+ Di14	EC4	[273]
R656C	Hughes (Hga) Di12	EC4	[20]
R656H	Moen (Moa) Di11	EC4	[20]
R656W	Di21	EC4	
E658K	Wright, $Wra^{+}b$ $Di3^{-}$	EC4. Interaction with GPA required	[178]
Band 3 High Transport (HT)			
P868L	Band 3 HT	In middle of TM14. Higher V_{max} for transport, altered DIDS reactivity	[191]
Southeast Asian Ovalocytosis (SAO)			
Del400-408	Band 3 SAO	Removes bend proximal to TM1,including Pro403. Misfolded and inactive protein, localized to ER in transfected cells, present in red cell membrane as heterodimer	[22, 274-276]

Table 2. Hereditary Stomatocytosis and other Mutants Inducing a Cation Leak			
Mutation	**Red Cell Cation Leak Fold Increase Over Normal**	**Structural Context [3]**	**References [23]**
L687P (HSt)	7-8	Near C-terminus of TM8, packs against TM3 and 10. TM8 is at interface of care and gate domain.	[200, 201]
D705Y (HS)	8	At N-terminus of TM9. In contact with loop connecting TM2 and 3. Also causes HS.	[200, 201]
R730C (HSt)	6	Near N-terminus of TM10. Essential residue for transport that may play a direct role in anion binding.	[202]
S731P (HSt)	30-87	Near N-terminus of TM10, near anion binding site. Proline could destabilize helix.	[200, 201]
H734R (HSt)	87-94	Near C-terminus of TM10. Essential residue for transport.	[200, 201]
E758K (HS & HSt)	N/D	In cytosolic loop near N-terminus of TM11 and interacts with loop connecting TM8 and 9. Cation flux may be through alternative pathway.	[203]
R760Q (HS)	4-6	At N-terminus of TM11 on cytosolic side of membrane interacting with H1, TM2 and loop connecting to TM3. HS Band 3 Prague II.	[200]
S762R (HSt)	7	Near N-terminus of TM11, interacts with His734 in TM10.	[277]
G796R (HSt)	13	Middle of TM12 close to TM5. May affect helix-helix packing by introduction of charged residue.	[204]

Table 3. Hereditary Spherocytosis (HS) Mutants			
Mutation	**Name**	**Structural Context**	**References**
G455E	Prague V	Gly455 is helix-terminating residue located at the end of the TM 2 helix. In contrast, glutamate is an excellent helix former and might extend the helix and introduces a charged residue at this position.	[24]
C479W	Edmonton	Cys479 is located one turn before the end of the helix in TM3, which terminates at Gly483. It faces inward towards TM4 and 8 and a large residue at this position could disrupt protein packing. Tryptophan residues are often found at the membrane interface and could move TM3 towards the membrane surface during biosynthesis, thereby affected protein folding.	[278]
V488M	Coimbra	V488 is located within the first turn of the helix forming TM4 facing towards the extracellular loop preceding TM8.	[279]
R490C	Bicetre	R490 is located one turn from the beginning of the TM4 helix and faces towards the protein interior, particularly the loop region preceding TM10.	[280]
R518C	Dresden	R518 is located on the cytosolic side of membrane at the beginning of the TM5 helix facing the polar region at the end of TM12.	[281]
M663K	Tambaú	M663 is one turn into the long helix forming TM8 and introduces a positive charge that may affect the position of the helix during	[282]

		biosynthesis	
S667F	Courcouronnes	Ser667 is one turn further along the helix in TM8 than Met663. Both Met663 and Ser667 point back towards the extracellular ends of TM3/4.	[227]
L707P		Leu707 is near the cytosolic end of the TM9 helix and is close to the cytosolic end of TM4. Retained in the ER	[24, 205]
G714R	Okinawa	Gly714 is part of a glycine cluster within the short TM9 helix, packing against Gly494 of the TM4 helix. An arginine mutation would be major disruption of this helix-helix interaction	[283]
R760Q/W		Arg760 is located at the N-terminal end of TM11 and points towards the cytosolic end of TM2, perhaps stabilizing the negative helix dipole. Retained in the ER	[205]
G771D	Chur	Gly771 is located in a bend region at the end of TM11 connected to extracellular helix H3. An aspartate at this position may compromise formation of the bend in TM11 and place a charged residue in a non-polar environment.	[284]
I783N	Napoli II	Ile783 is located just before the beginning of TM11 and is replaced by a more polar residue.	[285]
R808C/H	Jablonec, Nara	Arg808 is located in a short cytosolic helical segment H4 (Gln804– Phe813) that joins TM11 and 12. Arg808 may interact with the polar head-groups of neighbouring lipids (Fig. 18).	[24, 205, 283]

H834P	Birmingham	His834 is located one turn into the helix that forms TM13 pointing back towards the cytosolic loop that connects TM12 and 13.	[24, 205]
T837M/A	Philadelphia, Tokyo	Thr837 is located on the side of the TM13 helix as is His834 one turn further along the helix. Both residue faces towards a short cytosolic helix that follows TM helix 12.	[24, 205, 286]
A858D		Ala858 is located one turn into the helix that forms TM14. Alanine is good helix former, while aspartate is a poor helix former. Thus, this mutation may destabilize the TM14 helix.	[287, 288]
R870W	Prague III	Arg870 is located one turn from the cytosolic end of the TM14 helix and may be involved in interactions with lipid head groups, helping to position this final helix in the membrane. Retained in the ER	[24, 205]

Table 4. Distal Renal Tubular Acidosis (dRTA) Mutations			
Mutation	**Type/Name**	**Structural Context**	**References**
C479W	Recessive, Edmonton	Near the end of TM3 (See HS description above). Retained in ER, also causes HS.	[278]
V488M	Recessive, Coimbra	N-terminal of TM4 helix. (See HS description above). Causes HS as well in the homozygous state.	[279]
G494S	Recessive	Gly494 is within TM4 and involved in helix packing.	[289]
E522K	Recessive	E522K mutation is a charge reversal. Glu522 is located at the first turn of N-terminal region of TM5 helix and faces towards to the cytosolic loop connecting TM13 and 14. 20% of normal level at the plasma membrane.	[290]
R589H/S/C	Dominant	Arg589 is located one helical turn in from the cytosolic end of the TM6 helix. The side-chain points directly towards to a cluster of hydroxyl groups donated by Thr798, Ser799 and Ser801 one turn away from the cytosolic end of TM12 helix. Retained in ER and rescued by blocking interaction with the ER chaperone calnexin.	[223, 225, 226, 291]
R602H	Recessive	Arg602 is located in the first helical turn of the N-terminal region of TM7 facing back toward the cytosolic loop connecting TM6 and 7. Basolateral localization.	(Cordat, unpublished results)
G609R	Dominant	Gly609 is located in a bend region in the middle of TM7 and an arginine substitution at this position is predicted to be	[213]

		very disruptive introducing a positive charge within a TM segment. Apical and basolateral targeting.	
S613F	Dominant	Ser613 is close to the bend within TM7 located at Pro611 and is packed close to TM1. A large non-polar substitution at this position would disrupt the bend and protein packing. Intracellular retention.	[223, 225, 291]
S667F	Recessive for incomplete dRTA	Ser667 is located two helical turns in from the extracellular N-terminal end of TM8. A hydrophobic substitution would affect the polarity of this region. Retained in the ER in MDCK cells.	[227]
G701D	Recessive	Gly701 is located in a hydrophilic loop connecting TM8 and 9 on the cytosolic side of the membrane. The trafficking of this mutant can be rescued by the co-expression of Glycophorin A. Localized to Golgi, normal transport in red cells, rescued by GPA.	[186, 225]
S773P	Recessive	Ser773 is located at a ~90° bend in TM helix 11 that connect to helix H3. A proline substitution would change the flexibility of this region. Impaired trafficking to cell surface.	[292]
DelV850	Recessive	Val850 is located in the last turn of TM13 helix. A deletion at this position would cause a rotation of the last two residues of the helical segment by 100° just before the turn into TM14 and would likely affect packing	[186]

		of TM13 with TM14. The next residue is the DIDS-reactive Lys851, which would now point away from the inhibitor site. Near normal transport in red cells.	
A858D	Mild Dominant	A858D (See HS description above). Causes incomplete dRTA.	[186]
A888L/D889X	Dominant	Truncation of C-terminal tail.	[293]
R901STOP	Dominant, Walton	Truncation of C-terminal tail. Near normal transport in red cells, mis-sorted to apical membrane, retained in ER in MDCK cells.	[223, 294, 295]
D905dup	Dominant	Insertion in C-terminal tail.	[289]
D905Gfs15	Dominant, Qingdoa	C-terminal tail. Insertion of single base results in frameshift and novel 15 amino acid C-terminal sequence to residue 919.	[296]
M909T	Dominant	C-terminal tail. Mis-localized to both apical and basolateral membranes. Highlights importance of C-terminal tail in targeting in polarized cells.	[215]

References

[1] R.A.F. Reithmeier, A membrane metabolon linking carbonic anhydrase with chloride/bicarbonate anion exchangers, Blood Cells Molecules and Diseases 27 (2001) 85-89.

[2] D. Sterling, R.A. Reithmeier, J.R. Casey, A transport metabolon. Functional interaction of carbonic anhydrase II and chloride/bicarbonate exchangers, J Biol Chem 276 (2001) 47886-47894.

[3] T. Arakawa, T. Kobayashi-Yurugi, Y. Alguel, H. Iwanari, H. Hatae, M. Iwata, Y. Abe, T. Hino, C. Ikeda-Suno, H. Kuma, D. Kang, T. Murata, T. Hamakubo, A.D. Cameron, T. Kobayashi, N. Hamasaki, S. Iwata, Crystal structure of the anion exchanger domain of human erythrocyte band 3, Science 350 (2015) 680-684.

[4] G. Fairbanks, T.L. Steck, D.F. Wallach, Electrophoretic analysis of the major polypeptides of the human erythrocyte membrane, Biochemistry 10 (1971) 2606-2617.

[5] T.L. Steck, B. Ramos, E. Strapazon, Proteolytic dissection of band 3, the predominant transmembrane polypeptide of the human erythrocyte membrane, Biochemistry 15 (1976) 1153-1161.

[6] T.L. Steck, Cross-linking the major proteins of the isolated erythrocyte membrane, J Mol Biol 66 (1972) 295-305.

[7] R.A.F. Reithmeier, Fragmentation of the Band-3 Polypeptide from Human-Erythrocyte Membranes - Size and Detergent Binding of the Membrane-Associated Domain, Journal of Biological Chemistry 254 (1979) 3054-3060.

[8] Z.I. Cabantchik, A. Rothstein, Membrane proteins related to anion permeability of human red blood cells. I. Localization of disulfonic stilbene binding sites in proteins involved in permeation, J Membr Biol 15 (1974) 207-226.

[9] L. Zaki, H. Fasold, B. Schuhmann, H. Passow, Chemical modification of membrane proteins in relation to inhibition of anion exchange in human red blood cells, J Cell Physiol 86 (1975) 471-494.

[10] M.K. Ho, G. Guidotti, A membrane protein from human erythrocytes involved in anion exchange, J Biol Chem 250 (1975) 675-683.

[11] T.J. Mueller, M. Morrison, Detection of a variant of protein 3, the major transmembrane protein of the human erythrocyte, J Biol Chem 252 (1977) 6573-6576.

[12] P. Jarolim, H.L. Rubin, S. Zhai, K.E. Sahr, S.C. Liu, T.J. Mueller, J. Palek, Band 3 Memphis: a widespread polymorphism with abnormal electrophoretic mobility of erythrocyte band 3 protein caused by substitution AAG----GAG (Lys----Glu) in codon 56, Blood 80 (1992) 1592-1598.

[13] R.R. Kopito, H.F. Lodish, Primary structure and transmembrane orientation of the murine anion exchange protein, Nature 316 (1985) 234-238.

[14] M.J. Tanner, P.G. Martin, S. High, The complete amino acid sequence of the human erythrocyte membrane anion-transport protein deduced from the cDNA sequence, Biochem J 256 (1988) 703-712.

[15] S.E. Lux, K.M. John, R.R. Kopito, H.F. Lodish, Cloning and characterization of band 3, the human erythrocyte anion-exchange protein (AE1), Proc Natl Acad Sci U S A 86 (1989) 9089-9093.

[16] F.C. Brosius, 3rd, S.L. Alper, A.M. Garcia, H.F. Lodish, The major kidney band 3 gene transcript predicts an amino-terminal truncated band 3 polypeptide, J Biol Chem 264 (1989) 7784-7787.

[17] F.A. Spring, L.J. Bruce, D.J. Anstee, M.J. Tanner, A red cell band 3 variant with altered stilbene disulphonate binding is associated with the Diego (Dia) blood group antigen, Biochem J 288 (Pt 3) (1992) 713-716.
[18] P. Jarolim, J.L. Murray, H.L. Rubin, G. Coghlan, T. Zelinski, A Thr552 -->Ile substitution in erythroid band 3 gives rise to the Warrior blood group antigen, Transfusion 37 (1997) 398-405.
[19] P. Jarolim, J.L. Murray, H.L. Rubin, E. Smart, J.M. Moulds, Blood group antigens Rb(a), Tr(a), and Wd(a) are located in the third ectoplasmic loop of erythroid band 3, Transfusion 37 (1997) 607-615.
[20] P. Jarolim, H.L. Rubin, D. Zakova, J. Storry, M.E. Reid, Characterization of seven low incidence blood group antigens carried by erythrocyte band 3 protein, Blood 92 (1998) 4836-4843.
[21] M.J. Tanner, L. Bruce, P.G. Martin, D.M. Rearden, G.L. Jones, Melanesian hereditary ovalocytes have a deletion in red cell band 3, Blood 78 (1991) 2785-2786.
[22] P. Jarolim, J. Palek, D. Amato, K. Hassan, P. Sapak, G.T. Nurse, H.L. Rubin, S. Zhai, K.E. Sahr, S.C. Liu, Deletion in erythrocyte band 3 gene in malaria-resistant Southeast Asian ovalocytosis, Proc Natl Acad Sci U S A 88 (1991) 11022-11026.
[23] D. Barneaud-Rocca, B. Pellissier, F. Borgese, H. Guizouarn, Band 3 missense mutations and stomatocytosis: insight into the molecular mechanism responsible for monovalent cation leak, Int J Cell Biol 2011 (2011) 136802.
[24] P. Jarolim, J.L. Murray, H.L. Rubin, W.M. Taylor, J.T. Prchal, S.K. Ballas, L.M. Snyder, L. Chrobak, W.D. Melrose, V. Brabec, J. Palek, Characterization of 13 novel band 3 gene defects in hereditary spherocytosis with band 3 deficiency, Blood 88 (1996) 4366-4374.
[25] F.E. Karet, K.E. Finberg, A. Nayir, A. Bakkaloglu, S. Ozen, S.A. Hulton, S.A. Sanjad, E.A. Al-Sabban, J.F. Medina, R.P. Lifton, Localization of a gene for autosomal recessive distal renal tubular acidosis with normal hearing (rdRTA2) to 7q33-34, Am J Hum Genet 65 (1999) 1656-1665.
[26] P.T. Yenchitsomanus, S. Kittanakom, N. Rungroj, E. Cordat, R.A. Reithmeier, Molecular mechanisms of autosomal dominant and recessive distal renal tubular acidosis caused by SLC4A1 (AE1) mutations, J Mol Genet Med 1 (2005) 49-62.
[27] M.L. Jennings, M.P. Anderson, Chemical modification and labeling of glutamate residues at the stilbenedisulfonate site of human red blood cell band 3 protein, J Biol Chem 262 (1987) 1691-1697.
[28] M.L. Jennings, J.S. Smith, Anion-proton cotransport through the human red blood cell band 3 protein. Role of glutamate 681, J Biol Chem 267 (1992) 13964-13971.
[29] D. Zhang, A. Kiyatkin, J.T. Bolin, P.S. Low, Crystallographic structure and functional interpretation of the cytoplasmic domain of erythrocyte membrane band 3, Blood 96 (2000) 2925-2933.
[30] V. Shnitsar, J. Li, X. Li, C. Calmettes, A. Basu, J.R. Casey, T.F. Moraes, R.A. Reithmeier, A Substrate Access Tunnel in the Cytosolic Domain is not an Essential Feature of the SLC4 Family of Bicarbonate Transporters, J Biol Chem (2013).
[31] D.N. Wang, W. Kuhlbrandt, V.E. Sarabia, R.A.F. Reithmeier, 2-Dimensional Structure of the Membrane Domain of Human Band-3, the Anion Transport Protein of the Erythrocyte-Membrane, Embo Journal 12 (1993) 2233-2239.
[32] T.L. Steck, J.J. Koziarz, M.K. Singh, G. Reddy, H. Kohler, Preparation and analysis of seven major, topographically defined fragments of band 3, the predominant

transmembrane polypeptide of human erythrocyte membranes, Biochemistry 17 (1978) 1216-1222.
[33] R.A.F. Reithmeier, S.L. Chan, M. Popov, Structure of the erythrocyte Band 3 anion exchanger, in: W.N. Konings, H.R. Kaback, J.S. Lolkema (Eds.), Transport processes in eukaryotic and prokaryotic organisms, vol. 2, Elsevier Science B. V., Amsterdam, 1996, pp. 281-309.
[34] S. Grinstein, S. Ship, A. Rothstein, Anion transport in relation to proteolytic dissection of band 3 protein, Biochim Biophys Acta 507 (1978) 294-304.
[35] D.N. Wang, V.E. Sarabia, R.A.F. Reithmeier, W. Kuhlbrandt, 3-Dimensional Map of the Dimeric Membrane Domain of the Human Erythrocyte Anion-Exchanger, Band-3, Embo Journal 13 (1994) 3230-3235.
[36] T. Yamaguchi, Y. Ikeda, Y. Abe, H. Kuma, D. Kang, N. Hamasaki, T. Hirai, Structure of the membrane domain of human erythrocyte anion exchanger 1 revealed by electron crystallography, J Mol Biol 397 (2010) 179-189.
[37] T. Hirai, N. Hamasaki, T. Yamaguchi, Y. Ikeda, Topology models of anion exchanger 1 that incorporate the anti-parallel V-shaped motifs found in the EM structure, Biochem Cell Biol 89 (2011) 148-156.
[38] M.J. Lemieux, R.A.F. Reithmeier, D.N. Wang, Importance of detergent and phospholipid in the crystallization of the human erythrocyte anion-exchanger membrane domain, Journal of Structural Biology 137 (2002) 322-332.
[39] T. Hino, S. Iwata, T. Murata, Generation of functional antibodies for mammalian membrane protein crystallography, Curr Opin Struct Biol 23 (2013) 563-568.
[40] P.S. Low, D. Zhang, J.T. Bolin, Localization of mutations leading to altered cell shape and anion transport in the crystal structure of the cytoplasmic domain of band 3, Blood Cells Mol Dis 27 (2001) 81-84.
[41] P.S. Low, Structure and function of the cytoplasmic domain of band 3: center of erythrocyte membrane-peripheral protein interactions, Biochim Biophys Acta 864 (1986) 145-167.
[42] M.J. Tanner, Advances in the molecular biology of erythrocyte antigens, Curr Opin Hematol 2 (1995) 139-145.
[43] Y. Abe, T. Chaen, X.R. Jin, T. Hamasaki, N. Hamasaki, Mass spectrometric analyses of transmembrane proteins in human erythrocyte membrane, J Biochem 136 (2004) 97-106.
[44] D. Kang, K. Okubo, N. Hamasaki, N. Kuroda, H. Shiraki, A structural study of the membrane domain of band 3 by tryptic digestion. Conformational change of band 3 in situ induced by alkali treatment, J Biol Chem 267 (1992) 19211-19217.
[45] M. Popov, L.Y. Tam, J. Li, R.A.F. Reithmeier, Mapping the ends of transmembrane segments in a polytopic membrane protein - Scanning N-glycosylation mutagenesis of extracytosolic loops in the anion exchanger, Band 3, Journal of Biological Chemistry 272 (1997) 18325-18332.
[46] J.C. Cheung, J. Li, R.A.F. Reithmeier, Topology of transmembrane segments 1-4 in the human chloride/bicarbonate anion exchanger 1 (AE1) by scanning N-glycosylation mutagenesis, Biochemical Journal 390 (2005) 137-144.
[47] K. Ota, M. Sakaguchi, N. Hamasaki, K. Mihara, Assessment of topogenic functions of anticipated transmembrane segments of human band 3, J Biol Chem 273 (1998) 28286-28291.

[48] K. Ota, M. Sakaguchi, N. Hamasaki, K. Mihara, Membrane integration of the second transmembrane segment of band 3 requires a closely apposed preceding signal-anchor sequence, J Biol Chem 275 (2000) 29743-29748.
[49] K. Oikawa, D.M. Lieberman, R.A.F. Reithmeier, Conformation and Stability of the Anion Transport Protein of Human-Erythrocyte Membranes, Biochemistry 24 (1985) 2843-2848.
[50] F. Lu, S. Li, Y. Jiang, J. Jiang, H. Fan, G. Lu, D. Deng, S. Dang, X. Zhang, J. Wang, N. Yan, Structure and mechanism of the uracil transporter UraA, Nature 472 (2011) 243-246.
[51] E. Cordat, R.A.F. Reithmeier, Structure, function, and trafficking of SLC4 and SLC26 anion transporters, in: M.O. Bevensee (Ed.), Current Topics in Membranes, vol. 73, Elsevier Inc., Amsterdam, 2014, pp. 1-67.
[52] R.A.F. Reithmeier, T.F. Moraes, Solute carriers keep on rockin', Nature Structural & Molecular Biology 22 (2015) 752-754.
[53] M.L. Jennings, Oligomeric structure and the anion transport function of human erythrocyte band 3 protein, J Membr Biol 80 (1984) 105-117.
[54] J.R. Casey, R.A. Reithmeier, Analysis of the oligomeric state of Band 3, the anion transport protein of the human erythrocyte membrane, by size exclusion high performance liquid chromatography. Oligomeric stability and origin of heterogeneity, J Biol Chem 266 (1991) 15726-15737.
[55] H.M. Van Dort, R. Moriyama, P.S. Low, Effect of band 3 subunit equilibrium on the kinetics and affinity of ankyrin binding to erythrocyte membrane vesicles, J Biol Chem 273 (1998) 14819-14826.
[56] S.W. Pimplikar, R.A.F. Reithmeier, Affinity-Chromatography of Band-3, the Anion Transport Protein of Erythrocyte-Membranes, Journal of Biological Chemistry 261 (1986) 9770-9778.
[57] S.W. Pimplikar, R.A.F. Reithmeier, Studies on the Interaction of Matrix-Bound Inhibitor with Band-3, the Anion Transport Protein of Human-Erythrocyte Membranes, Biochimica Et Biophysica Acta 942 (1988) 253-261.
[58] I.G. Macara, L.C. Cantley, Interactions between transport inhibitors at the anion binding sites of the band 3 dimer, Biochemistry 20 (1981) 5095-5105.
[59] I.G. Macara, L.C. Cantley, Mechanism of anion exchange across the red cell membrane by band 3: interactions between stilbenedisulfonate and NAP-taurine binding sites, Biochemistry 20 (1981) 5695-5701.
[60] J.A. Quilty, E. Cordat, R.A. Reithmeier, Impaired trafficking of human kidney anion exchanger (kAE1) caused by hetero-oligomer formation with a truncated mutant associated with distal renal tubular acidosis, Biochem J 368 (2002) 895-903.
[61] P.T. Yenchitsomanus, N. Sawasdee, A. Paemanee, T. Keskanokwong, S. Vasuvattakul, S. Bejrachandra, W. Kunachiwa, S. Fucharoen, P. Jittphakdee, W. Yindee, C. Promwong, Anion exchanger 1 mutations associated with distal renal tubular acidosis in the Thai population, J Hum Genet 48 (2003) 451-456.
[62] J.V. Staros, D.G. Morgan, D.R. Appling, A membrane-impermeant, cleavable cross-linker. Dimers of human erythrocyte band 3 subunits cross-linked at the extracytoplasmic membrane face, J Biol Chem 256 (1981) 5890-5893.
[63] M.L. Jennings, J.S. Nicknish, Localization of a site of intermolecular cross-linking in human red blood cell band 3 protein, J Biol Chem 260 (1985) 5472-5479.

[64] J.M. Salhany, R.L. Sloan, K.A. Cordes, In situ cross-linking of human erythrocyte band 3 by bis(sulfosuccinimidyl)suberate. Evidence for ligand modulation of two alternate quaternary forms: covalent band 3 dimers and noncovalent tetramers formed by the association of two covalent dimers, J Biol Chem 265 (1990) 17688-17693.
[65] S. Lourdel, T. Grand, J. Burgos, W. Gonzalez, F.V. Sepulveda, J. Teulon, ClC-5 mutations associated with Dent's disease: a major role of the dimer interface, Pflugers Arch 463 (2012) 247-256.
[66] J. Sun, J.R. Bankston, J. Payandeh, T.R. Hinds, W.N. Zagotta, N. Zheng, Crystal structure of the plant dual-affinity nitrate transporter NRT1.1, Nature 507 (2014) 73-77.
[67] J.L. Robertson, L. Kolmakova-Partensky, C. Miller, Design, function and structure of a monomeric ClC transporter, Nature 468 (2010) 844-847.
[68] Z.I. Cabantchik, P.A. Knauf, A. Rothstein, The anion transport system of the red blood cell. The role of membrane protein evaluated by the use of 'probes', Biochim Biophys Acta 515 (1978) 239-302.
[69] J.J. Falke, S.I. Chan, Molecular mechanisms of band 3 inhibitors. 1. Transport site inhibitors, Biochemistry 25 (1986) 7888-7894.
[70] J.J. Falke, S.I. Chan, Molecular mechanisms of band 3 inhibitors. 2. Channel blockers, Biochemistry 25 (1986) 7895-7898.
[71] J.J. Falke, S.I. Chan, Molecular mechanisms of band 3 inhibitors. 3. Translocation inhibitors, Biochemistry 25 (1986) 7899-7906.
[72] A. Rao, P. Martin, R.A.F. Reithmeier, L.C. Cantley, Location of the Stilbenedisulfonate Binding-Site of the Human-Erythrocyte Anion-Exchange System by Resonance Energy-Transfer, Biochemistry 18 (1979) 4505-4516.
[73] C. Landoltmarticorena, J.R. Casey, R.A.F. Reithmeier, Transmembrane Helix-Helix Interactions and Accessibility of H2dids on Labeled Band-3, the Erythrocyte Anion-Exchange Protein, Molecular Membrane Biology 12 (1995) 173-182.
[74] D.M. Lieberman, R.A.F. Reithmeier, Characterization of the Stilbenedisulfonate Binding-Site of the Band-3 Polypeptide of Human-Erythrocyte Membranes, Biochemistry 22 (1983) 4028-4033.
[75] K. Okubo, D. Kang, N. Hamasaki, M.L. Jennings, Red blood cell band 3. Lysine 539 and lysine 851 react with the same H2DIDS (4,4'-diisothiocyanodihydrostilbene-2,2'-disulfonic acid) molecule, J Biol Chem 269 (1994) 1918-1926.
[76] M.L. Jennings, H. Passow, Anion transport across the erythrocyte membrane, in situ proteolysis of band 3 protein, and cross-linking of proteolytic fragments by 4,4'-diisothiocyano dihydrostilbene-2,2'-disulfonate, Biochim Biophys Acta 554 (1979) 498-519.
[77] C. Landolt-Marticorena, K.A. Williams, C.M. Deber, R.A.F. Reithmeier, Nonrandom Distribution of Amino-Acids in the Transmembrane Segments of Human Type-I Single Span Membrane-Proteins, Journal of Molecular Biology 229 (1993) 602-608.
[78] Y. Okawa, J. Li, A. Basu, J.R. Casey, R.A. Reithmeier, Differential roles of tryptophan residues in the functional expression of human anion exchanger 1 (AE1, Band 3, SLC4A1), Mol Membr Biol 31 (2014) 211-227.
[79] P.A. Knauf, F.Y. Law, T.W. Leung, S.J. Atherton, Relocation of the disulfonic stilbene sites of AE1 (band 3) on the basis of fluorescence energy transfer measurements, Biochemistry 43 (2004) 11917-11931.

[80] A.M. Garcia, H.F. Lodish, Lysine 539 of human band 3 is not essential for ion transport or inhibition by stilbene disulfonates, J Biol Chem 264 (1989) 19607-19613.
[81] D. Bartel, H. Hans, H. Passow, Identification by site-directed mutagenesis of Lys-558 as the covalent attachment site of H2DIDS in the mouse erythroid band 3 protein, Biochim Biophys Acta 985 (1989) 355-358.
[82] P.G. Wood, H. Muller, M. Sovak, H. Passow, Role of Lys 558 and Lys 869 in substrate and inhibitor binding to the murine band 3 protein: a study of the effects of site-directed mutagenesis of the band 3 protein expressed in the oocytes of Xenopus laevis, J Membr Biol 127 (1992) 139-148.
[83] I.G. Macara, S. Kuo, L.C. Cantley, Evidence that inhibitors of anion exchange induce a transmembrane conformational change in band 3, J Biol Chem 258 (1983) 1785-1792.
[84] J.J. Falke, S.I. Chan, Evidence that anion transport by band 3 proceeds via a ping-pong mechanism involving a single transport site. A 35 Cl NMR study, J Biol Chem 260 (1985) 9537-9544.
[85] W.E. Wojcicki, A.H. Beth, Structural and binding properties of the stilbenedisulfonate sites on erythrocyte band 3: an electron paramagnetic resonance study using spin-labeled stilbenedisulfonates, Biochemistry 32 (1993) 9454-9464.
[86] R.A.F. Reithmeier, C.A. Pirraglia, D.M. Lieberman, J.R. Casey, A.W. F., Towards crystallization of band 3, in: N. Hamasaki, M.L. Jennings (Eds.), Anion transport protein of teh red blood cell membrane, Elsevier, Amsterdam, 1989, pp. 213-223.
[87] R. Dutzler, E.B. Campbell, M. Cadene, B.T. Chait, R. MacKinnon, X-ray structure of a ClC chloride channel at 3.0 A reveals the molecular basis of anion selectivity, Nature 415 (2002) 287-294.
[88] P. Bonar, H.P. Schneider, H.M. Becker, J.W. Deitmer, J.R. Casey, Three-Dimensional Model for the Human Cl/HCO Exchanger, AE1, by Homology to the E. coli ClC Protein, J Mol Biol (2013).
[89] D. Barneaud-Rocca, C. Etchebest, H. Guizouarn, Structural Model of the Anion Exchanger 1 (SLC4A1) and Identification of Transmembrane Segments Forming the Transport Site, J Biol Chem 288 (2013) 26372-26384.
[90] M.N. Chernova, L. Jiang, M. Crest, M. Hand, D.H. Vandorpe, K. Strange, S.L. Alper, Electrogenic sulfate/chloride exchange in Xenopus oocytes mediated by murine AE1 E699Q, J Gen Physiol 109 (1997) 345-360.
[91] S. Muller-Berger, D. Karbach, D. Kang, N. Aranibar, P.G. Wood, H. Ruterjans, H. Passow, Roles of histidine 752 and glutamate 699 in the pH dependence of mouse band 3 protein-mediated anion transport, Biochemistry 34 (1995) 9325-9332.
[92] D. Karbach, M. Staub, P.G. Wood, H. Passow, Effect of site-directed mutagenesis of the arginine residues 509 and 748 on mouse band 3 protein-mediated anion transport, Biochim Biophys Acta 1371 (1998) 114-122.
[93] X.R. Jin, Y. Abe, C.Y. Li, N. Hamasaki, Histidine-834 of human erythrocyte band 3 has an essential role in the conformational changes that occur during the band 3-mediated anion exchange, Biochemistry 42 (2003) 12927-12932.
[94] S. Muller-Berger, D. Karbach, J. Konig, S. Lepke, P.G. Wood, H. Appelhans, H. Passow, Inhibition of mouse erythroid band 3-mediated chloride transport by site-directed mutagenesis of histidine residues and its reversal by second site mutation of Lys 558, the locus of covalent H2DIDS binding, Biochemistry 34 (1995) 9315-9324.

[95] C. Miller, ClC chloride channels viewed through a transporter lens, Nature 440 (2006) 484-489.
[96] O. Jardetzky, Simple allosteric model for membrane pumps, Nature 211 (1966) 969-970.
[97] D. Liu, S.D. Kennedy, P.A. Knauf, Source of transport site asymmetry in the band 3 anion exchange protein determined by NMR measurements of external Cl- affinity, Biochemistry 35 (1996) 15228-15235.
[98] S. Grinstein, L. McCulloch, A. Rothstein, Transmembrane effects of irreversible inhibitors of anion transport in red blood cells. Evidence for mobile transport sites, J Gen Physiol 73 (1979) 493-514.
[99] J.J. Falke, K.J. Kanes, S.I. Chan, The minimal structure containing the band 3 anion transport site. A 35Cl NMR study, J Biol Chem 260 (1985) 13294-13303.
[100] J.J. Falke, K.J. Kanes, S.I. Chan, The kinetic equation for the chloride transport cycle of band 3. A 35Cl and 37Cl NMR study, J Biol Chem 260 (1985) 9545-9551.
[101] L.A. Kelley, S. Mezulis, C.M. Yates, M.N. Wass, M.J. Sternberg, The Phyre2 web portal for protein modeling, prediction and analysis, Nat Protoc 10 (2015) 845-858.
[102] H. Passow, Molecular aspects of band 3 protein-mediated anion transport across the red blood cell membrane, Rev Physiol Biochem Pharmacol 103 (1986) 61-203.
[103] S.L. Alper, Molecular physiology and genetics of Na+-independent SLC4 anion exchangers, J Exp Biol 212 (2009) 1672-1683.
[104] E. Cordat, J.R. Casey, Bicarbonate transport in cell physiology and disease, Biochem J 417 (2009) 423-439.
[105] M.F. Romero, C.M. Fulton, W.F. Boron, The SLC4 family of HCO 3 - transporters, Pflugers Arch 447 (2004) 495-509.
[106] A. Pushkin, I. Kurtz, SLC4 base (HCO3 -, CO3 2-) transporters: classification, function, structure, genetic diseases, and knockout models, Am J Physiol Renal Physiol 290 (2006) F580-599.
[107] M.F. Romero, Molecular pathophysiology of SLC4 bicarbonate transporters, Curr Opin Nephrol Hypertens 14 (2005) 495-501.
[108] L.K. Drickamer, Orientation of the band 3 polypeptide from human erythrocyte membranes. Identification of NH2-terminal sequence and site of carbohydrate attachment, J Biol Chem 253 (1978) 7242-7248.
[109] J.R. Casey, Y. Ding, R.R. Kopito, The role of cysteine residues in the erythrocyte plasma membrane anion exchange protein, AE1, J Biol Chem 270 (1995) 8521-8527.
[110] J.D. Groves, M.J. Tanner, Role of N-glycosylation in the expression of human band 3-mediated anion transport, Mol Membr Biol 11 (1994) 31-38.
[111] J.R. Casey, C.A. Pirraglia, R.A.F. Reithmeier, Enzymatic Deglycosylation of Human Band-3, the Anion Transport Protein of the Erythrocyte-Membrane - Effect on Protein-Structure and Transport-Properties, Journal of Biological Chemistry 267 (1992) 11940-11948.
[112] M. Popov, R.A.F. Reithmeier, Calnexin interaction with N-glycosylation mutants of a polytopic membrane glycoprotein, the human erythrocyte anion exchanger 1 (band 3), Journal of Biological Chemistry 274 (1999) 17635-17642.
[113] S.T. Patterson, R.A. Reithmeier, Cell surface rescue of kidney anion exchanger 1 mutants by disruption of chaperone interactions, J Biol Chem 285 (2010) 33423-33434.

[114] S.T. Patterson, J. Li, J.A. Kang, A. Wickrema, D.B. Williams, R.A. Reithmeier, Loss of specific chaperones involved in membrane glycoprotein biosynthesis during the maturation of human erythroid progenitor cells, J Biol Chem 284 (2009) 14547-14557.
[115] A.J. Pang, R.A. Reithmeier, Interaction of anion exchanger 1 and glycophorin A in human erythroleukaemic K562 cells, Biochem J 421 (2009) 345-356.
[116] R.C. Williamson, A.M. Toye, Glycophorin A: Band 3 aid, Blood Cells Mol Dis 41 (2008) 35-43.
[117] J.D. Groves, M.J. Tanner, Glycophorin A facilitates the expression of human band 3-mediated anion transport in Xenopus oocytes, J Biol Chem 267 (1992) 22163-22170.
[118] J.D. Groves, M.J. Tanner, The effects of glycophorin A on the expression of the human red cell anion transporter (band 3) in Xenopus oocytes, J Membr Biol 140 (1994) 81-88.
[119] M.T. Young, R. Beckmann, A.M. Toye, M.J. Tanner, Red-cell glycophorin A-band 3 interactions associated with the movement of band 3 to the cell surface, Biochem J 350 Pt 1 (2000) 53-60.
[120] K. Okubo, N. Hamasaki, K. Hara, M. Kageura, Palmitoylation of cysteine 69 from the COOH-terminal of band 3 protein in the human erythrocyte membrane. Acylation occurs in the middle of the consensus sequence of F--I-IICLAVL found in band 3 protein and G2 protein of Rift Valley fever virus, J Biol Chem 266 (1991) 16420-16424.
[121] J.C. Cheung, R.A.F. Reithmeier, Palmitoylation is not required for trafficking of human anion exchanger 1 to the cell surface, Biochemical Journal 378 (2004) 1015-1021.
[122] D. Kang, D. Karbach, H. Passow, Anion transport function of mouse erythroid band 3 protein (AE1) does not require acylation of cysteine residue 861, Biochim Biophys Acta 1194 (1994) 341-344.
[123] M.M. Kay, G.J. Bosman, G.J. Johnson, A.H. Beth, Band-3 polymers and aggregates, and hemoglobin precipitates in red cell aging, Blood Cells 14 (1988) 275-295.
[124] L.J. Bruce, D.J. Anstee, F.A. Spring, M.J. Tanner, Band 3 Memphis variant II. Altered stilbene disulfonate binding and the Diego (Dia) blood group antigen are associated with the human erythrocyte band 3 mutation Pro854-->Leu, J Biol Chem 269 (1994) 16155-16158.
[125] R.R. Kopito, H.F. Lodish, Structure of the murine anion exchange protein, J Cell Biochem 29 (1985) 1-17.
[126] Y. Kawano, K. Okubo, F. Tokunaga, T. Miyata, S. Iwanaga, N. Hamasaki, Localization of the pyridoxal phosphate binding site at the COOH-terminal region of erythrocyte band 3 protein, J Biol Chem 263 (1988) 8232-8238.
[127] M. Popov, J. Li, R.A.F. Reithmeier, Transmembrane folding of the human erythrocyte anion exchanger (AE1, Band 3) determined by scanning and insertional N-glycosylation mutagenesis, Biochemical Journal 339 (1999) 269-279.
[128] J.C. Cheung, R.A.F. Reithmeier, Scanning N-glycosylation mutagenesis of membrane proteins, Methods 41 (2007) 451-459.
[129] J. Fujinaga, X.B. Tang, J.R. Casey, Topology of the membrane domain of human erythrocyte anion exchange protein, AE1, J Biol Chem 274 (1999) 6626-6633.
[130] Q. Zhu, J.R. Casey, The substrate anion selectivity filter in the human erythrocyte Cl-/HCO3- exchange protein, AE1, J Biol Chem 279 (2004) 23565-23573.
[131] E.R. Geertsma, Y.N. Chang, F.R. Shaik, Y. Neldner, E. Pardon, J. Steyaert, R. Dutzler, Structure of a prokaryotic fumarate transporter reveals the architecture of the SLC26 family, Nat Struct Mol Biol 22 (2015) 803-808.

[132] Z.I. Cabantchik, A. Rothstein, Membrane proteins related to anion permeability of human red blood cells. II. Effects of proteolytic enzymes on disulfonic stilbene sites of surface proteins, J Membr Biol 15 (1974) 227-248.
[133] M.L. Jennings, M.F. Adams, Modification by papain of the structure and function of band 3, the erythrocyte anion transport protein, Biochemistry 20 (1981) 7118-7123.
[134] M.L. Jennings, M. Adams-Lackey, G.H. Denney, Peptides of human erythrocyte band 3 protein produced by extracellular papain cleavage, J Biol Chem 259 (1984) 4652-4660.
[135] J.D. Groves, M.J. Tanner, Co-expressed complementary fragments of the human red cell anion exchanger (band 3, AE1) generate stilbene disulfonate-sensitive anion transport, J Biol Chem 270 (1995) 9097-9105.
[136] J.D. Groves, L. Wang, M.J. Tanner, Functional reassembly of the anion transport domain of human red cell band 3 (AE1) from multiple and non-complementary fragments, FEBS Lett 433 (1998) 223-227.
[137] M.L. Jennings, M.P. Anderson, R. Monaghan, Monoclonal antibodies against human erythrocyte band 3 protein. Localization of proteolytic cleavage sites and stilbenedisulfonate-binding lysine residues, J Biol Chem 261 (1986) 9002-9010.
[138] N. Hamasaki, K. Okubo, H. Kuma, D. Kang, Y. Yae, Proteolytic cleavage sites of band 3 protein in alkali-treated membranes: fidelity of hydropathy prediction for band 3 protein, J Biochem 122 (1997) 577-585.
[139] T. Kanki, M. Sakaguchi, A. Kitamura, T. Sato, K. Mihara, N. Hamasaki, The tenth membrane region of band 3 is initially exposed to the luminal side of the endoplasmic reticulum and then integrated into a partially folded band 3 intermediate, Biochemistry 41 (2002) 13973-13981.
[140] K.C. Appell, P.S. Low, Evaluation of structural interdependence of membrane-spanning and cytoplasmic domains of band 3, Biochemistry 21 (1982) 2151-2157.
[141] H.M. Van Dort, P.S. Low, K.A. Cordes, L.M. Schopfer, J.M. Salhany, Calorimetric evidence for allosteric subunit interactions associated with inhibitor binding to band 3 transporter, J Biol Chem 269 (1994) 59-61.
[142] N. Hamasaki, H. Kuma, K. Ota, M. Sakaguchi, K. Mihara, A new concept in polytopic membrane proteins following from the study of band 3 protein, Biochem Cell Biol 76 (1998) 729-733.
[143] S.Q. Liu, P.A. Knauf, Lys-430, site of irreversible inhibition of band 3 Cl- flux by eosin-5-maleimide, is not at the transport site, Am J Physiol 264 (1993) C1155-1164.
[144] R.J. Pan, R.J. Cherry, The eosin-5-maleimide binding site on human erythrocyte band 3: investigation of membrane sidedness and location of charged residues by triplet state quenching, Biochemistry 37 (1998) 10238-10245.
[145] D. Liu, S.D. Kennedy, P.A. Knauf, 35Cl nuclear magnetic resonance line broadening shows that eosin-5-maleimide does not block the external anion access channel of band 3, Biophys J 69 (1995) 399-408.
[146] P.A. Knauf, N.M. Strong, J. Penikas, R.B. Wheeler, Jr., S.Q. Liu, Eosin-5-maleimide inhibits red cell Cl- exchange at a noncompetitive site that senses band 3 conformation, Am J Physiol 264 (1993) C1144-1154.
[147] H. Nanri, N. Hamasaki, S. Minakami, Affinity labeling of erythrocyte band 3 protein with pyridoxal 5-phosphate. Involvement of the 35,000-dalton fragment in anion transport, J Biol Chem 258 (1983) 5985-5989.

[148] Y. Kawano, N. Hamasaki, Isolation of a 5,300-dalton peptide containing a pyridoxal phosphate binding site from the 38,000-dalton domain of band 3 of human erythrocyte membranes, J Biochem 100 (1986) 191-199.
[149] S. Takazaki, Y. Abe, D. Kang, C. Li, X. Jin, T. Ueda, N. Hamasaki, The functional role of arginine 901 at the C-terminus of the human anion transporter band 3 protein, J Biochem 139 (2006) 903-912.
[150] R. Bohm, L. Zaki, Towards the localization of the essential arginine residues in the band 3 protein of human red blood cell membranes, Biochim Biophys Acta 1280 (1996) 238-242.
[151] K. Izuhara, K. Okubo, N. Hamasaki, Conformational change of band 3 protein induced by diethyl pyrocarbonate modification in human erythrocyte ghosts, Biochemistry 28 (1989) 4725-4728.
[152] D. Askin, G.B. Bloomberg, E.J. Chambers, M.J. Tanner, NMR solution structure of a cytoplasmic surface loop of the human red cell anion transporter, band 3, Biochemistry 37 (1998) 11670-11678.
[153] M.M. Kay, Molecular mapping of human band 3 aging antigenic sites and active amino acids using synthetic peptides, J Protein Chem 11 (1992) 595-602.
[154] L. Zaki, T. Julien, Anion transport in red blood cells and arginine-specific reagents. Interaction between the substrate-binding site and the binding site of arginine-specific reagents, Biochim Biophys Acta 818 (1985) 325-332.
[155] L. Zaki, R. Bohm, M. Merckel, Chemical labelling of arginyl-residues involved in anion transport mediated by human band 3 protein and some aspects of its location in the peptide chain, Cell Mol Biol (Noisy-le-grand) 42 (1996) 1053-1063.
[156] E. Betakis, G. Fritzsch, L. Zaki, Inhibition of anion transport in the human red blood cell membrane with para- and meta-methoxyphenylglyoxal, Biochim Biophys Acta 1110 (1992) 75-80.
[157] L. Zaki, Anion transport in red blood cells and arginine-specific reagents. The location of [14C]phenylglyoxal binding sites in the anion transport protein in the membrane of human red cells, FEBS Lett 169 (1984) 234-240.
[158] P.J. Bjerrum, J.O. Wieth, C.L. Borders, Jr., Selective phenylglyoxalation of functionally essential arginyl residues in the erythrocyte anion transport protein, J Gen Physiol 81 (1983) 453-484.
[159] E.M. Gartner, K. Liebold, B. Legrum, H. Fasold, H. Passow, Three different actions of phenylglyoxal on band 3 protein-mediated anion transport across the red blood cell membrane, Biochim Biophys Acta 1323 (1997) 208-222.
[160] R.A. Reithmeier, A. Rao, Reactive sulfhydryl groups of the band 3 polypeptide from human erythrocyte membranes. Identification of the sulfhydryl groups involved in Cu2+-o-phenanthroline cross-linking, J Biol Chem 254 (1979) 6151-6155.
[161] A. Rao, R.A. Reithmeier, Reactive sulfhydryl groups of the band 3 polypeptide from human erythroycte membranes. Location in the primary structure, J Biol Chem 254 (1979) 6144-6150.
[162] Q. Zhu, J.R. Casey, Topology of transmembrane proteins by scanning cysteine accessibility mutagenesis methodology, Methods 41 (2007) 439-450.
[163] X.B. Tang, J. Fujinaga, R. Kopito, J.R. Casey, Topology of the region surrounding Glu681 of human AE1 protein, the erythrocyte anion exchanger, J Biol Chem 273 (1998) 22545-22553.

[164] X.B. Tang, M. Kovacs, D. Sterling, J.R. Casey, Identification of residues lining the translocation pore of human AE1, plasma membrane anion exchange protein, J Biol Chem 274 (1999) 3557-3564.
[165] Q. Zhu, D.W. Lee, J.R. Casey, Novel topology in C-terminal region of the human plasma membrane anion exchanger, AE1, J Biol Chem 278 (2003) 3112-3120.
[166] X.B. Tang, J.R. Casey, Trapping of inhibitor-induced conformational changes in the erythrocyte membrane anion exchanger AE1, Biochemistry 38 (1999) 14565-14572.
[167] S.D. Wainwright, W.J. Mawby, M.J. Tanner, The membrane domain of the human erythrocyte anion transport protein. Epitope mapping of a monoclonal antibody defines the location of a cytoplasmic loop near the C-terminus of the protein, Biochem J 272 (1990) 265-268.
[168] M.M. Kay, G.J. Bosman, C. Lawrence, Functional topography of band 3: specific structural alteration linked to functional aberrations in human erythrocytes, Proc Natl Acad Sci U S A 85 (1988) 492-496.
[169] A.M. Taylor, Q. Zhu, J.R. Casey, Cysteine-directed cross-linking localizes regions of the human erythrocyte anion-exchange protein (AE1) relative to the dimeric interface, Biochem J 359 (2001) 661-668.
[170] A. Basu, S. Mazor, J.R. Casey, Distance measurements within a concatamer of the plasma membrane Cl(-)/HCO(3)(-) exchanger, AE1, Biochemistry 49 (2010) 9226-9240.
[171] P.A. Knauf, L.J. Spinelli, N.A. Mann, Flufenamic acid senses conformation and asymmetry of human erythrocyte band 3 anion transport protein, Am J Physiol 257 (1989) C277-289.
[172] E. Sabban, V. Marchesi, M. Adesnik, D.D. Sabatini, Erythrocyte membrane protein band 3: its biosynthesis and incorporation into membranes, J Cell Biol 91 (1981) 637-646.
[173] L.Y. Tam, T.W. Loo, D.M. Clarke, R.A.F. Reithmeier, Identification of an Internal Topogenic Signal Sequence in Human Band-3, the Erythrocyte Anion-Exchanger, Journal of Biological Chemistry 269 (1994) 32542-32550.
[174] J.D. Groves, M.J. Tanner, Topology studies with biosynthetic fragments identify interacting transmembrane regions of the human red-cell anion exchanger (band 3; AE1), Biochem J 344 Pt 3 (1999) 687-697.
[175] J.D. Groves, M.J. Tanner, Structural model for the organization of the transmembrane spans of the human red-cell anion exchanger (band 3; AE1), Biochem J 344 Pt 3 (1999) 699-711.
[176] L. Wang, J.D. Groves, W.J. Mawby, M.J. Tanner, Complementation studies with Co-expressed fragments of the human red cell anion transporter (Band 3; AE1). The role of some exofacial loops in anion transport, J Biol Chem 272 (1997) 10631-10638.
[177] J.D. Groves, L. Wang, M.J. Tanner, Complementation studies with co-expressed fragments of human red cell band 3 (AE1): the assembly of the anion-transport domain in xenopus oocytes and a cell-free translation system, Biochem J 332 (Pt 1) (1998) 161-171.
[178] L.J. Bruce, S.M. Ring, D.J. Anstee, M.E. Reid, S. Wilkinson, M.J. Tanner, Changes in the blood group Wright antigens are associated with a mutation at amino acid 658 in human erythrocyte band 3: a site of interaction between band 3 and glycophorin A under certain conditions, Blood 85 (1995) 541-547.
[179] J.R. Casey, D.M. Lieberman, R.A.F. Reithmeier, Purification and Characterization of Band-3 Protein, Methods in Enzymology 173 (1989) 494-512.

[180] J. Yu, T.L. Steck, Isolation and characterization of band 3, the predominant polypeptide of the human erythrocyte membrane, J Biol Chem 250 (1975) 9170-9175.
[181] M.T. Young, M.J. Tanner, Distinct regions of human glycophorin A enhance human red cell anion exchanger (band 3; AE1) transport function and surface trafficking, J Biol Chem 278 (2003) 32954-32961.
[182] H. Hassoun, T. Hanada, M. Lutchman, K.E. Sahr, J. Palek, M. Hanspal, A.H. Chishti, Complete deficiency of glycophorin A in red blood cells from mice with targeted inactivation of the band 3 (AE1) gene, Blood 91 (1998) 2146-2151.
[183] L.J. Bruce, R.J. Pan, D.L. Cope, M. Uchikawa, R.B. Gunn, R.J. Cherry, M.J. Tanner, Altered structure and anion transport properties of band 3 (AE1, SLC4A1) in human red cells lacking glycophorin A, J Biol Chem 279 (2004) 2414-2420.
[184] L.J. Bruce, J.D. Groves, Y. Okubo, B. Thilaganathan, M.J. Tanner, Altered band 3 structure and function in glycophorin A- and B-deficient (MkMk) red blood cells, Blood 84 (1994) 916-922.
[185] O. Wrong, L.J. Bruce, R.J. Unwin, A.M. Toye, M.J. Tanner, Band 3 mutations, distal renal tubular acidosis, and Southeast Asian ovalocytosis, Kidney Int 62 (2002) 10-19.
[186] L.J. Bruce, O. Wrong, A.M. Toye, M.T. Young, G. Ogle, Z. Ismail, A.K. Sinha, P. McMaster, I. Hwaihwanje, G.B. Nash, S. Hart, E. Lavu, R. Palmer, A. Othman, R.J. Unwin, M.J. Tanner, Band 3 mutations, renal tubular acidosis and South-East Asian ovalocytosis in Malaysia and Papua New Guinea: loss of up to 95% band 3 transport in red cells, Biochem J 350 Pt 1 (2000) 41-51.
[187] M.J. Tanner, Band 3 anion exchanger and its involvement in erythrocyte and kidney disorders, Curr Opin Hematol 9 (2002) 133-139.
[188] E.Y. Almomani, C.Y. Chu, E. Cordat, Mis-trafficking of bicarbonate transporters: implications to human diseases, Biochem Cell Biol 89 157-177.
[189] T.L. Steck, G. Fairbanks, D.F. Wallach, Disposition of the major proteins in the isolated erythrocyte membrane. Proteolytic dissection, Biochemistry 10 (1971) 2617-2624.
[190] A. Schawalder, K. Hue-Roye, L. Castilho, A. Chaudhuri, M.E. Reid, Analysis in non-human primates reveals that the ancestral Band 3 gene encodes Dib and the Band 3-Memphis phenotype, J Med Primatol 35 (2006) 144-148.
[191] L.J. Bruce, M.M. Kay, C. Lawrence, M.J. Tanner, Band 3 HT, a human red-cell variant associated with acanthocytosis and increased anion transport, carries the mutation Pro-868-->Leu in the membrane domain of band 3, Biochem J 293 (Pt 2) (1993) 317-320.
[192] N. Mohandas, R. Winardi, D. Knowles, A. Leung, M. Parra, E. George, J. Conboy, J. Chasis, Molecular basis for membrane rigidity of hereditary ovalocytosis. A novel mechanism involving the cytoplasmic domain of band 3, J Clin Invest 89 (1992) 686-692.
[193] M.L. Jennings, P.G. Gosselink, Anion exchange protein in Southeast Asian ovalocytes: heterodimer formation between normal and variant subunits, Biochemistry 34 (1995) 3588-3595.
[194] V.E. Sarabia, J.R. Casey, R.A.F. Reithmeier, Molecular Characterization of the Band-3 Protein from Southeast-Asian Ovalocytes, Journal of Biological Chemistry 268 (1993) 10676-10680.
[195] R. Moriyama, H. Ideguchi, C.R. Lombardo, H.M. Van Dort, P.S. Low, Structural and functional characterization of band 3 from Southeast Asian ovalocytes, J Biol Chem 267 (1992) 25792-25797.

[196] E.J. Chambers, G.B. Bloomberg, S.M. Ring, M.J. Tanner, Structural studies on the effects of the deletion in the red cell anion exchanger (band 3, AE1) associated with South East Asian ovalocytosis, J Mol Biol 285 (1999) 1289-1307.
[197] J.C. Cheung, R.A.F. Reithmeier, Membrane integration and topology of the first transmembrane segment in normal and Southeast Asian ovalocytosis human erythrocyte anion exchanger 1, Molecular Membrane Biology 22 (2005) 203-214.
[198] J.C. Cheung, E. Cordat, R.A. Reithmeier, Trafficking defects of the Southeast Asian ovalocytosis deletion mutant of anion exchanger 1 membrane proteins, Biochem J 392 (2005) 425-434.
[199] J.M. Salhany, L.M. Schopfer, Interactions between mutant and wild-type band 3 subunits in hereditary Southeast Asian ovalocytic red blood cell membranes, Biochemistry 35 (1996) 251-257.
[200] L.J. Bruce, H.C. Robinson, H. Guizouarn, F. Borgese, P. Harrison, M.J. King, J.S. Goede, S.E. Coles, D.M. Gore, H.U. Lutz, R. Ficarella, D.M. Layton, A. Iolascon, J.C. Ellory, G.W. Stewart, Monovalent cation leaks in human red cells caused by single amino-acid substitutions in the transport domain of the band 3 chloride-bicarbonate exchanger, AE1, Nat Genet 37 (2005) 1258-1263.
[201] H. Guizouarn, S. Martial, N. Gabillat, F. Borgese, Point mutations involved in red cell stomatocytosis convert the electroneutral anion exchanger 1 to a nonselective cation conductance, Blood 110 (2007) 2158-2165.
[202] A.K. Stewart, P.S. Kedar, B.E. Shmukler, D.H. Vandorpe, A. Hsu, B. Glader, A. Rivera, C. Brugnara, S.L. Alper, Functional characterization and modified rescue of novel AE1 mutation R730C associated with overhydrated cation leak stomatocytosis, Am J Physiol Cell Physiol 300 (2011) C1034-1046.
[203] A.K. Stewart, D.H. Vandorpe, J.F. Heneghan, F. Chebib, K. Stolpe, A. Akhavein, E.J. Edelman, Y. Maksimova, P.G. Gallagher, S.L. Alper, The GPA-dependent, spherostomatocytosis mutant AE1 E758K induces GPA-independent, endogenous cation transport in amphibian oocytes, Am J Physiol Cell Physiol 298 (2010) C283-297.
[204] A. Iolascon, L. De Falco, F. Borgese, M.R. Esposito, R.A. Avvisati, P. Izzo, C. Piscopo, H. Guizouarn, A. Biondani, A. Pantaleo, L. De Franceschi, A novel erythroid anion exchange variant (Gly796Arg) of hereditary stomatocytosis associated with dyserythropoiesis, Haematologica 94 (2009) 1049-1059.
[205] J.A. Quilty, R.A.F. Reithmeier, Trafficking and folding defects in hereditary spherocytosis mutants of the human red cell anion exchanger, Traffic 1 (2000) 987-998.
[206] P. Jarolim, J. Palek, H.L. Rubin, J.T. Prchal, C. Korsgren, C.M. Cohen, Band 3 Tuscaloosa: Pro327----Arg327 substitution in the cytoplasmic domain of erythrocyte band 3 protein associated with spherocytic hemolytic anemia and partial deficiency of protein 4.2, Blood 80 (1992) 523-529.
[207] S.P. Bustos, R.A. Reithmeier, Protein 4.2 interaction with hereditary spherocytosis mutants of the cytoplasmic domain of human anion exchanger 1, Biochem J 433 (2010) 313-322.
[208] S.P. Bustos, R.A.F. Reithmeier, Structure and stability of hereditary spherocytosis mutants of the cytosolic domain of the erythrocyte anion exchanger 1 protein, Biochemistry 45 (2006) 1026-1034.

[209] Z. Zhou, S.C. DeSensi, R.A. Stein, S. Brandon, L. Song, C.E. Cobb, E.J. Hustedt, A.H. Beth, Structure of the cytoplasmic domain of erythrocyte band 3 hereditary spherocytosis variant P327R: band 3 Tuscaloosa, Biochemistry 46 (2007) 10248-10257.
[210] E. Cordat, Unraveling trafficking of the kidney anion exchanger 1 in polarized MDCK epithelial cells, Biochem Cell Biol 84 (2006) 949-959.
[211] V.L. Schuster, S.M. Bonsib, M.L. Jennings, Two types of collecting duct mitochondria-rich (intercalated) cells: lectin and band 3 cytochemistry, Am J Physiol 251 (1986) C347-355.
[212] S.L. Alper, J. Natale, S. Gluck, H.F. Lodish, D. Brown, Subtypes of intercalated cells in rat kidney collecting duct defined by antibodies against erythroid band 3 and renal vacuolar H+-ATPase, Proc Natl Acad Sci U S A 86 (1989) 5429-5433.
[213] N. Rungroj, M.A. Devonald, A.W. Cuthbert, F. Reimann, V. Akkarapatumwong, P.T. Yenchitsomanus, W.M. Bennett, F.E. Karet, A novel missense mutation in AE1 causing autosomal dominant distal renal tubular acidosis retains normal transport function but is mistargeted in polarized epithelial cells, J Biol Chem 279 (2004) 13833-13838.
[214] E.Y. Almomani, C.Y. Chu, E. Cordat, Mis-trafficking of bicarbonate transporters: implications to human diseases, Biochem Cell Biol 89 (2011) 157-177.
[215] A.C. Fry, Y. Su, V. Yiu, A.W. Cuthbert, H. Trachtman, F.E. Karet Frankl, Mutation conferring apical-targeting motif on AE1 exchanger causes autosomal dominant distal RTA, J Am Soc Nephrol 23 (2012) 1238-1249.
[216] P. Jarolim, H.L. Rubin, S.C. Liu, M.R. Cho, V. Brabec, L.H. Derick, S.J. Yi, S.T. Saad, S. Alper, C. Brugnara, et al., Duplication of 10 nucleotides in the erythroid band 3 (AE1) gene in a kindred with hereditary spherocytosis and band 3 protein deficiency (band 3PRAGUE), J Clin Invest 93 (1994) 121-130.
[217] M.A. Devonald, A.N. Smith, J.P. Poon, G. Ihrke, F.E. Karet, Non-polarized targeting of AE1 causes autosomal dominant distal renal tubular acidosis, Nat Genet 33 (2003) 125-127.
[218] J.A. Quilty, J. Li, R.A. Reithmeier, Impaired trafficking of distal renal tubular acidosis mutants of the human kidney anion exchanger kAE1, Am J Physiol Renal Physiol 282 (2002) F810-820.
[219] A.M. Toye, L.J. Bruce, R.J. Unwin, O. Wrong, M.J. Tanner, Band 3 Walton, a C-terminal deletion associated with distal renal tubular acidosis, is expressed in the red cell membrane but retained internally in kidney cells, Blood 99 (2002) 342-347.
[220] J.W. Vince, R.A. Reithmeier, Carbonic anhydrase II binds to the carboxyl terminus of human band 3, the erythrocyte C1-/HCO3- exchanger, J Biol Chem 273 (1998) 28430-28437.
[221] J.W. Vince, R.A. Reithmeier, Identification of the carbonic anhydrase II binding site in the Cl(-)/HCO(3)(-) anion exchanger AE1, Biochemistry 39 (2000) 5527-5533.
[222] T.F. Moraes, R.A. Reithmeier, Membrane transport metabolons, Biochim Biophys Acta 1818 (2012) 2687-2706.
[223] A.M. Toye, G. Banting, M.J. Tanner, Regions of human kidney anion exchanger 1 (kAE1) required for basolateral targeting of kAE1 in polarised kidney cells: mis-targeting explains dominant renal tubular acidosis (dRTA), J Cell Sci 117 (2004) 1399-1410.
[224] R.C. Williamson, A.C. Brown, W.J. Mawby, A.M. Toye, Human kidney anion exchanger 1 localisation in MDCK cells is controlled by the phosphorylation status of two critical tyrosines, J Cell Sci 121 (2008) 3422-3432.

[225] E. Cordat, S. Kittanakom, P.T. Yenchitsomanus, J. Li, K. Du, G.L. Lukacs, R.A. Reithmeier, Dominant and recessive distal renal tubular acidosis mutations of kidney anion exchanger 1 induce distinct trafficking defects in MDCK cells, Traffic 7 (2006) 117-128.
[226] J.A. Quilty, J. Li, R.A. Reithmeier, Impaired trafficking of distal renal tubular acidosis mutants of the human kidney anion exchanger kAE1, American Journal of Physiology-Renal Physiology 282 (2002) F810-F820.
[227] A.M. Toye, R.C. Williamson, M. Khanfar, B. Bader-Meunier, T. Cynober, M. Thibault, G. Tchernia, M. Dechaux, J. Delaunay, L.J. Bruce, Band 3 Courcouronnes (Ser667Phe): a trafficking mutant differentially rescued by wild-type band 3 and glycophorin A, Blood 111 (2008) 5380-5389.
[228] A.K. Stewart, F.T. Chebib, S.W. Akbar, M.J. Salas, R.A. Sonik, B.E. Shmukler, S.L. Alper, Interactions of mouse glycophorin A with the dRTA-related mutant G719D of the mouse Cl-/HCO3- exchanger Ae1, Biochem Cell Biol 89 (2011) 224-235.
[229] D. Ungsupravate, N. Sawasdee, S. Khositseth, W. Udomchaiprasertkul, S. Khoprasert, J. Li, R.A. Reithmeier, P.T. Yenchitsomanus, Impaired trafficking and intracellular retention of mutant kidney anion exchanger 1 proteins (G701D and A858D) associated with distal renal tubular acidosis, Mol Membr Biol 27 92-103.
[230] D. Ungsupravate, N. Sawasdee, S. Khositseth, W. Udomchaiprasertkul, S. Khoprasert, J. Li, R.A. Reithmeier, P.T. Yenchitsomanus, Impaired trafficking and intracellular retention of mutant kidney anion exchanger 1 proteins (G701D and A858D) associated with distal renal tubular acidosis, Mol Membr Biol 27 (2010) 92-103.
[231] E. Cordat, R.A. Reithmeier, Expression and interaction of two compound heterozygous distal renal tubular acidosis mutants of kidney anion exchanger 1 in epithelial cells, Am J Physiol Renal Physiol 291 (2006) F1354-1361.
[232] S. Kittanakom, E. Cordat, R.A.F. Reithmeier, Dominant-negative effect of Southeast Asian ovalocytosis anion exchanger 1 in compound heterozygous distal renal tubular acidosis, Biochemical Journal 410 (2008) 271-281.
[233] P.T. Yenchitsomanus, S. Vasuvattakul, S. Kirdpon, S. Wasanawatana, W. Susaengrat, S. Sreethiphayawan, D. Chuawatana, S. Mingkum, N. Sawasdee, P. Thuwajit, P. Wilairat, P. Malasit, S. Nimmannit, Autosomal recessive distal renal tubular acidosis caused by G701D mutation of anion exchanger 1 gene, Am J Kidney Dis 40 (2002) 21-29.
[234] R.A.F. Reithmeier, The Erythrocyte Anion Transporter (Band-3), Current Opinion in Structural Biology 3 (1993) 515-523.
[235] M.F. Romero, A.P. Chen, M.D. Parker, W.F. Boron, The SLC4 family of bicarbonate (HCO(3)(-)) transporters, Mol Aspects Med 34 (2013) 159-182.
[236] I. Choi, SLC4A transporters, Curr Top Membr 70 (2012) 77-103.
[237] K. Alka, J.R. Casey, Bicarbonate transport in health and disease, IUBMB Life 66 (2014) 596-615.
[238] S.L. Alper, Molecular physiology of SLC4 anion exchangers, Exp Physiol 91 (2006) 153-161.
[239] B.S. Lee, R.B. Gunn, R.R. Kopito, Functional differences among nonerythroid anion exchangers expressed in a transfected human cell line, J Biol Chem 266 (1991) 11448-11454.
[240] M.F. Romero, The electrogenic Na+/HCO3- cotransporter, NBC, JOP 2 (2001) 182-191.

[241] M.O. Bevensee, B.M. Schmitt, I. Choi, M.F. Romero, W.F. Boron, An electrogenic Na(+)-HCO(-)(3) cotransporter (NBC) with a novel COOH-terminus, cloned from rat brain, Am J Physiol Cell Physiol 278 (2000) C1200-1211.
[242] M.F. Romero, W.F. Boron, Electrogenic Na+/HCO3- cotransporters: cloning and physiology, Annu Rev Physiol 61 (1999) 699-723.
[243] M.D. Parker, E.P. Ourmozdi, M.J. Tanner, Human BTR1, a new bicarbonate transporter superfamily member and human AE4 from kidney, Biochem Biophys Res Commun 282 (2001) 1103-1109.
[244] H. Tsuganezawa, K. Kobayashi, M. Iyori, T. Araki, A. Koizumi, S. Watanabe, A. Kaneko, T. Fukao, T. Monkawa, T. Yoshida, D.K. Kim, Y. Kanai, H. Endou, M. Hayashi, T. Saruta, A new member of the HCO3(-) transporter superfamily is an apical anion exchanger of beta-intercalated cells in the kidney, J Biol Chem 276 (2001) 8180-8189.
[245] J. Takano, K. Noguchi, M. Yasumori, M. Kobayashi, Z. Gajdos, K. Miwa, H. Hayashi, T. Yoneyama, T. Fujiwara, Arabidopsis boron transporter for xylem loading, Nature 420 (2002) 337-340.
[246] M. Park, Q. Li, N. Shcheynikov, W. Zeng, S. Muallem, NaBC1 is a ubiquitous electrogenic Na+ -coupled borate transporter essential for cellular boron homeostasis and cell growth and proliferation, Mol Cell 16 (2004) 331-341.
[247] W. Zhang, D.G. Ogando, J.A. Bonanno, A.G. Obukhov, Human SLC4A11 Is a Novel NH3/H+ Co-transporter, J Biol Chem 290 (2015) 16894-16905.
[248] G.L. Vilas, S.K. Loganathan, J. Liu, A.K. Riau, J.D. Young, J.S. Mehta, E.N. Vithana, J.R. Casey, Transmembrane water-flux through SLC4A11: a route defective in genetic corneal diseases, Hum Mol Genet 22 (2013) 4579-4590.
[249] S.S. Jalimarada, D.G. Ogando, E.N. Vithana, J.A. Bonanno, Ion transport function of SLC4A11 in corneal endothelium, Invest Ophthalmol Vis Sci 54 (2013) 4330-4340.
[250] D.G. Ogando, S.S. Jalimarada, W. Zhang, E.N. Vithana, J.A. Bonanno, SLC4A11 is an EIPA-sensitive Na(+) permeable pHi regulator, Am J Physiol Cell Physiol 305 (2012) C716-727.
[251] T. Sander, M.R. Toliat, A. Heils, G. Leschik, C. Becker, F. Ruschendorf, K. Rohde, S. Mundlos, P. Nurnberg, Association of the 867Asp variant of the human anion exchanger 3 gene with common subtypes of idiopathic generalized epilepsy, Epilepsy Res 51 (2002) 249-255.
[252] G.L. Vilas, D.E. Johnson, P. Freund, J.R. Casey, Characterization of an epilepsy-associated variant of the human Cl-/HCO3(-) exchanger AE3, Am J Physiol Cell Physiol 297 (2009) C526-536.
[253] H.S. Yang, E. Kim, S. Lee, H.J. Park, D.S. Cooper, I. Rajbhandari, I. Choi, Mutation of Aspartate 555 of the Sodium/Bicarbonate Transporter SLC4A4/NBCe1 Induces Chloride Transport, J Biol Chem 284 (2009) 15970-15979.
[254] T. Igarashi, J. Inatomi, T. Sekine, S.H. Cha, Y. Kanai, M. Kunimi, K. Tsukamoto, H. Satoh, M. Shimadzu, F. Tozawa, T. Mori, M. Shiobara, G. Seki, H. Endou, Mutations in SLC4A4 cause permanent isolated proximal renal tubular acidosis with ocular abnormalities, Nat Genet 23 (1999) 264-266.
[255] D. Dinour, M.H. Chang, J. Satoh, B.L. Smith, N. Angle, A. Knecht, I. Serban, E.J. Holtzman, M.F. Romero, A novel missense mutation in the sodium bicarbonate

cotransporter (NBCe1/SLC4A4) causes proximal tubular acidosis and glaucoma through ion transport defects, J Biol Chem 279 (2004) 52238-52246.
[256] S. Horita, H. Yamada, J. Inatomi, N. Moriyama, T. Sekine, T. Igarashi, Y. Endo, M. Dasouki, M. Ekim, L. Al-Gazali, M. Shimadzu, G. Seki, T. Fujita, Functional analysis of NBC1 mutants associated with proximal renal tubular acidosis and ocular abnormalities, J Am Soc Nephrol 16 (2005) 2270-2278.
[257] M. Suzuki, M.H. Vaisbich, H. Yamada, S. Horita, Y. Li, T. Sekine, N. Moriyama, T. Igarashi, Y. Endo, T.P. Cardoso, L.C. de Sa, V.H. Koch, G. Seki, T. Fujita, Functional analysis of a novel missense NBC1 mutation and of other mutations causing proximal renal tubular acidosis, Pflugers Arch 455 (2008) 583-593.
[258] Y.F. Lo, S.S. Yang, G. Seki, H. Yamada, S. Horita, O. Yamazaki, T. Fujita, T. Usui, J.D. Tsai, I.S. Yu, S.W. Lin, S.H. Lin, Severe metabolic acidosis causes early lethality in NBC1 W516X knock-in mice as a model of human isolated proximal renal tubular acidosis, Kidney Int 79 (2011) 730-741.
[259] S.D. McAlear, M.O. Bevensee, A cysteine-scanning mutagenesis study of transmembrane domain 8 of the electrogenic sodium/bicarbonate cotransporter NBCe1, J Biol Chem 281 (2006) 32417-32427.
[260] Q. Zhu, R. Azimov, L. Kao, D. Newman, W. Liu, N. Abuladze, A. Pushkin, I. Kurtz, NBCe1-A Transmembrane Segment 1 Lines the Ion Translocation Pathway, J Biol Chem 284 (2009) 8918-8929.
[261] Q. Zhu, L. Kao, R. Azimov, D. Newman, W. Liu, A. Pushkin, N. Abuladze, I. Kurtz, Topological location and structural importance of the NBCe1-A residues mutated in proximal renal tubular acidosis, J Biol Chem 285 (2010) 13416-13426.
[262] Q. Zhu, L. Kao, R. Azimov, N. Abuladze, D. Newman, A. Pushkin, W. Liu, C. Chang, I. Kurtz, Structural and functional characterization of the C-terminal transmembrane region of NBCe1-A, J Biol Chem 285 (2010) 37178-37187.
[263] Q. Zhu, W. Liu, L. Kao, R. Azimov, D. Newman, N. Abuladze, I. Kurtz, Topology of NBCe1 protein transmembrane segment 1 and structural effect of proximal renal tubular acidosis (pRTA) S427L mutation, J Biol Chem 288 (2013) 7894-7906.
[264] P.J. Stansfeld, M.S.P. Sansom, Molecular simulation approaches to membrane proteins, Structure 19 (2011) 1562-1572.
[265] V.A. Gregg, R.A.F. Reithmeier, Effect of Cholesterol on Phosphate-Uptake by Human Red-Blood-Cells, Febs Letters 157 (1983) 159-164.
[266] T. Muhlebach, R.J. Cherry, Influence of cholesterol on the rotation and self-association of band 3 in the human erythrocyte membrane, Biochemistry 21 (1982) 4225-4228.
[267] D. Schubert, K. Boss, Band 3 protein-cholesterol interactions in erythrocyte membranes. Possible role in anion transport and dependency on membrane phospholipid, FEBS Lett 150 (1982) 4-8.
[268] A.C. Kalli, M.S.P. Sansom, R.A.F. Reithmeier, Molecular dynamics simulations of the bacterial UraA H⁺-Uracil symporter in lipid bilayers reveal a closed state and a selective interaction with cardiolipin, PLoS Comput. Biol. 11 (2015) e1004123.
[269] L.R. Maneri, P.S. Low, Structural stability of the erythrocyte anion transporter, band 3, in different lipid environments. A differential scanning calorimetric study, J Biol Chem 263 (1988) 16170-16178.

[270] K. McManus, K. Lupe, G. Coghlan, T. Zelinski, An amino acid substitution in the putative second extracellular loop of RBC band 3 accounts for the Froese blood group polymorphism, Transfusion 40 (2000) 1246-1249.
[271] L.J. Bruce, T. Zelinski, K. Ridgwell, M.J. Tanner, The low-incidence blood group antigen, Wda, is associated with the substitution Val557-->Met in human erythrocyte band 3 (AE1), Vox Sang 71 (1996) 118-120.
[272] T. Zelinski, K. McManus, F. Punter, M. Moulds, G. Coghlan, A Gly565-->Ala substitution in human erythroid band 3 accounts for the Wu blood group polymorphism, Transfusion 38 (1998) 745-748.
[273] T. Zelinski, A. Rusnak, K. McManus, G. Coghlan, Distinctive Swann blood group genotypes: molecular investigations, Vox Sang 79 (2000) 215-218.
[274] A.E. Schofield, P.G. Martin, D. Spillett, M.J. Tanner, The structure of the human red blood cell anion exchanger (EPB3, AE1, band 3) gene, Blood 84 (1994) 2000-2012.
[275] A.E. Schofield, M.J. Tanner, J.C. Pinder, B. Clough, P.M. Bayley, G.B. Nash, A.R. Dluzewski, D.M. Reardon, T.M. Cox, R.J. Wilson, et al., Basis of unique red cell membrane properties in hereditary ovalocytosis, J Mol Biol 223 (1992) 949-958.
[276] J.C. Cheung, E. Cordat, R.A.F. Reithmeier, Trafficking defects of the Southeast Asian ovalocytosis deletion mutant of anion exchanger 1 membrane proteins, Biochemical Journal 392 (2005) 425-434.
[277] H. Guizouarn, F. Borgese, N. Gabillat, P. Harrison, J.S. Goede, C. McMahon, G.W. Stewart, L.J. Bruce, South-east Asian ovalocytosis and the cryohydrocytosis form of hereditary stomatocytosis show virtually indistinguishable cation permeability defects, Br J Haematol 152 (2011) 655-664.
[278] C. Chu, N. Woods, N. Sawasdee, H. Guizouarn, B. Pellissier, F. Borgese, P.T. Yenchitsomanus, M. Gowrishankar, E. Cordat, Band 3 Edmonton I, a novel mutant of the anion exchanger 1 causing spherocytosis and distal renal tubular acidosis, Biochem J 426 (2009) 379-388.
[279] N. Alloisio, P. Texier, A. Vallier, M.L. Ribeiro, L. Morle, M. Bozon, E. Bursaux, P. Maillet, P. Goncalves, M.J. Tanner, G. Tamagnini, J. Delaunay, Modulation of clinical expression and band 3 deficiency in hereditary spherocytosis, Blood 90 (1997) 414-420.
[280] D. Dhermy, C. Galand, O. Bournier, L. Boulanger, T. Cynober, P.O. Schismanoff, E. Bursaux, G. Tchernia, P. Boivin, M. Garbarz, Heterogenous band 3 deficiency in hereditary spherocytosis related to different band 3 gene defects, Br J Haematol 98 (1997) 32-40.
[281] S.W. Eber, J.M. Gonzalez, M.L. Lux, A.L. Scarpa, W.T. Tse, M. Dornwell, J. Herbers, W. Kugler, R. Ozcan, A. Pekrun, P.G. Gallagher, W. Schroter, B.G. Forget, S.E. Lux, Ankyrin-1 mutations are a major cause of dominant and recessive hereditary spherocytosis, Nat Genet 13 (1996) 214-218.
[282] P.R. Lima, M.O. Baratti, M.L. Chiattone, F.F. Costa, S.T. Saad, Band 3Tambau: a de novo mutation in the AE1 gene associated with hereditary spherocytosis. Implications for anion exchange and insertion into the red blood cell membrane, Eur J Haematol 74 (2005) 396-401.
[283] A. Kanzaki, S. Hayette, L. Morle, F. Inoue, R. Matsuyama, T. Inoue, A. Yawata, H. Wada, A. Vallier, N. Alloisio, Y. Yawata, J. Delaunay, Total absence of protein 4.2 and partial deficiency of band 3 in hereditary spherocytosis, Br J Haematol 99 (1997) 522-530.

[284] P. Maillet, N. Alloisio, L. Morle, J. Delaunay, Spectrin mutations in hereditary elliptocytosis and hereditary spherocytosis, Hum Mutat 8 (1996) 97-107.
[285] E. Miraglia del Giudice, A. Vallier, P. Maillet, S. Perrotta, S. Cutillo, A. Iolascon, M.J. Tanner, J. Delaunay, N. Alloisio, Novel band 3 variants (bands 3 Foggia, Napoli I and Napoli II) associated with hereditary spherocytosis and band 3 deficiency: status of the D38A polymorphism within the EPB3 locus, Br J Haematol 96 (1997) 70-76.
[286] S. Iwase, H. Ideguchi, M. Takao, J. Horiguchi-Yamada, M. Iwasaki, S. Takahara, T. Sekikawa, S. Mochizuki, H. Yamada, Band 3 Tokyo: Thr837-->Ala837 substitution in erythrocyte band 3 protein associated with spherocytic hemolysis, Acta Haematol 100 (1998) 200-203.
[287] B.E. Shmukler, P.S. Kedar, P. Warang, M. Desai, M. Madkaikar, K. Ghosh, R.B. Colah, S.L. Alper, Hemolytic anemia and distal renal tubular acidosis in two Indian patients homozygous for SLC4A1/AE1 mutation A858D, Am J Hematol 85 (2010) 824-828.
[288] R. Sinha, I. Agarwal, W.M. Bawazir, L.J. Bruce, Distal renal tubular acidosis with hereditary spherocytosis, Indian Pediatr 50 (2013) 693-695.
[289] Z. Zhang, K.X. Liu, J.W. He, W.Z. Fu, H. Yue, H. Zhang, C.Q. Zhang, Z.L. Zhang, Identification of two novel mutations in the SLC4A1 gene in two unrelated Chinese families with distal renal tubular acidosis, Arch Med Res 43 (2012) 298-304.
[290] Y.H. Chang, C.F. Shaw, S.H. Jian, K.H. Hsieh, Y.H. Chiou, P.J. Lu, Compound mutations in human anion exchanger 1 are associated with complete distal renal tubular acidosis and hereditary spherocytosis, Kidney Int 76 (2009) 774-783.
[291] L.J. Bruce, D.L. Cope, G.K. Jones, A.E. Schofield, M. Burley, S. Povey, R.J. Unwin, O. Wrong, M.J. Tanner, Familial distal renal tubular acidosis is associated with mutations in the red cell anion exchanger (Band 3, AE1) gene, J Clin Invest 100 (1997) 1693-1707.
[292] S. Kittanakom, E. Cordat, V. Akkarapatumwong, P. Yenchitsomanus, R.A.F. Reithmeier, Trafficking defects of a novel autosomal recessive distal renal tubular acidosis mutant (S773P) of the human kidney anion exchanger (kAE1), Journal of Biological Chemistry 279 (2004) 40960-40971.
[293] L. Cheidde, T.C. Vieira, P.R. Lima, S.T. Saad, I.P. Heilberg, A novel mutation in the anion exchanger 1 gene is associated with familial distal renal tubular acidosis and nephrocalcinosis, Pediatrics 112 (2003) 1361-1367.
[294] A.M. Toye, L.J. Bruce, R.J. Unwin, O. Wrong, M.J. Tanner, Band 3 Walton, a C-terminal deletion associated with distal renal tubular acidosis, is expressed in the red cell membrane but retained internally in kidney cells, Blood 99 (2002) 342-347.
[295] J.A. Quilty, E. Cordat, R.A.F. Reithmeier, Impaired trafficking of human kidney anion exchanger (kAE1) caused by hetero-oligomer formation with a truncated mutant associated with distal renal tubular acidosis, Biochemical Journal 368 (2002) 895-903.
[296] L. Shao, Y. Xu, Q. Dong, Y. Lang, S. Yue, Z. Miao, A novel SLC4A1 variant in an autosomal dominant distal renal tubular acidosis family with a severe phenotype, Endocrine 37 (2010) 473-478.

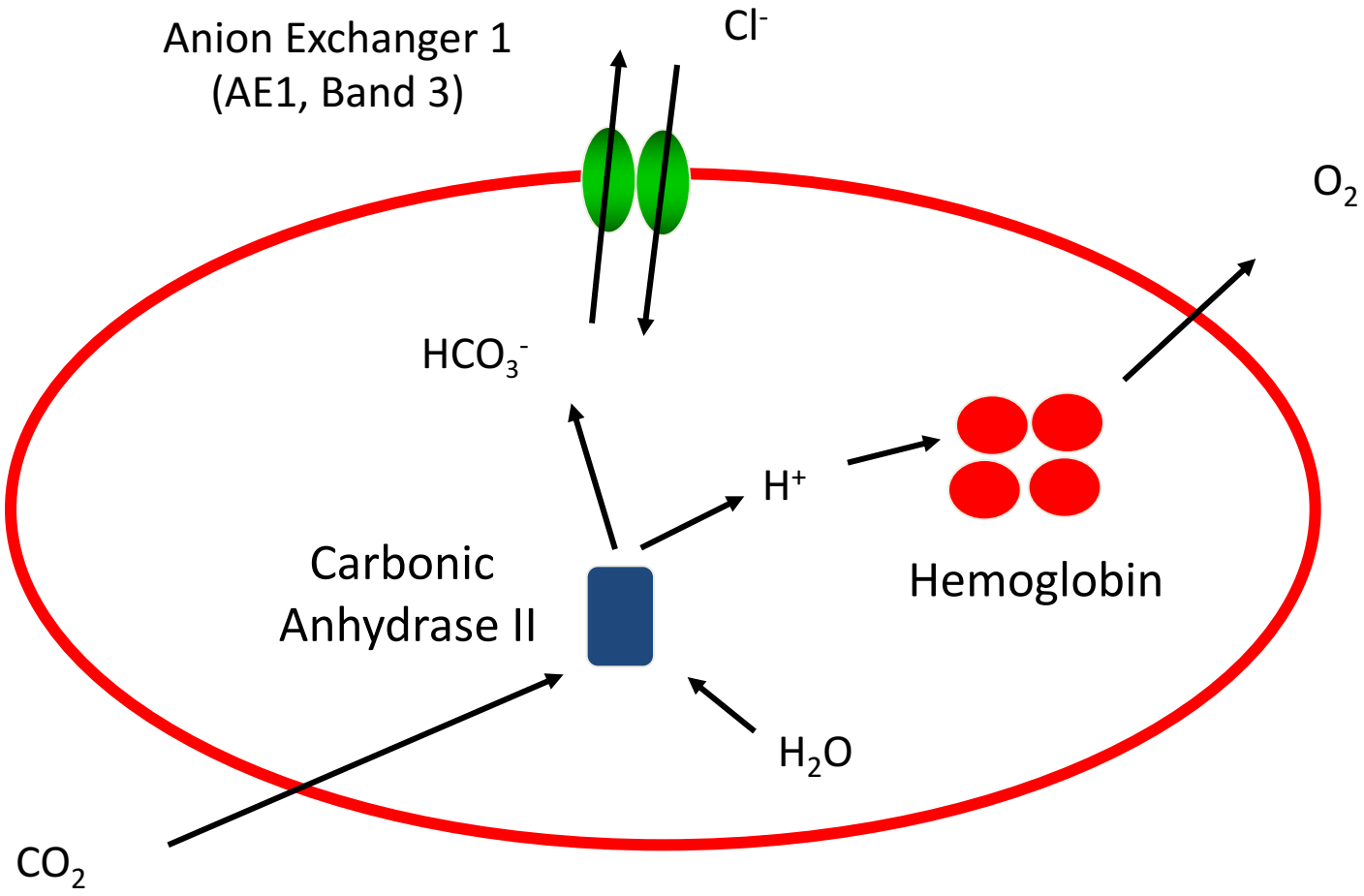

Reithmeier et al. Fig. 1

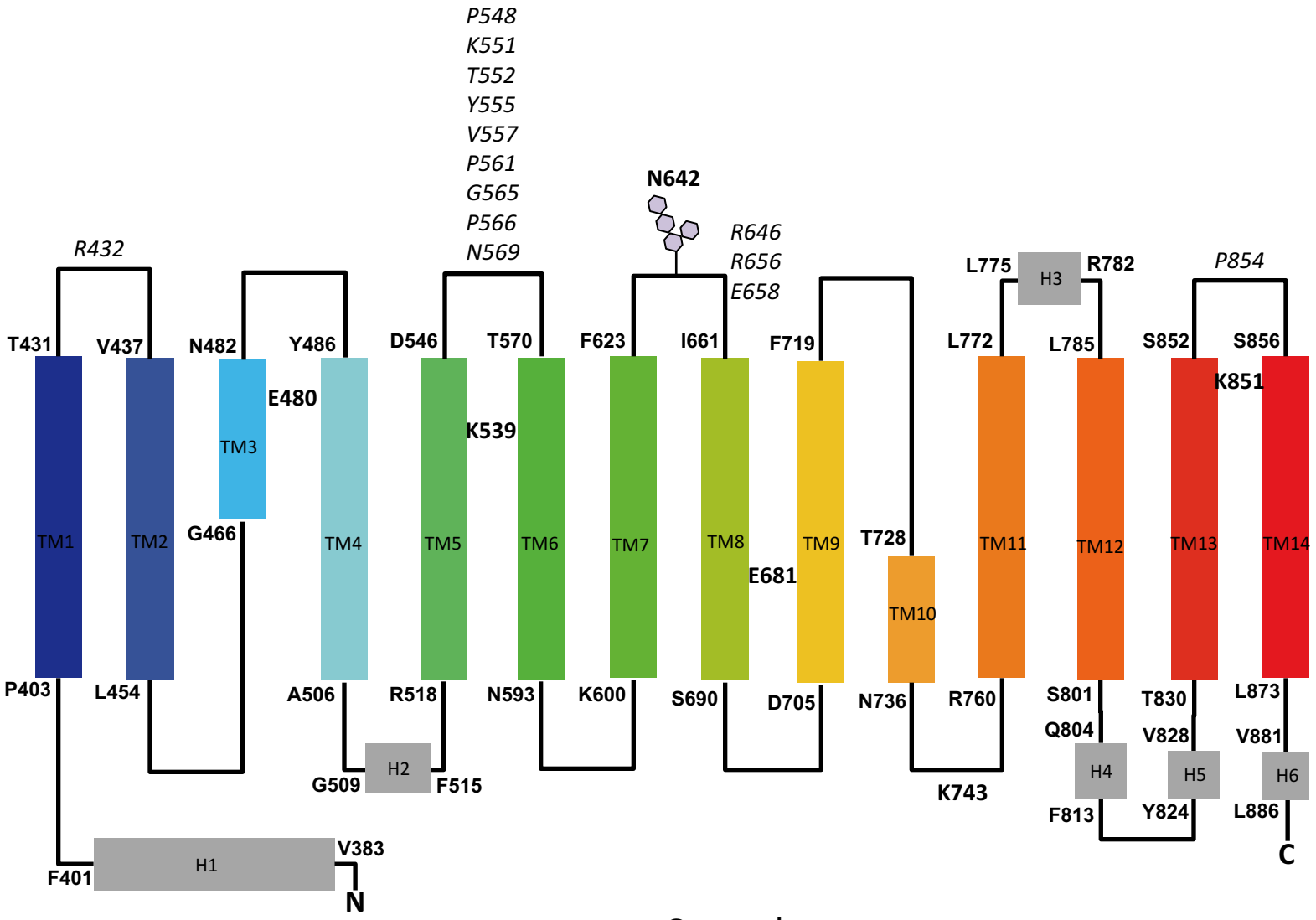

Reithmeier et al., Fig. 2.

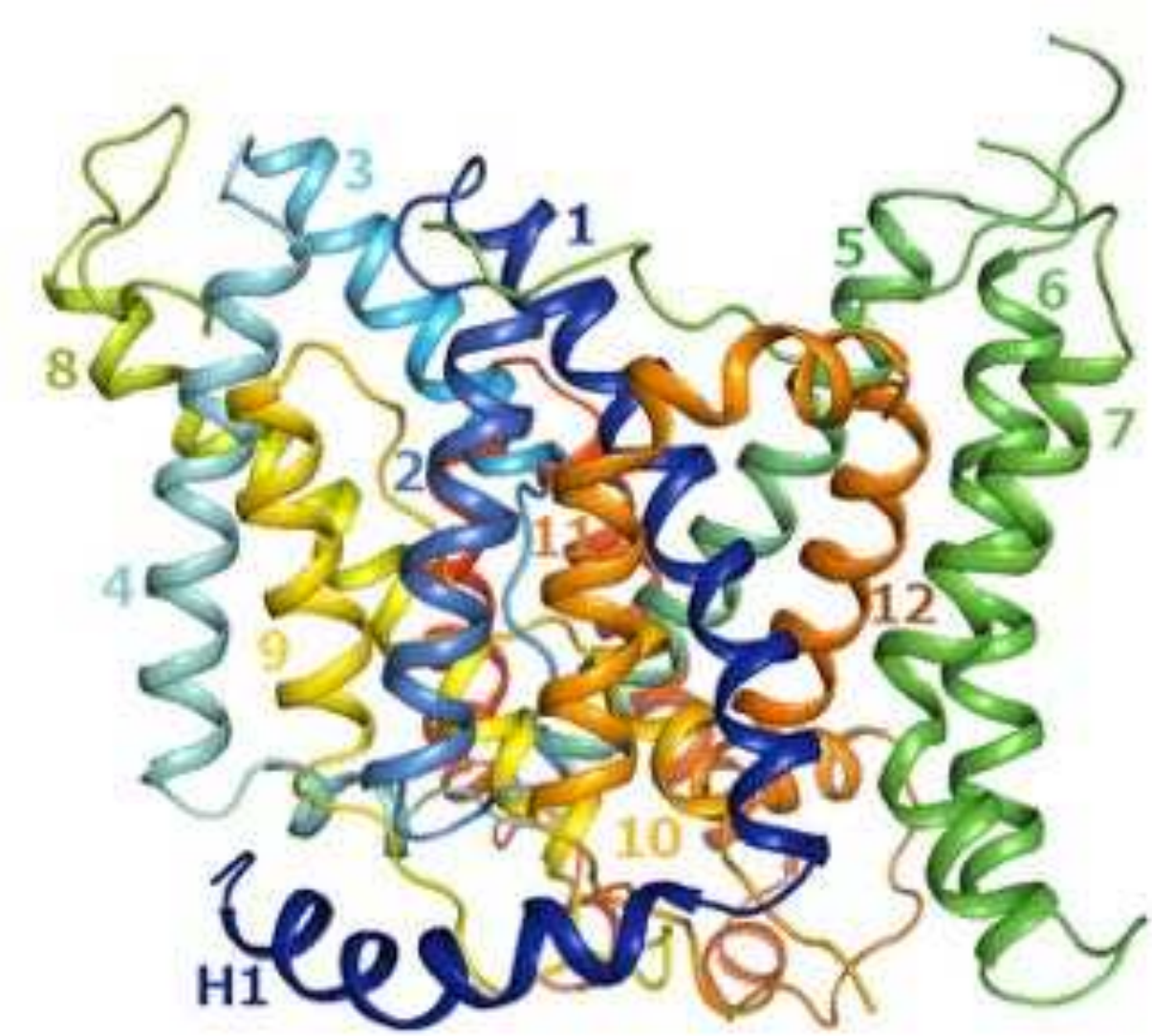

Reithmeier et al., Fig. 3A

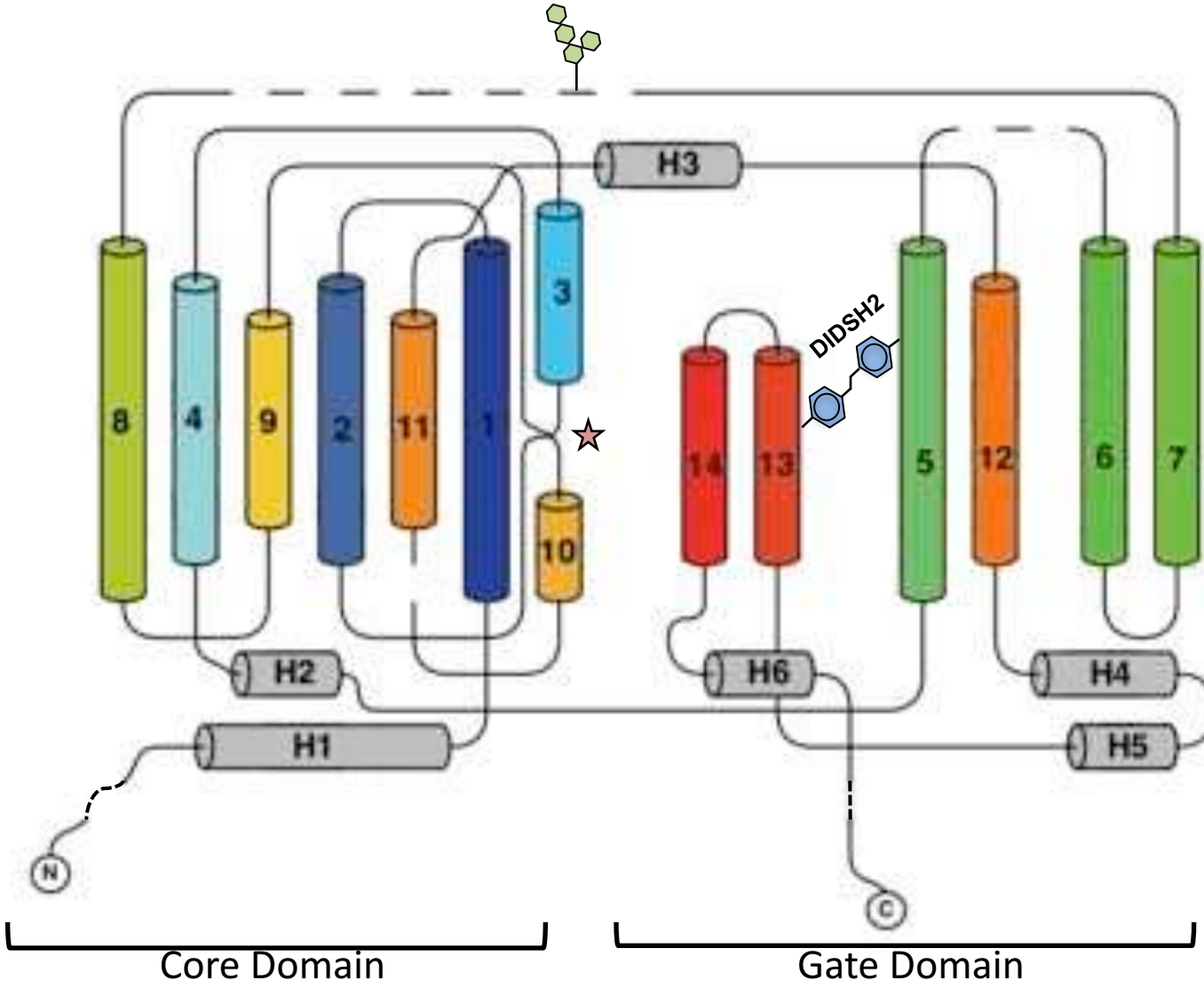

Reithmeier et al., Fig.

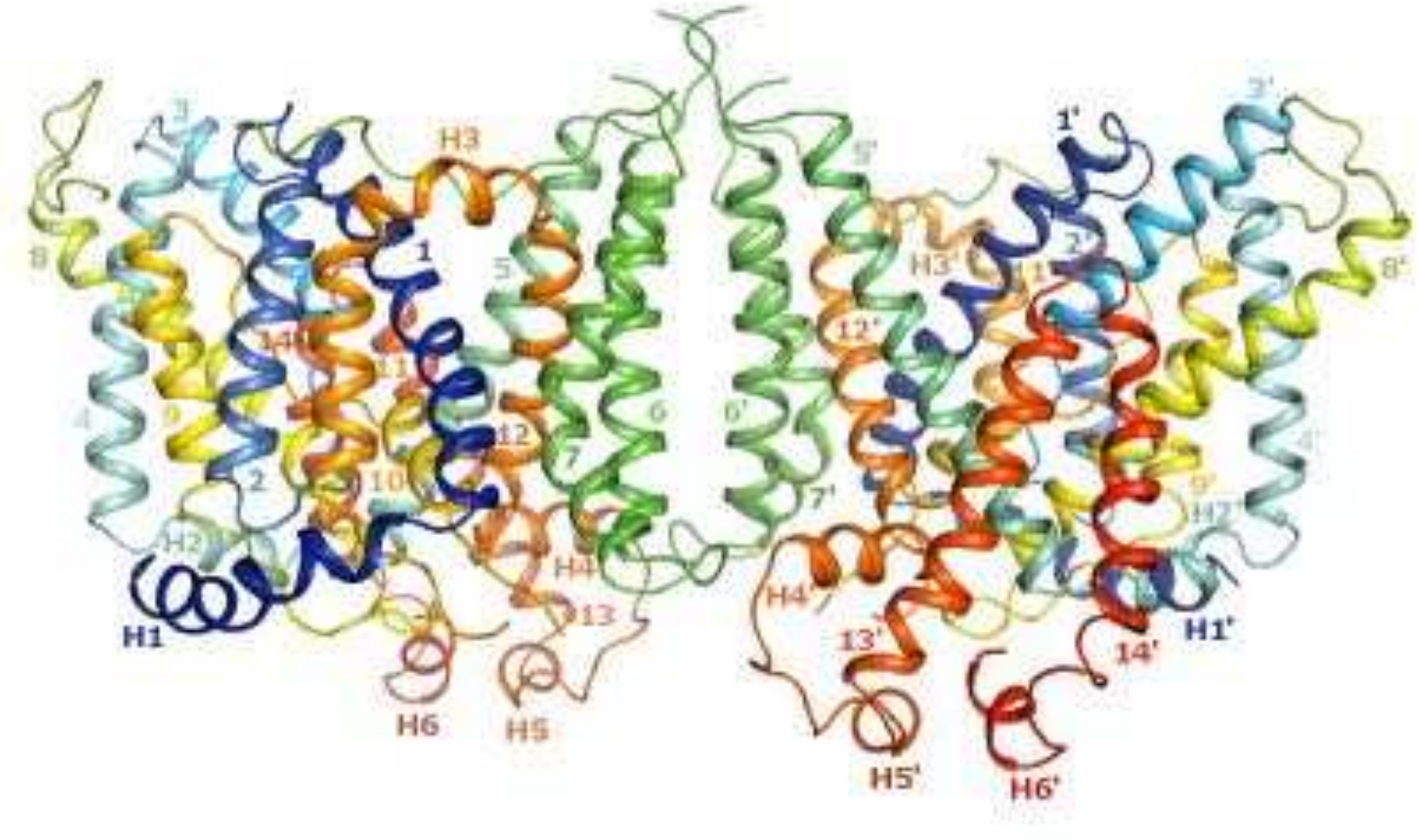

Reithmeier et al., Fig. 4A

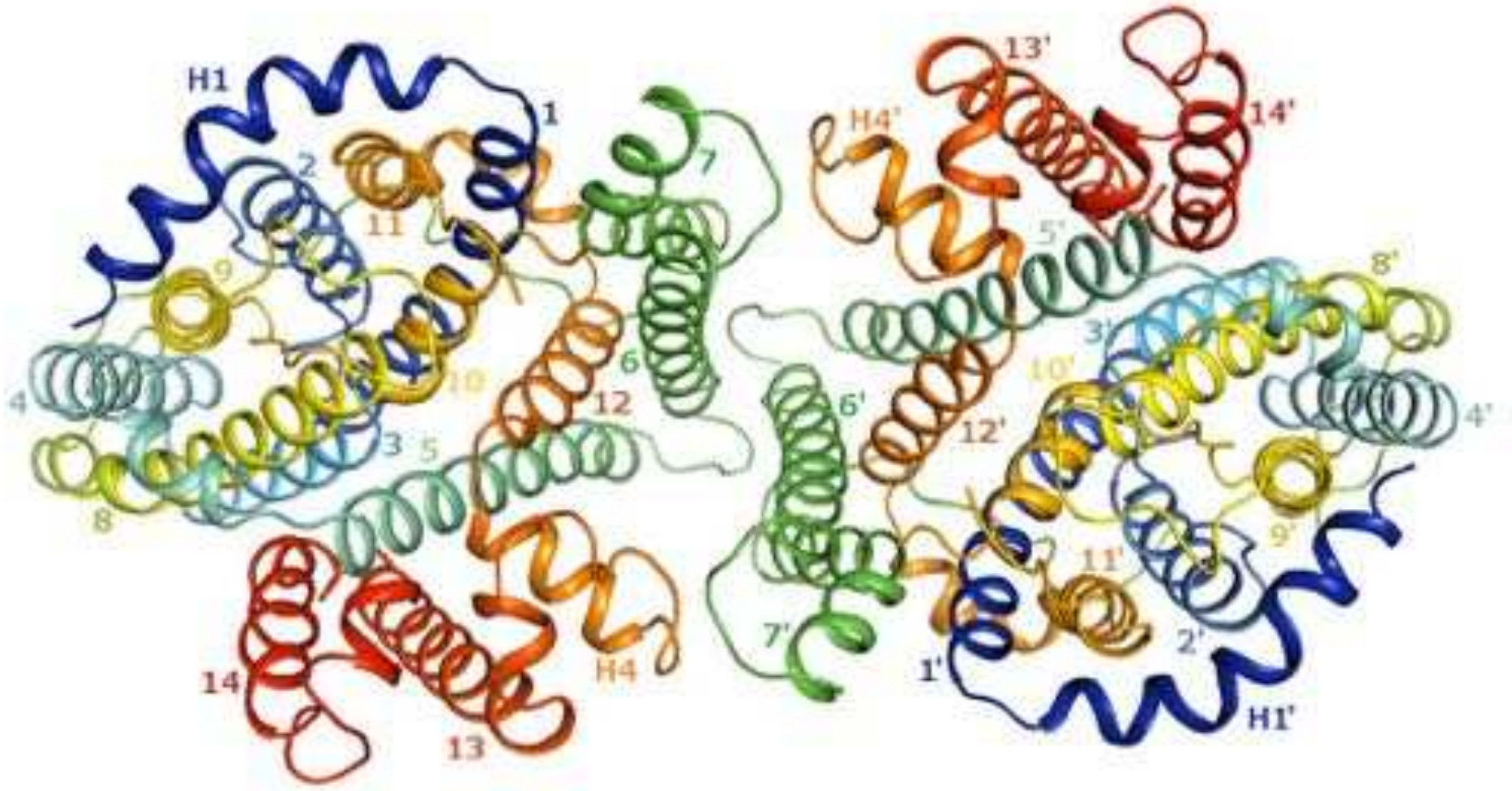

Reithmeier et al., Fig. 4B

A

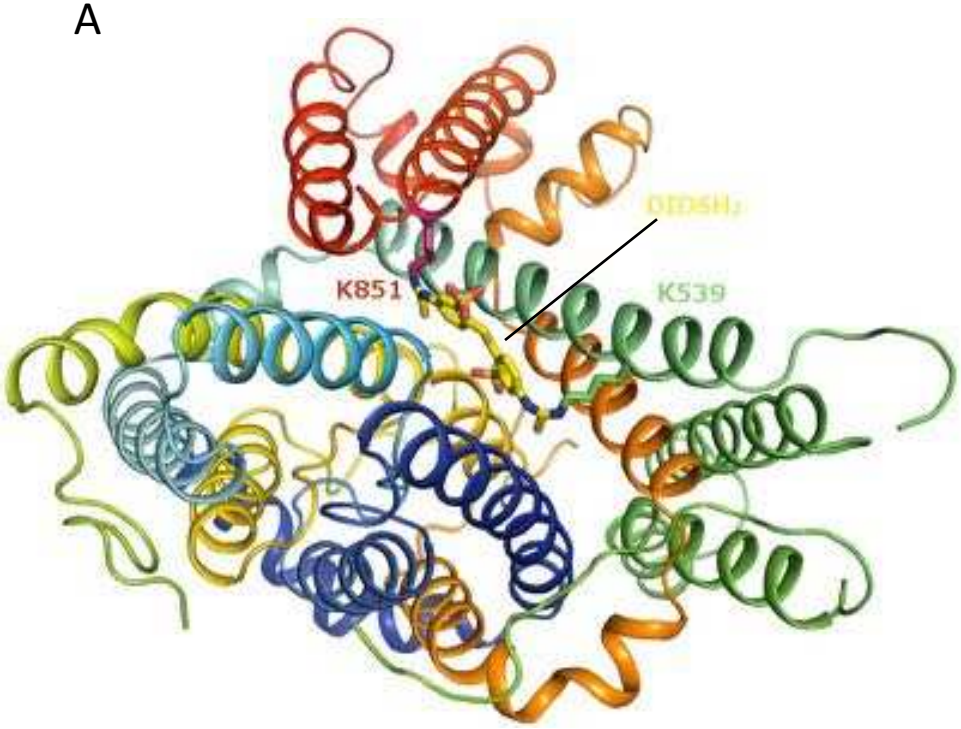

B

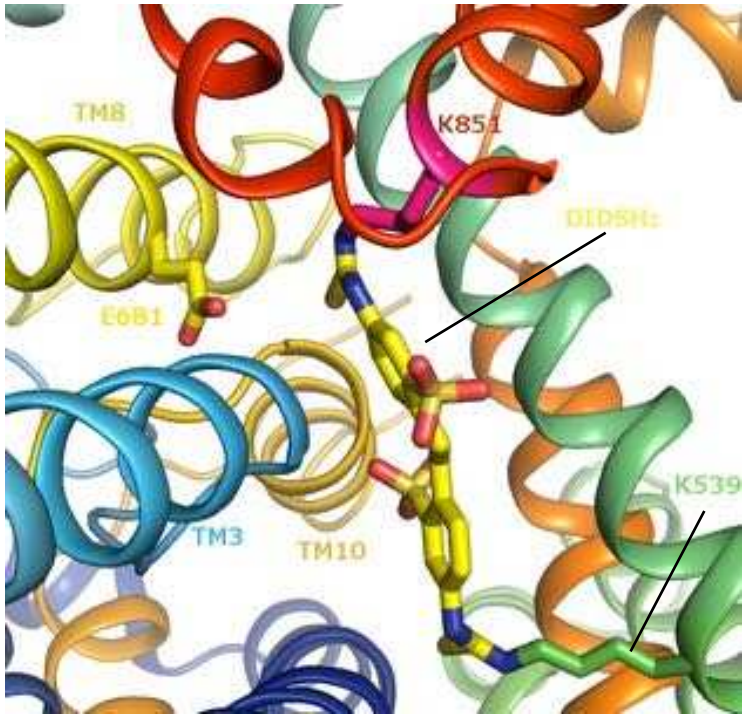

C

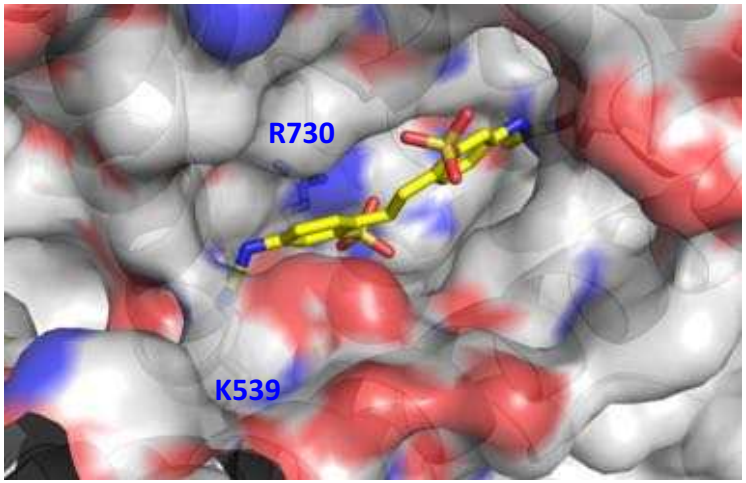

Reithmeier et al., Fig. 5

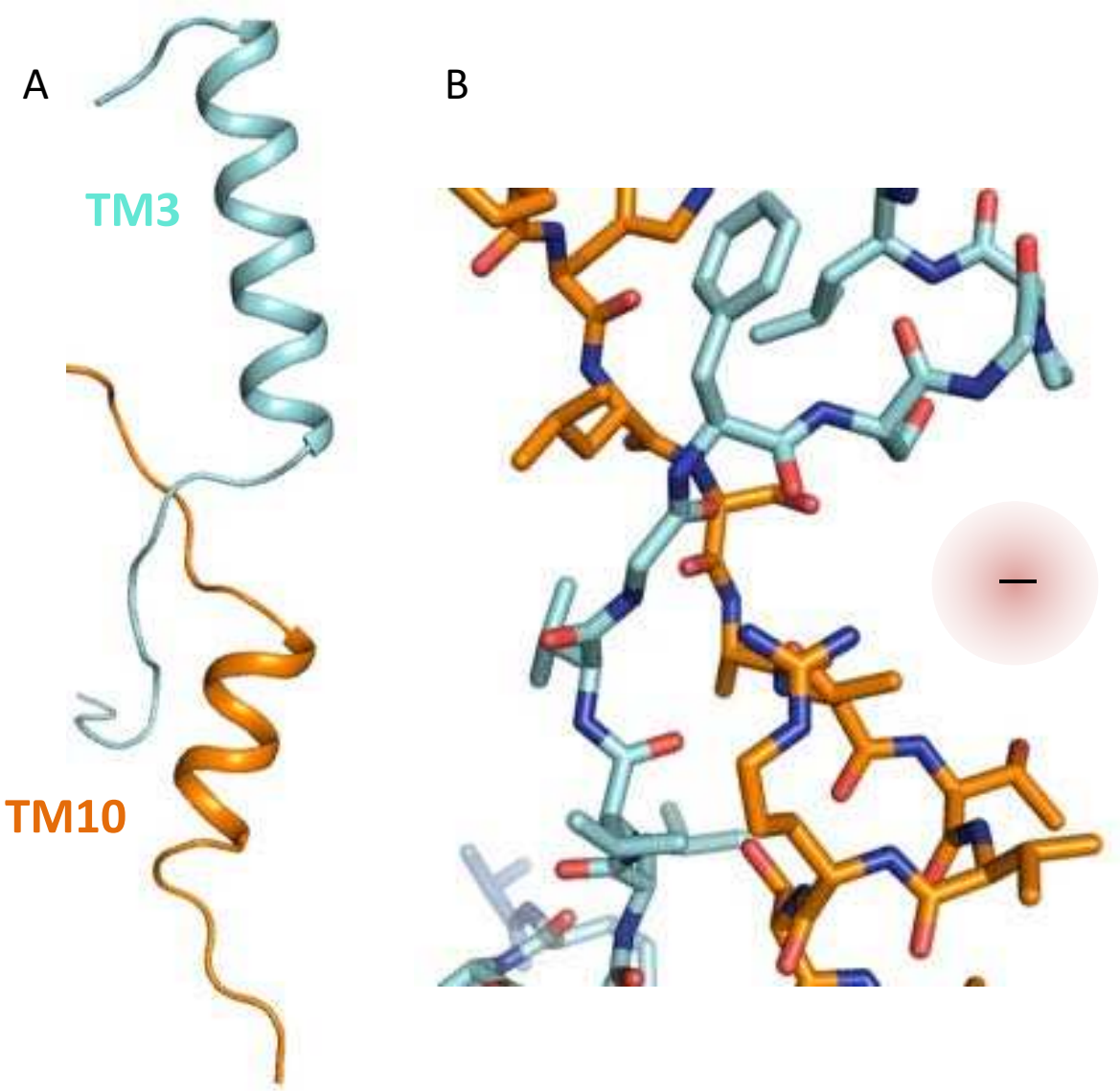

Reithmeier et al., Fig. 6

A

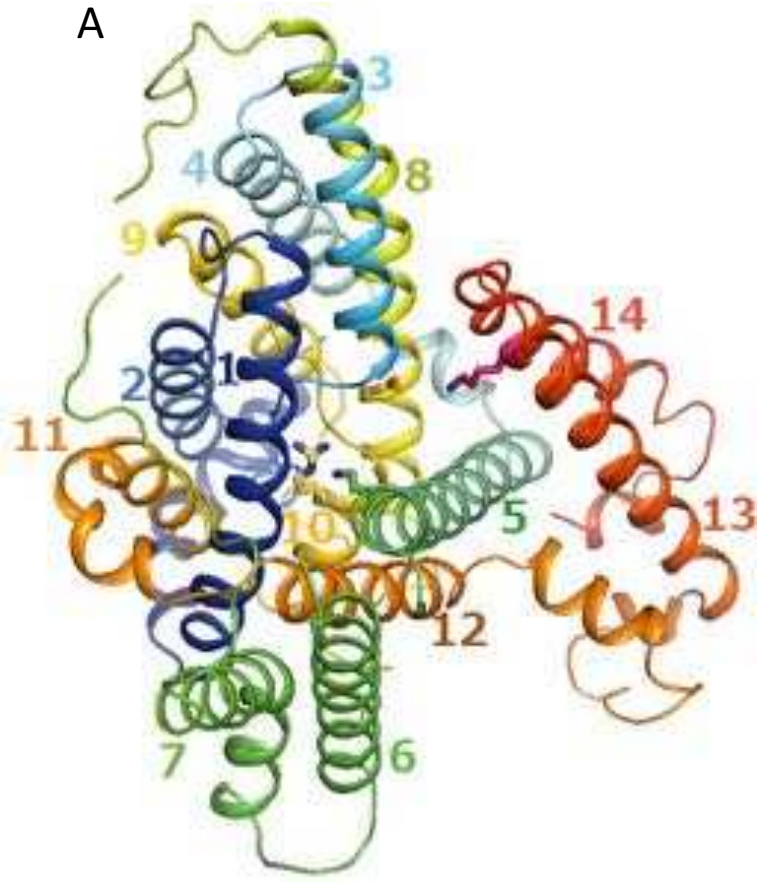

B

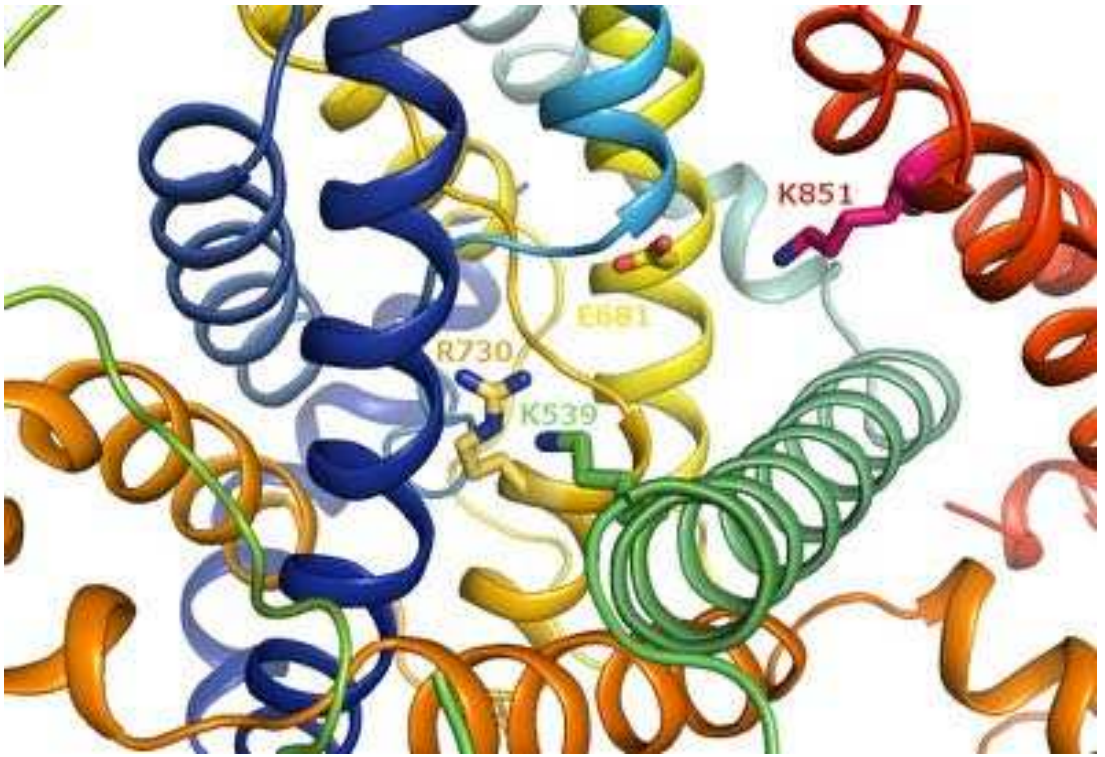

Reithmeier et al., Fig. 7

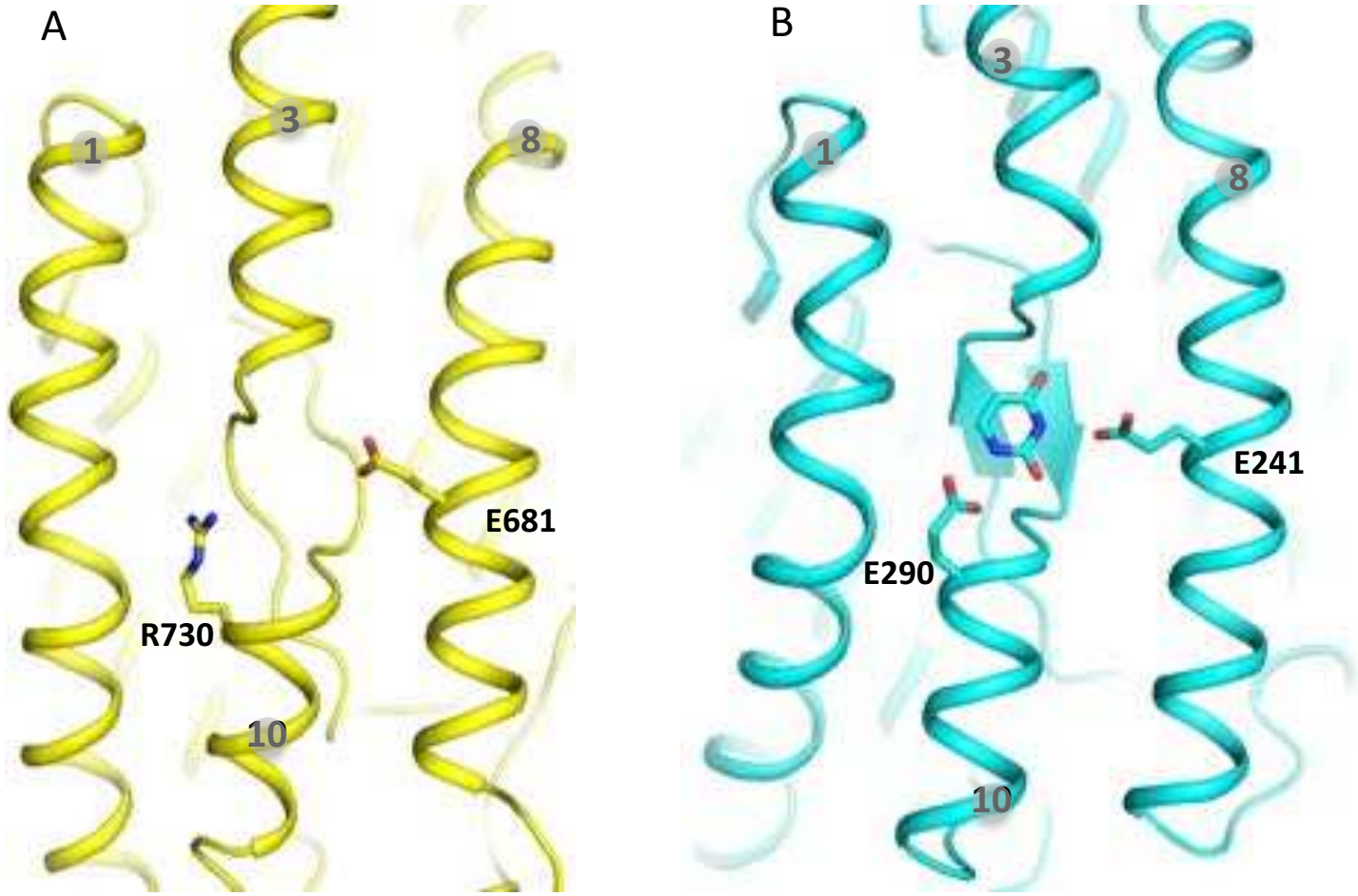

Reithmeier et al., Fig. 8

A TM 1-7

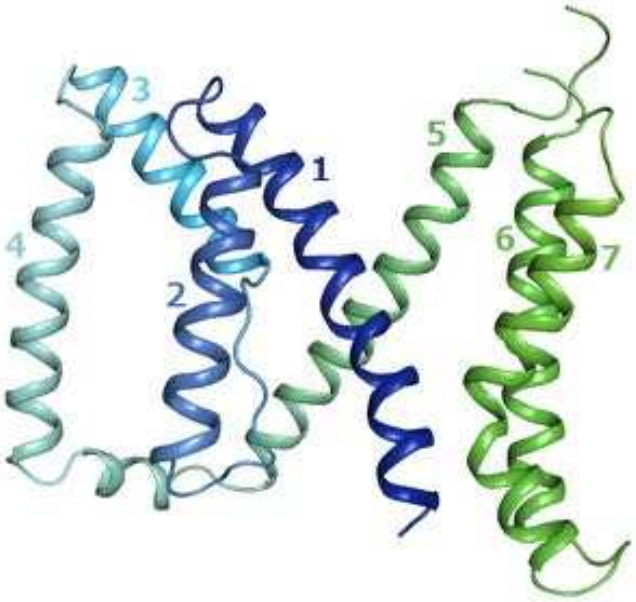

B TM 8-16

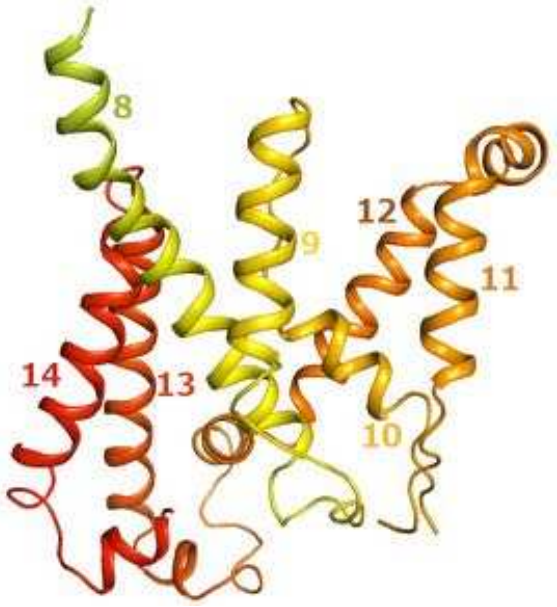

Reithmeier et al., Fig. 9

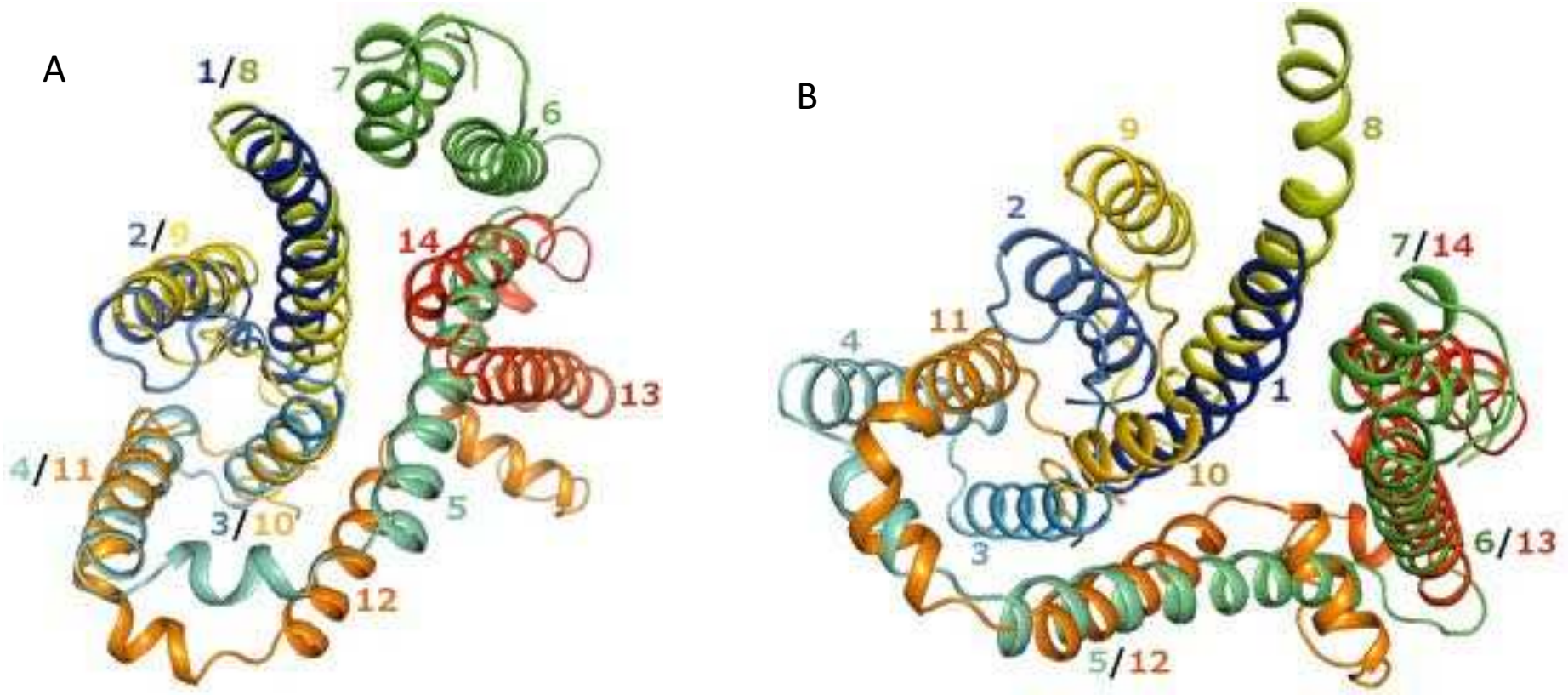

Reithmeier et al., Fig. 10

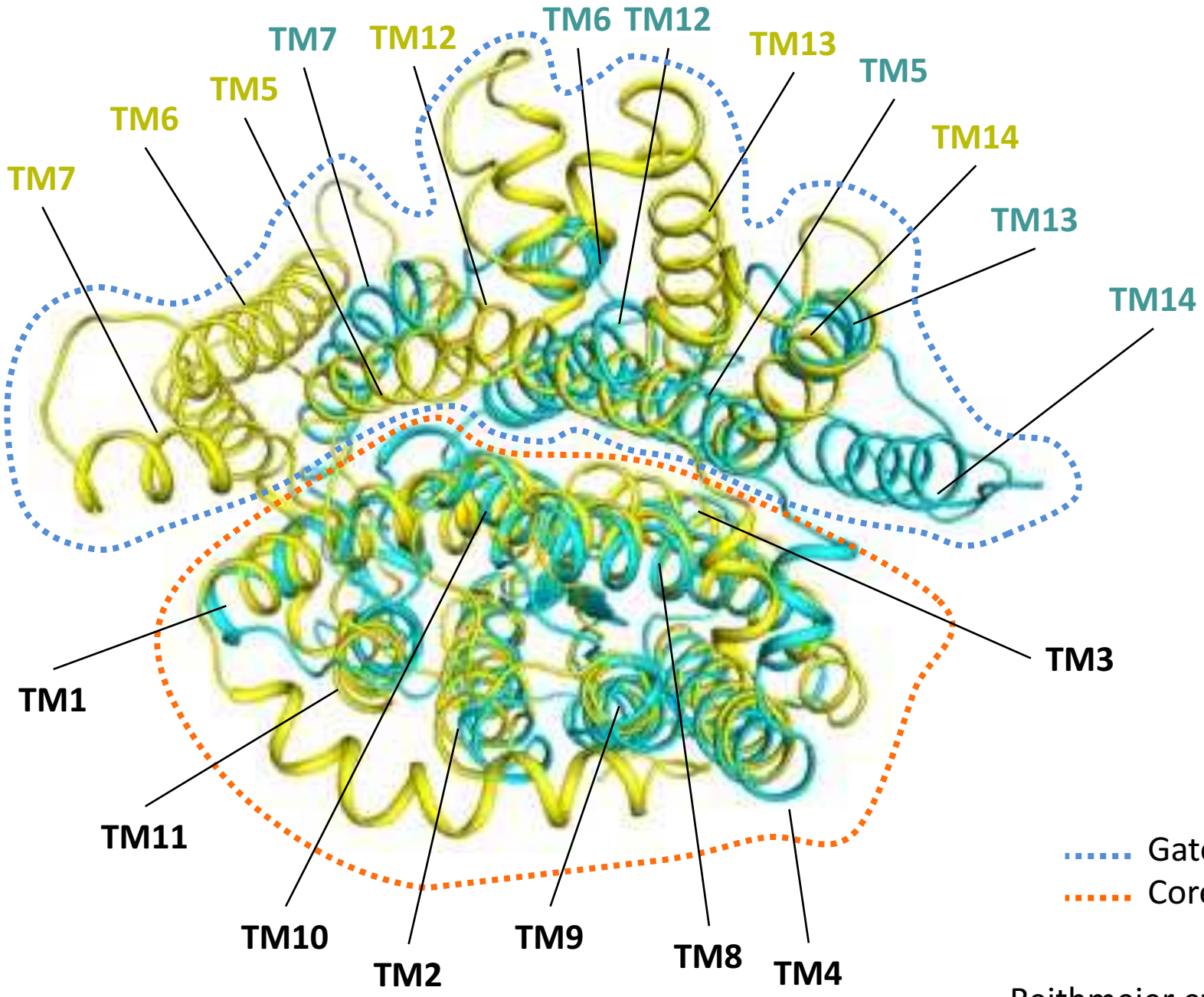

Reithmeier et al., Fig. 11

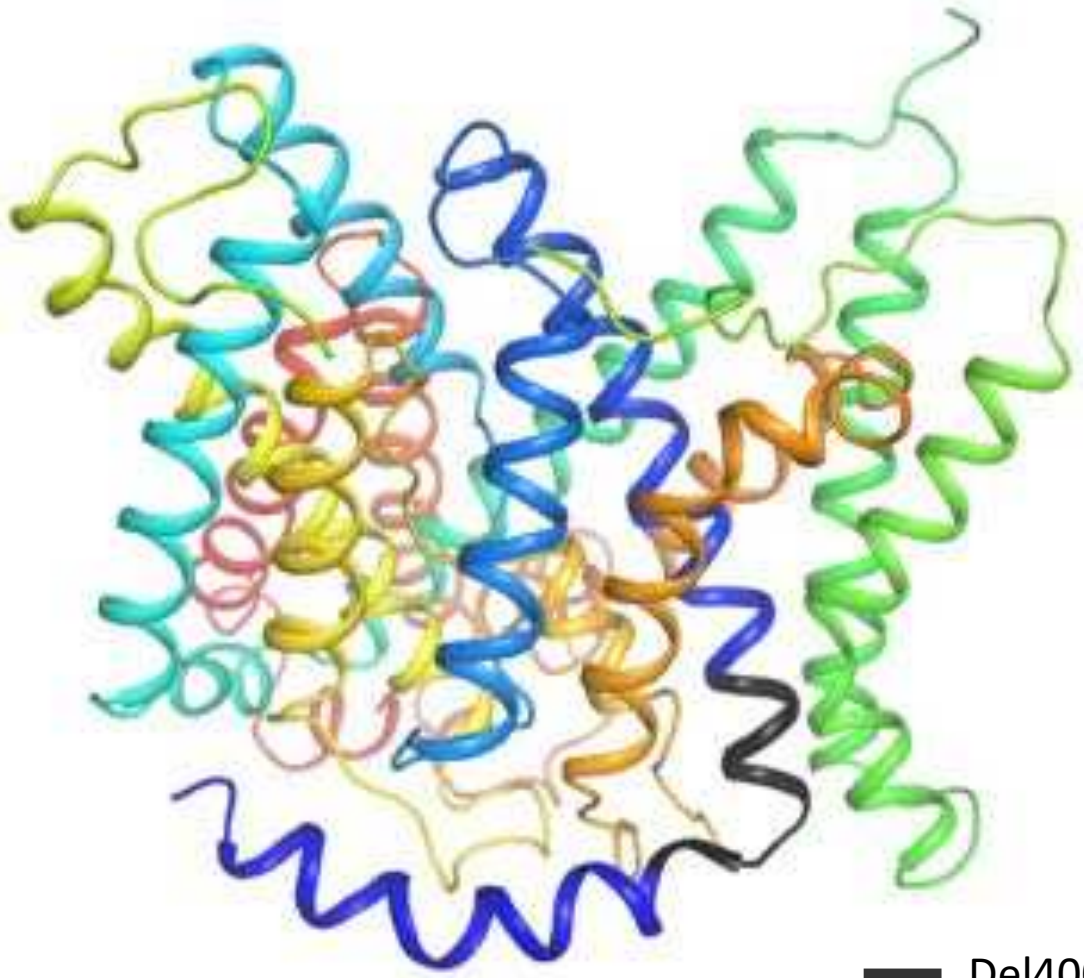

Del400-408

Reithmeier et al., Fig. 12

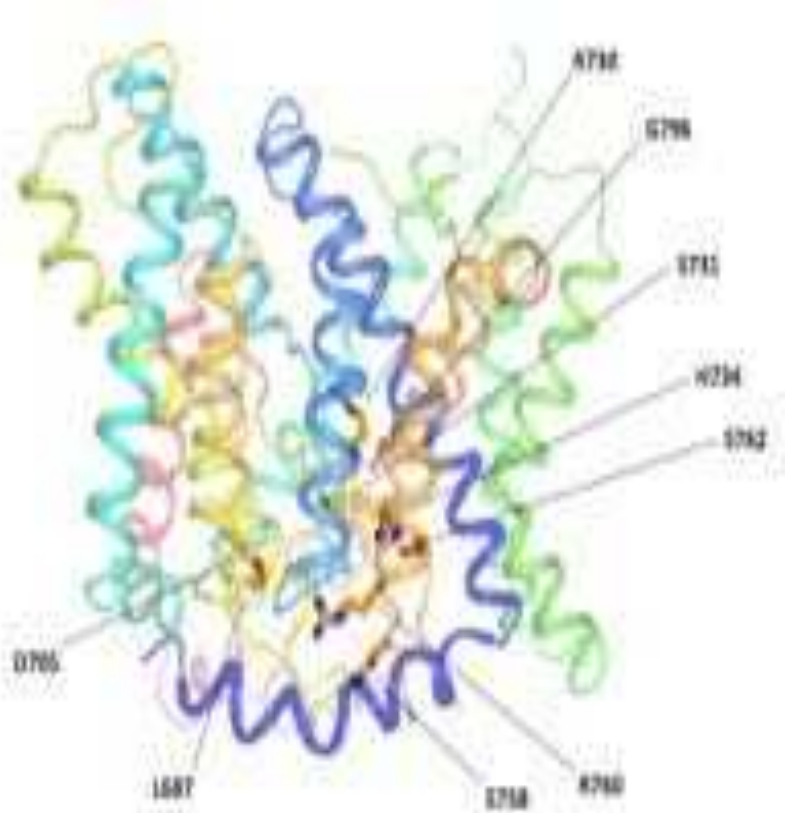

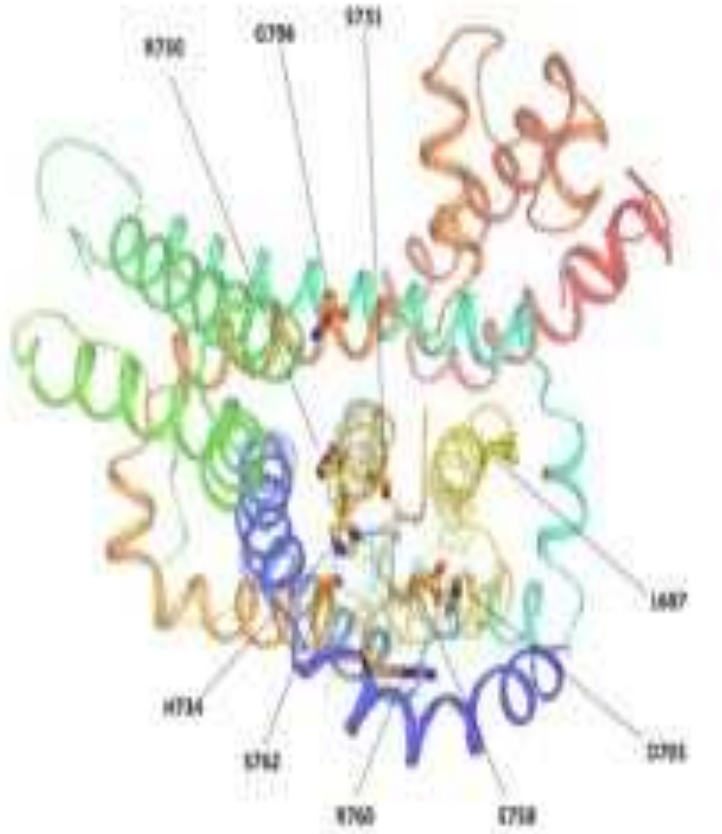

Reithmeier et al., Fig.13

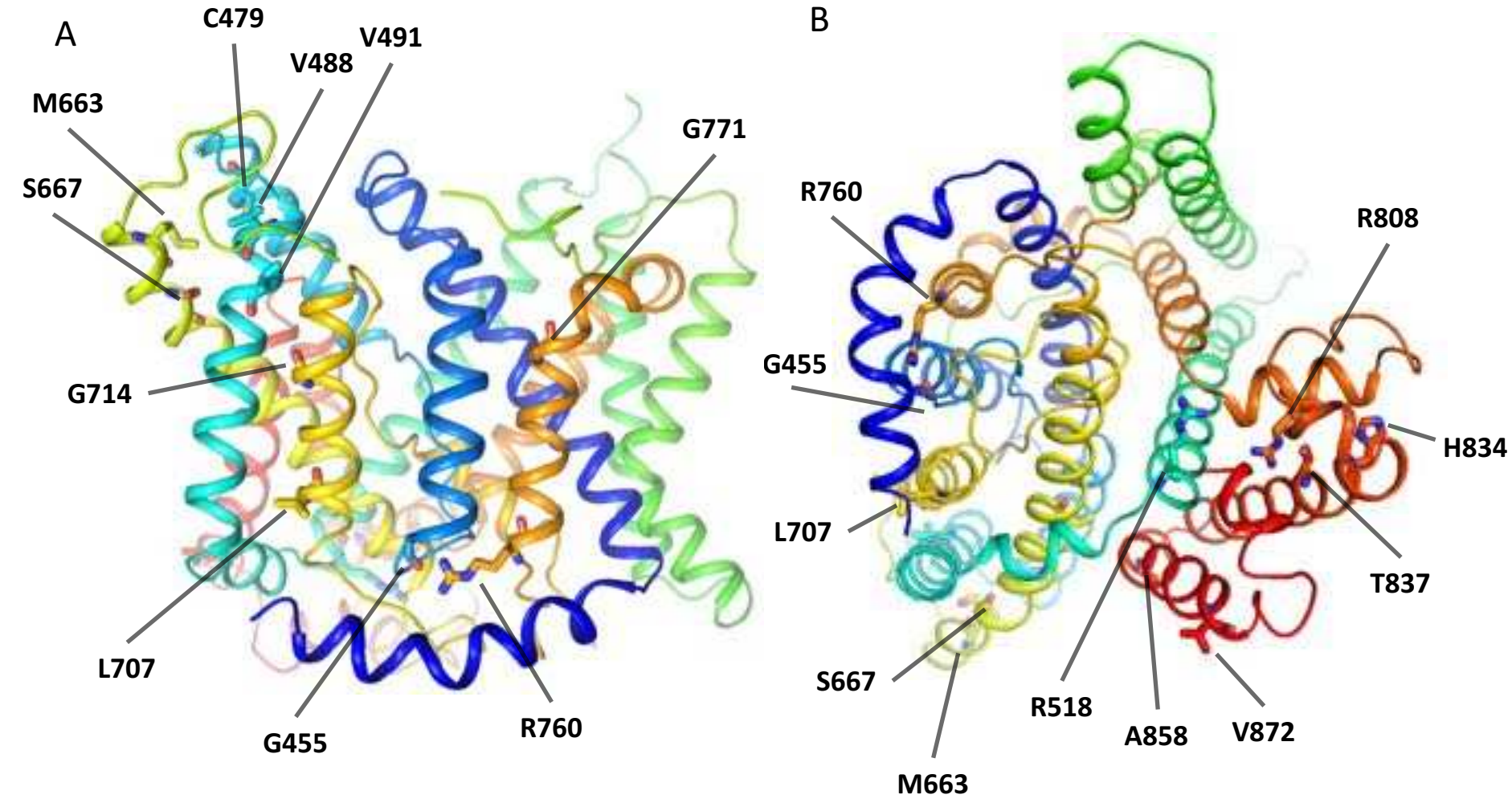

Reithmeier et al., Fig. 14

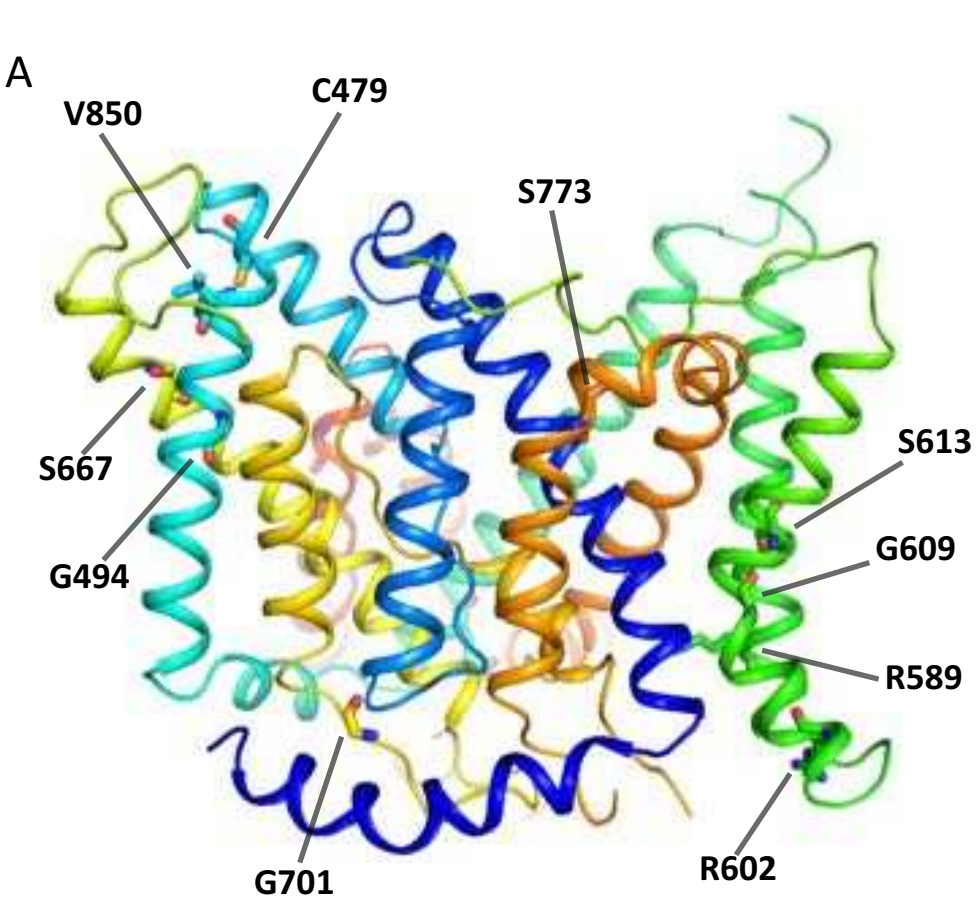

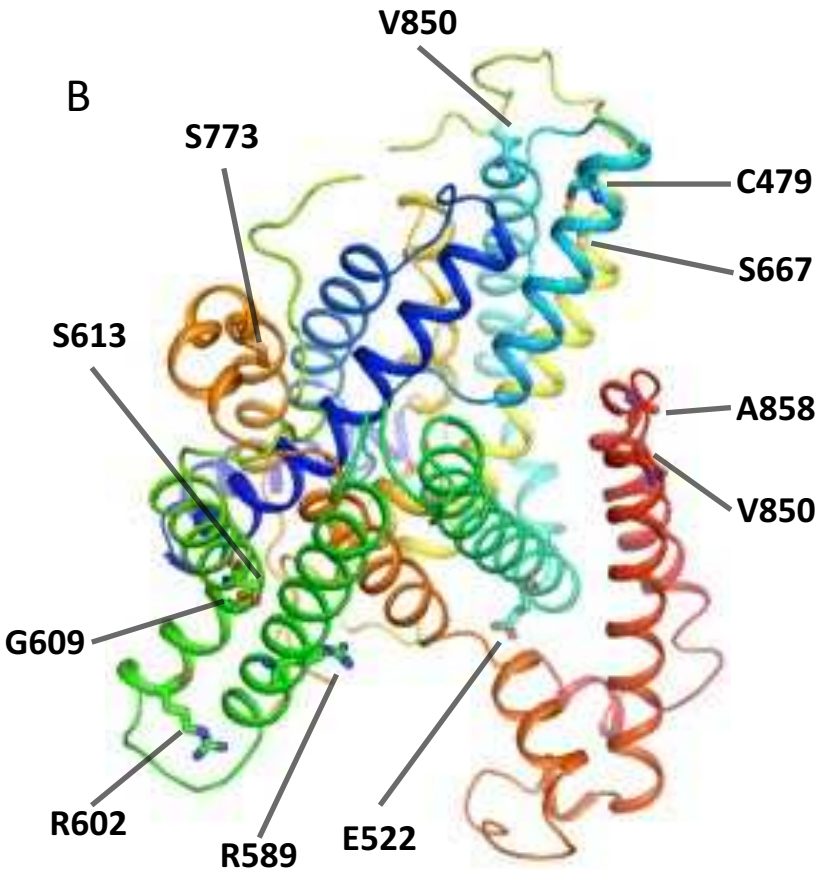

Reithmeier et al., Fig. 15

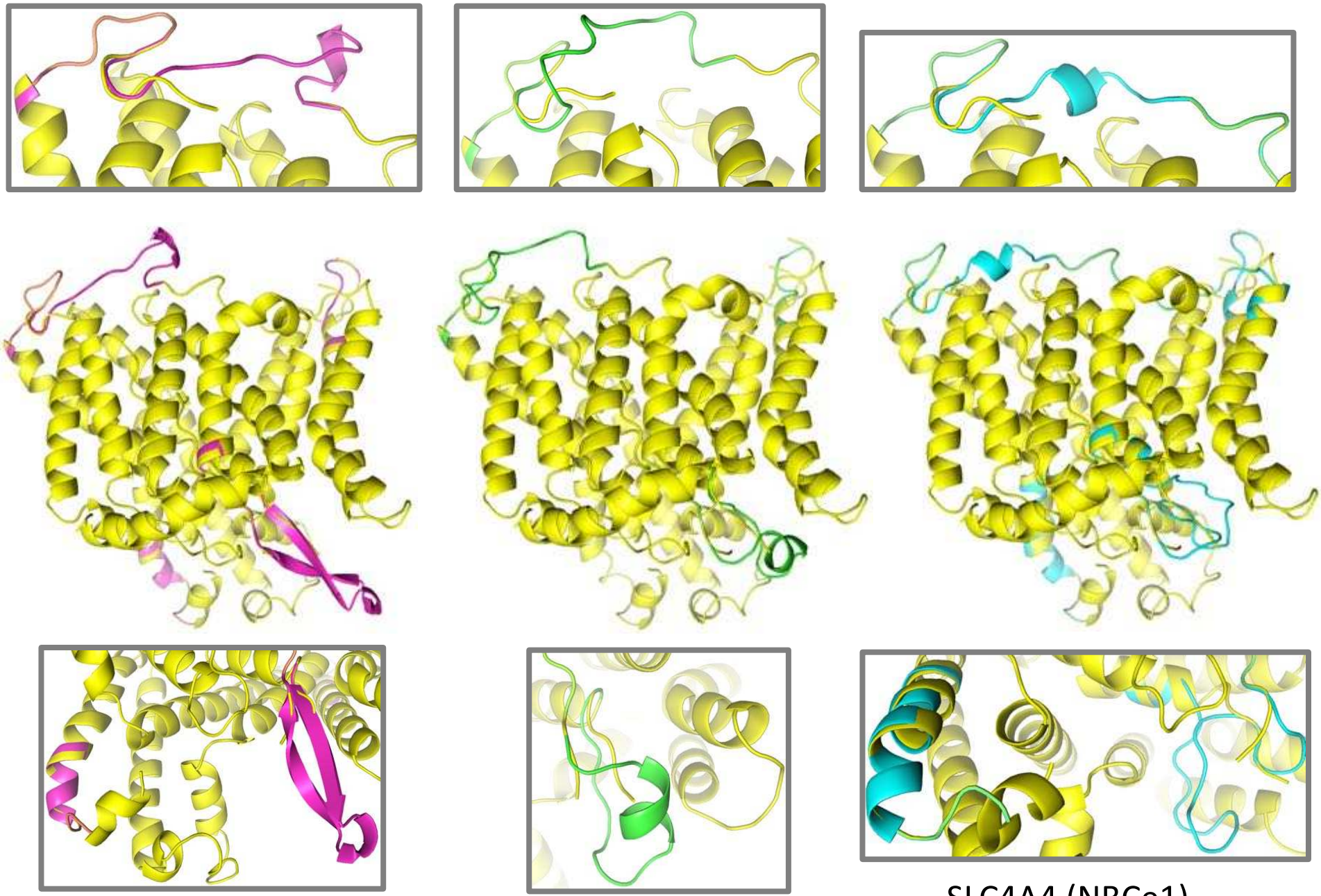

SLC4A2 (AE2)

SLC4A3 (AE3)

SLC4A4 (NBCe1)

Reithmeier et al., Fig. 16

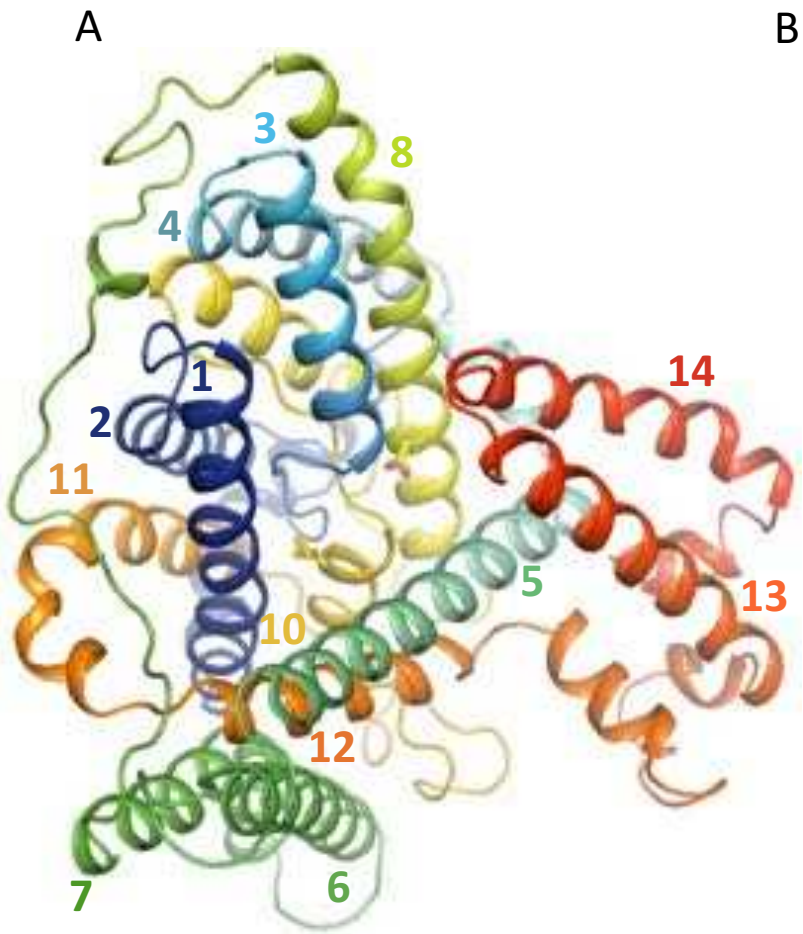

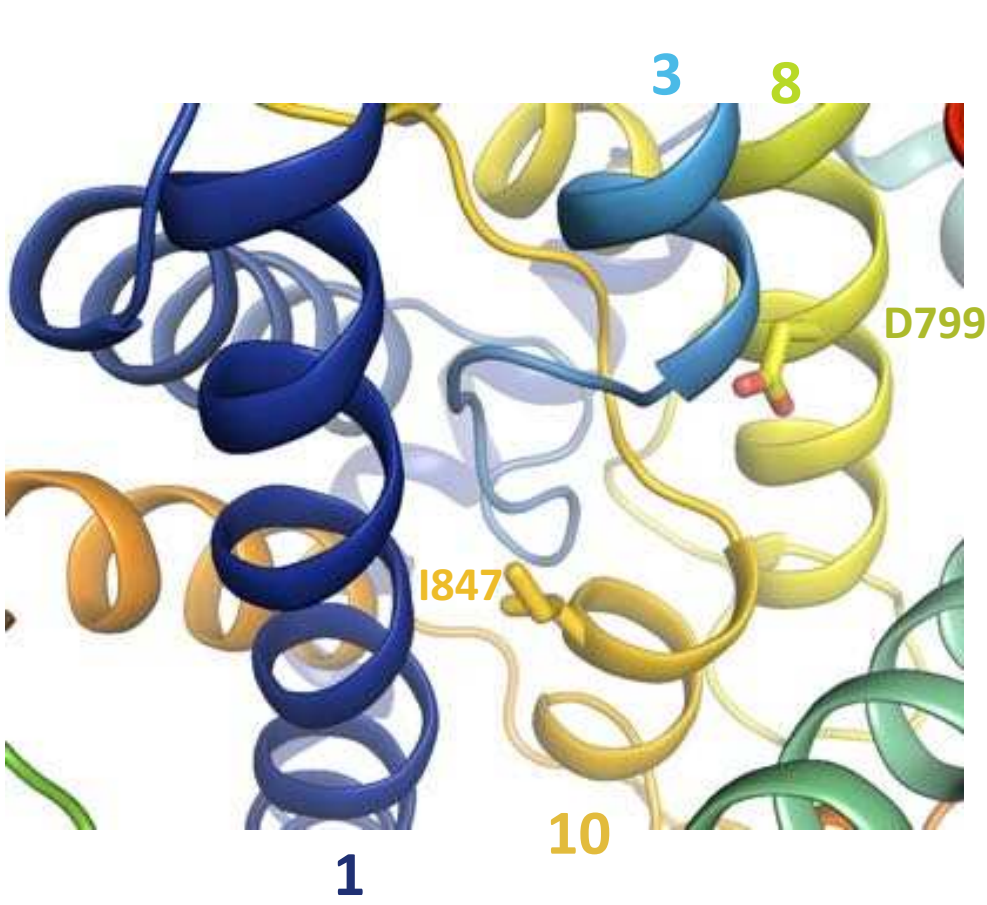

Reithmeier et al., Fig. 17

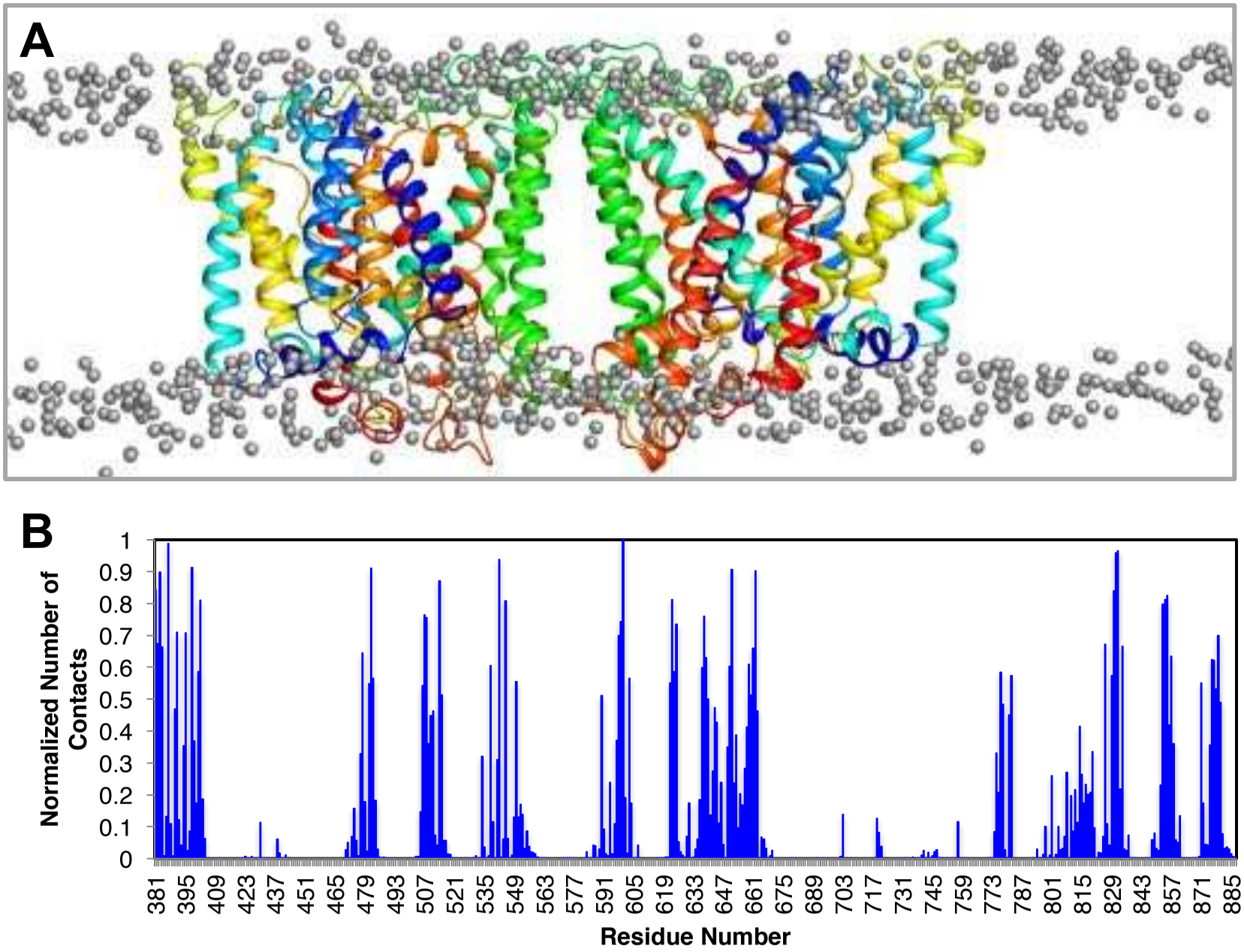

Reithmeier et al., Figure 18